Impacts of Land Management on Water Resources in the Crocodile River Catchment, Mpumalanga

Mary Nkosi

Student: 20021177

A dissertation submitted to the Department of Earth Sciences in the Faculty of Science, Engineering and Agriculture, University of Venda in fulfilment of the requirements for Master of Earth Science in Hydrology and Water Resources

Department of Earth Sciences

Faculty of Science, Engineering and Agriculture

University of Venda

Supervisor: Dr F.I. Mathivha

Co-Supervisor: Prof. J.O Odiyo

March 2022

Declaration

I, Mary Nkosi hereby declare that the dissertation titled **"Impacts of Land Management on Water Resources in the Crocodile River Catchment, Mpumalanga"** submitted to the University of Venda for the fulfilment of a Master of Earth Science in Hydrology and Water Resources degree has not previously been submitted for a degree at this or any other University, and that it is my own work in design and execution and that all reference materials contained therein have been duly acknowledged.

Signature: ___  ____ Date: 02-03-2022

Abstract

Land use/land cover (LULC) have a “cause and effect” relationship with the hydrology of catchment areas. The Crocodile River Catchment (CRC) has been reported to be fully utilised and at its limit. Due to its ecological and socio-economic importance, it is therefore imperative to quantify the changes in the river’s water resources. Using remote sensing (RS), QSWAT and Quantum GIS (QGIS) this study analysed and evaluated the long-term effects of LULC changes on the hydrology of the CRC between 1981 and 2020. LULC was classified into 8 major classes (cultivation land, forest plantation, water, grassland, built-up areas, bush/savannah and natural forest) for 1980/81, 2000/01 and 2020 to demonstrate the changes in land-use for the past 40 years. The study found that natural forests and grassland decreased by 12.8% and 1%, respectively. There was an increase in cultivated lands, forest plantations and built-up by 2.5%, 3.1% and 2.3%, respectively. Built-up areas, cultivated lands and forest plantations were identified as the major land-use activities and the hotspots for these were further mapped and analysed per quaternary catchment. The overall NDVI value for all LULC ranged between -0.3 and 0.9. The LULC maps were used as input data to the QSWAT model to evaluate LULC impacts on water resources. The model performance evaluation showed an NSE value between 0.41 to 0.79, PBIAS -4.44 to 44.7 and RSR 0.54 to 0.75 between simulated and the observed streamflow. For this study, these findings on model performance showed acceptable results. The results further showed a decreasing trend in streamflow from1981-2020. The decreasing trends were attributed to the increase in forest plantation and cultivation with built-up areas found to have minimum impacts on the catchment’s hydrological response because they occupied a small percentage of the catchment. The distribution of ET and surface runoff also varied with the LULC, however, climate was shown to have an influence on streamflow and the distribution of LULC in the catchment area, thus affecting the hydrological regime.

Keywords: LULC, Land use Hotspot, NDVI, QSWAT, Water resources,

Dedication

This study is dedicated to God, my family and Fhumulani for their undying support in my career development. To my son, Lubanzi, you are my motivation and my drive for working hard.

Acknowledgement

First, I want to thank God for everything He has done for me and for this opportunity. I would like to extend my gratitude to Digby Wells Environmental and NRF for the resources that made it possible for me to register for my postgraduate studies. I would like to acknowledge DWS for providing streamflow data and; ARC and SAWS for providing climate data (rainfall, solar radiation, temperature, wind speed and humidity).

Without my family, this project would not have been this easy, I am thankful for their understanding, their support and for their cheers; and especially my mother, without her prayers and her support this would not have been possible. I would like to acknowledge my friends as well for their support and assistance during the duration of this study.

I am thankful to my mentor and supervisor, Dr F.I. Mathivha, she has been more than a supervisor, and thank you for believing in me when I did not believe in myself. Your guidance and encouragement made all the difference, especially in the quality of the final dissertation. I would like to also extend my gratitude to the late Prof. J.O. Odiyo, his co-supervision in my proposal development assisted in shaping the concept presented in this dissertation. I am grateful for the opportunity to have worked with him. Lastly, I am grateful to the University of Venda and the former School of Environmental Sciences, especially, the former HWR Department for being my host and for the opportunity to complete this degree with the help of the staff.

List of Publication

1. Nkosi, M., Mathivha, F.I. and Odiyo, J.O., 2021. Impact of Land Management on Water Resources, a South African Context. Sustainability, 13, 701, https://doi.org/10.3390/su13020701.
2. Nkosi, M. and Mathivha F.I. Evaluating the influence of LULC on streamflow in the Crocodile River using SWAT (***in preparation***)
3. Nkosi, M. and Mathivha, F.I. Evaluating the impacts of Commercial Forest on Evapotranspiration in the Crocodile River (***in preparation***)

Table of Contents

List of Figures

List of Tables

List of Acronyms

ACRU	Agricultural Catchments Research Unit
AGNSP	Agricultural Non-point Source Pollutions
AGRR	Agriculture
ARC	Agricultural Research Council
ASTER	Advance Spaceborne Thermal Emission and Reflection Radiometer
AVHRR	Advanced Very High-Resolution Radiometer
BSVG	Bare area with no or scattered vegetation
CCD	Canopy Chlorophyll Density
CMA	Catchment Management Area
CN	Curve Number
CRC	Crocodile River Catchment
CUP	Calibration and Uncertainty Program
DEA	Department of Environmental Affairs
DEM	Digital Elevation Model
DN	Digital Number
DSS	Data Storage System
DWA	Department of Water Affairs
DVI	Difference Vegetation Index
ERTS-1	Earth Resources Technology Satellites
FAO	Food and Agricultural Organisation
FRSE	Forest Evergreen
FRST	Mixed Forest
GIS	Geographical Information Systems
GIMMS	Global Inventory Modelling and Mapping Studies
GRAS	Grassland
HEC-HMS	Hydrologic-Engineering Centre- Hydrologic Modelling System
HRU	Hydrological Response Unit
IUCMA	Inkomati-Usuthu Catchment Management Area
IWMA	Inkomati Water Management Area
IWRM	Integrated Water Resource Management
LADA	Land Degradation Assessment in Dry Land
LAI	Leaf Area Index

LULC	Land Use and Land Cover
MAE	Mean Absolute Error
MAR	Mean Annual Runoff
MODIS	Moderate Resolution Imaging Spectroradiometer
MPCOGTA	Mpumalanga Cooperative Governance and Traditional Affairs
MSI	Multispectral Instrument
NASA	National Aeronautics and Space Administration
NECASC	Northeast Climate Science Centre
NDVI	Normalized Difference Vegetation Index
NIR	Near-Infrared
NSE	Nash-Sutcliffe Coefficient
OLI	Operational Land Imager
PBIAS	Percent BIAS
PET	Potential Evaporation
QGIS	Quantum Geographical Information System
RS	Remote Sensing
RSR	RSME-observation Standard Ration
RVI	Ratio-based Vegetation Indices
SA	South Africa
SAVA	Savannah
SAWS	South African Weather Services
SCP	Semi-automatic Classification Plug-in
SOTER	Soil and Terrain Database
SoER	State of Environment
SRTM	Shuttle Radar Topography Mission
STATS	Statistics
SUFI	Sequential Uncertainty Fitting
SW	Surface Water
SWAT	Soil and Water Assessment Tool
SWIR	Shortwave Infrared
TIRS	Thermal Infrared Sensor
TM+	Thematic Mapping Plus
US	United States
USGS	United States Geological Survey

VNIR	Visible and Near-Infrared
VI	Vegetation Index
WATR	Water
WWF	World Wildlife Fund

CHAPTER 1: INTRODUCTION

1.1 Background

The world's population is growing at an unprecedented rate, and putting pressure on the earth's resources (Boucher, 2018). As the population grows, virgin land is encroached, resulting in forest clearing, putting many species at risk of becoming extinct and natural resources such as water at risk of being degraded (Baus, 2017). Baker and Miller (2013) indicated that in some cases, the interaction between human activities, water use and the need to sustain ecosystem health can often lead to water resource degradation which can result in water scarcity. The availability and quality of natural resources depend on the way in which the land is utilised and managed, for example, an increase in built-up areas is expected to decrease infiltration and percolation which in turn increase surface run-off and evaporation (Kumar *et al*., 2017). In South Africa, urban expansion has led to an increase in water demand, therefore, leading to overexploitation of water resources. According to Donnenfield *et al*. (2018), more than 60% of the rivers in the country are overexploited due to the rise in water demand as a result of the increase in urbanisation. Many of the country's catchments are failing to meet its water demand, among these is the Crocodile River catchment (CRC).

Natural forests in the CRC have been converted for agriculture and forestry production (State of Rivers Report, 2001). There are also mining and industrial activities occurring within the catchment, and it was reported by Sauka (2016) that about 1.5% of the catchment is under urban development. Due to these economic activities and the rapid land-use expansion of the catchment area, DWA (2014) reported that the Crocodile River is at its limit and its water is fully utilised. The quality of the river was reported to have been compromised in the past due to sewage pollution, intensive agricultural use of fertilisers and pesticides as well as mining and industrial waste (Nel and Driver, 2015). Remote Sensing (RS) and Geographical Information Systems (GIS) techniques have been frequently used to monitor changes in Land use/ Land Cover (LULC), especially in places where primary data-collection is a problem (Skidmore *et al.,* 1997). Information generated from these tools are important as they assist with the management and future planning of natural resources, especially, with climate change increasing the vulnerability of water resources (Skidmore *et al*., 1997). Through integrating hydrological modelling with GIS and RS, this study focused on evaluating,

analysing and spatially presenting changes of the CRC that resulted from land alteration and modification.

1.2 Problem statement

Land use activities, development and management of water resources are interdependent. Catchments areas are very sensitive to any changes induced on the land, for example, land erosion results in sedimentation (Welde and Gebremariam, 2017). Due to anthropogenic land-use changes, overpopulation, over-extraction of water, diversions of river systems and sedimentation load, freshwater ecosystems in Africa are at risk (Sauka, 2016). The Lowveld region of South Africa has developed rapidly over the past years and agricultural activities have expanded. Managing catchment natural species and natural environment is a problem in most parts of the Crocodile River Catchment, especially near Nelspruit (Linstrom, 2016). Soko and Gyedu-Ababio (2015) observed a decrease in species richness in the upper reaches of the catchment, due to the Kwena Dam.

As outlined in Linstrom (2016), most riparian zones which also serve as buffer zones are at risk, if not already destroyed through developments manifested through vegetation clearing, in the study area. Large amounts of water resources have been abstracted from the Crocodile River Catchment, which has resulted in low flow during dry season (Kleynhans *et al*., 2013). Changes in vegetation cover lead to changes in the composition and structure of a catchment, thereby affecting water intake and runoff. Due to the intensity of these activities, together with the expanding industrial and urban land uses, the catchment is noted to be water stressed by Soko and Gyedu-Ababio (2015).

1.3 Motivation

Development is expected to continue in the study area with an increase in water demand, therefore, better management of water has become important within this catchment over the recent years. It was indicated that water scarcity has been evident since the mid-80s and has been intensified by climate extremes, such as droughts and floods (Kleynhans *et al*., 2013). In addition, various studies, Bender and Gibson, (2010); Mutamba and Busari, (2011); DWA, (2014) have indicated that water quantity challenges are affecting water supply in the catchment area. An investigation done on water requirement in the Inkomati Water Management Area (IWMA) in 2009, showed

that there is a need to develop new water resource strategies (DWA, 2009). There are also challenges with ecosystem health of the CRC as reported by Mpumalanga SoE (2004) and Kleynhans *et al*., 2013). The river system's health is reported to be threatened by challenges like sedimentation, eutrophication, and flow modification. The increase in demand will exert more changes to the environment of the CRC and this would aggravate the risk of the catchment being degraded.

This study, therefore, focuses on land management and its impacts on the CRC water resources. It evaluates changes observed in surface run-off, streamflow discharge while also quantifying the changes in vegetation. With the use of GIS, RS and SWAT model, this study will compare changes in LULC and record the hydrological impacts. The process will yield information on the modifications of the CRC through LULC changes, thus assist in the development of land management and water resource strategies that will promote the catchment health and improve water supply. Furthermore, findings will portray the usefulness of the SWAT model in simulating streamflow in catchments with characteristics such as the CRC. There is not much updated literature on the study area pertaining to the application of RS and GIS, therefore, this study will be able to generate current comprehensive data.

1.4 Research questions

i. How has the LULC changed on Crocodile River Catchment over the past 40 years?
ii. Which activities and areas pose a threat to the quality and quantity of the River?
iii. How has the hydrological response of the catchment changed?

1.5 Objectives

The main objective of this study is to apply GIS and RS techniques in integration with SWAT in evaluating the effects of land use and land-cover changes on water resources in the Crocodile River Catchment. The specific objectives are to:

i. Evaluate LULC changes on CRC between 1980 - 2020,
ii. Identify hot spot areas and land uses that are a threat to CRC and
iii. Quantify and analyse changes in the catchment water resources over the study period.

1.6 Description of the study area

The Crocodile River Catchment is located in the Mpumalanga Province of South Africa and is governed by the Inkomati-Usuthu Water Management Area (WMA) as part of the second National Water Resource Strategy (NWRS 2) (Figure 1.1). It forms one of the significant rivers in South Africa in terms of ecology as a result of the diversity of riverine habitats. According to Roux *et al.* (1999), it houses at least 49 fish species making it one of the most biologically diverse rivers in South Africa. The catchment is about 2 000 m above sea level in the Steenkampsberg Mountains near Dullstroom. It is a slow flowing river with a length of 320 km, and it drains an area of 10 450 km^2 and the bedrock is mainly Dolerite intrusion, basaltic lava and sand pools (Kleynhans *et al*., 2013). Crocodile River has 4 major towns located along it, namely, - City of Mbombela, Barberton, White River and Malelane - (Inkomati Water Management Area, 2008).

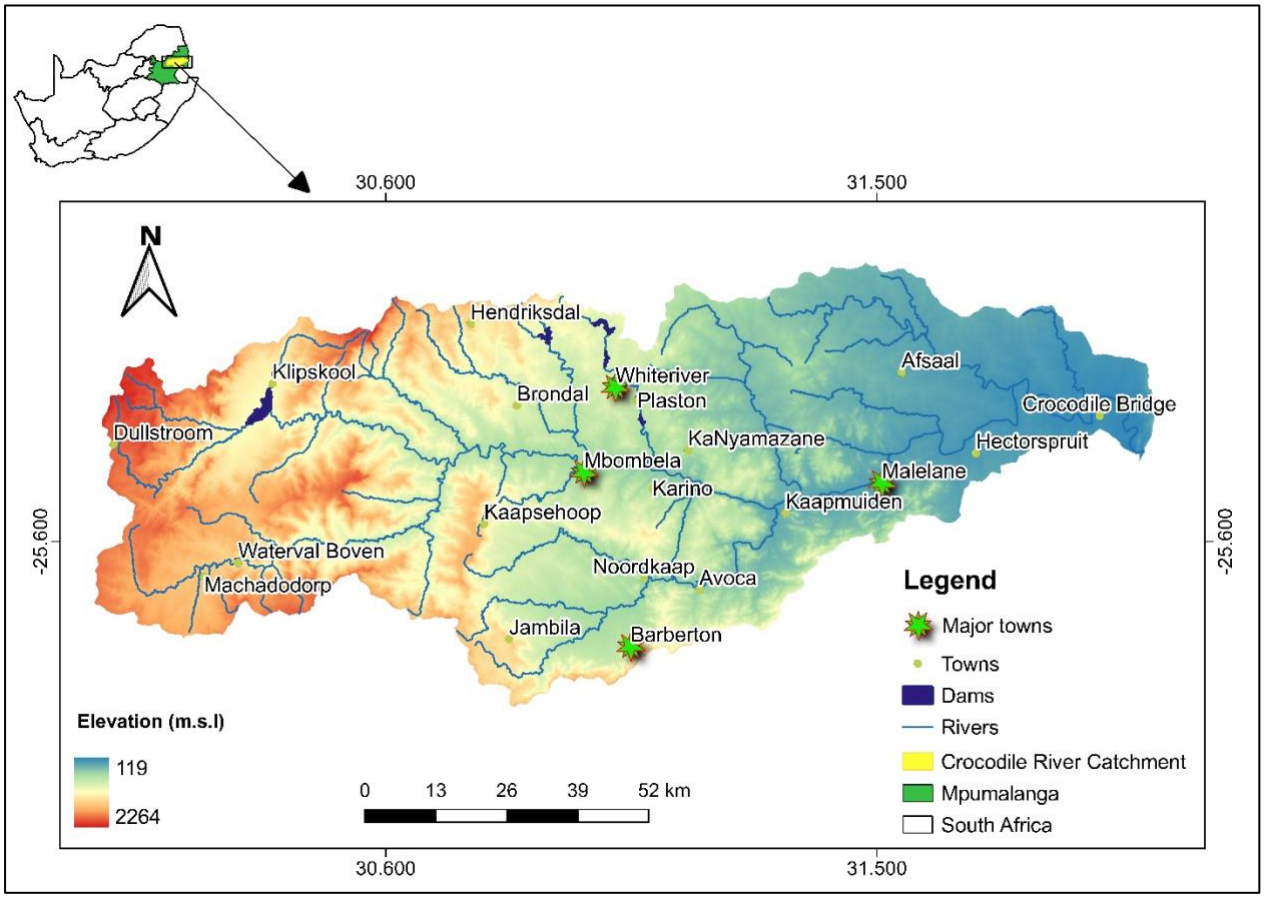

(Source: WR2012)

Figure 1.1: The location of the study area.

1.6.1 Hydrology and Water resources

The Crocodile River ranges from the cold mountain streams in the Drakensberg to the slow-moving temperate waters and it meanders through Lowveld (Kleynhans *et al*., 2013). It originates in the Steenkampsberg and flows in an easterly direction down to the Kwena Dam Basin. It further winds along the valley of the Schoemanskloof to the Montrose falls and then joins with the Elands River ((Source: WR2012)

Figure 1.*2*). As it flows in the easterly direction, it then converges with the Komati River in the Komatipoort to form the Inkomati River which borders South Africa and Mozambique (Sauki, 2016). Kleynhans *et al*. (2013) added that the upper catchment area is made of steep sided valleys and sharp cliff slopes on the edge of the Escarpment. The Elands River rises in Machadorp town and the other main tributaries for the river include the Kaap River, Komati River, Sabie River and White River. Each main river tributary contains one major dam. The Kwena Dam is the biggest and most important dam within the Crocodile River, supplying an area of 12.5 km^2, it is found where several rivers converge, namely, the Crocodile River, Lunsklip, Alex-se-Loop, Elandspruit and Badfonteinloop Rivers.

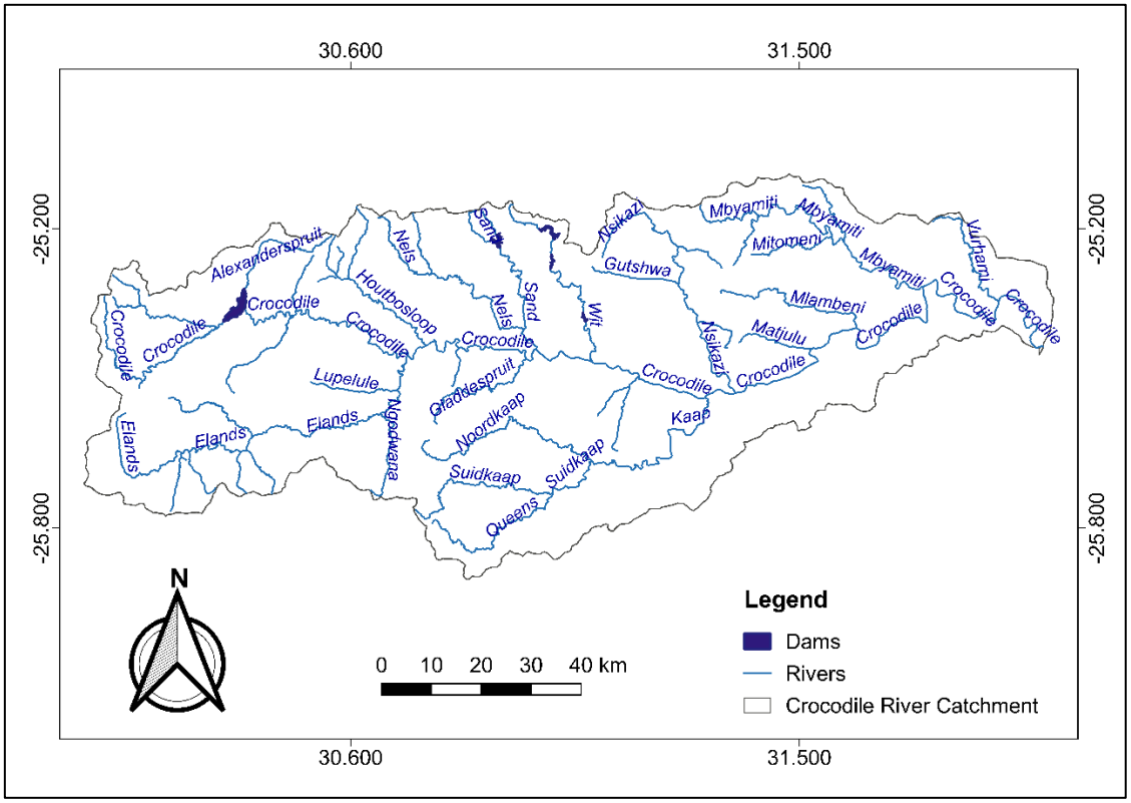

(Source: WR2012)

Figure 1.2: Rivers and dams of the catchment.

The Crocodile River has a natural mean annual runoff of 1 136 million cubic metres per year (Basson and Rossow, 2003), and it varies from between 200 and 500 million m^3/a in the western and northern parts of the catchment. According to van der Laan *et al*. (2012) and Sauka (2016), both the Kwena and Witklip Dams regulate the flow of this river. Water is released regularly for supply to farmers along the lower reaches and this helps flush away wastewater effluents. Approximately 859 million m^3/a can be abstracted from the catchment; this includes usable surface water, existing groundwater, usable returns, storages, and natural runoff. The east part of the catchment together with Sabie River supplies water to one of the major municipalities in the Province, Mbombela Local Municipality (MLM) (DWA, 2014).

1.6.2 Climate

1.6.2.1 Rainfall

The mean annual precipitation over the catchment is 880 mm. (Source: WR2012)

Figure 1.*3* shows the distribution of rainfall within the catchment. According to Riddell *et al*. (2013), the western upper plateau (highveld) receives approximately 730 mm/year, while the mountainous/escarpment region received the highest rainfall of almost 1600 mm and the eastern sub-tropical region (lowveld) receives between 550–850 mm/year. The dry lowveld part receives 600 mm of rainfall per year (van der Laan *et al*. 2012; Jackson 2014). Not only does rainfall varies with altitude, but it is also highly seasonal, more than 80% of the annual rainfall fall during summer (October - March) and the peak rainfall months are December and January (DWAF, 2004).

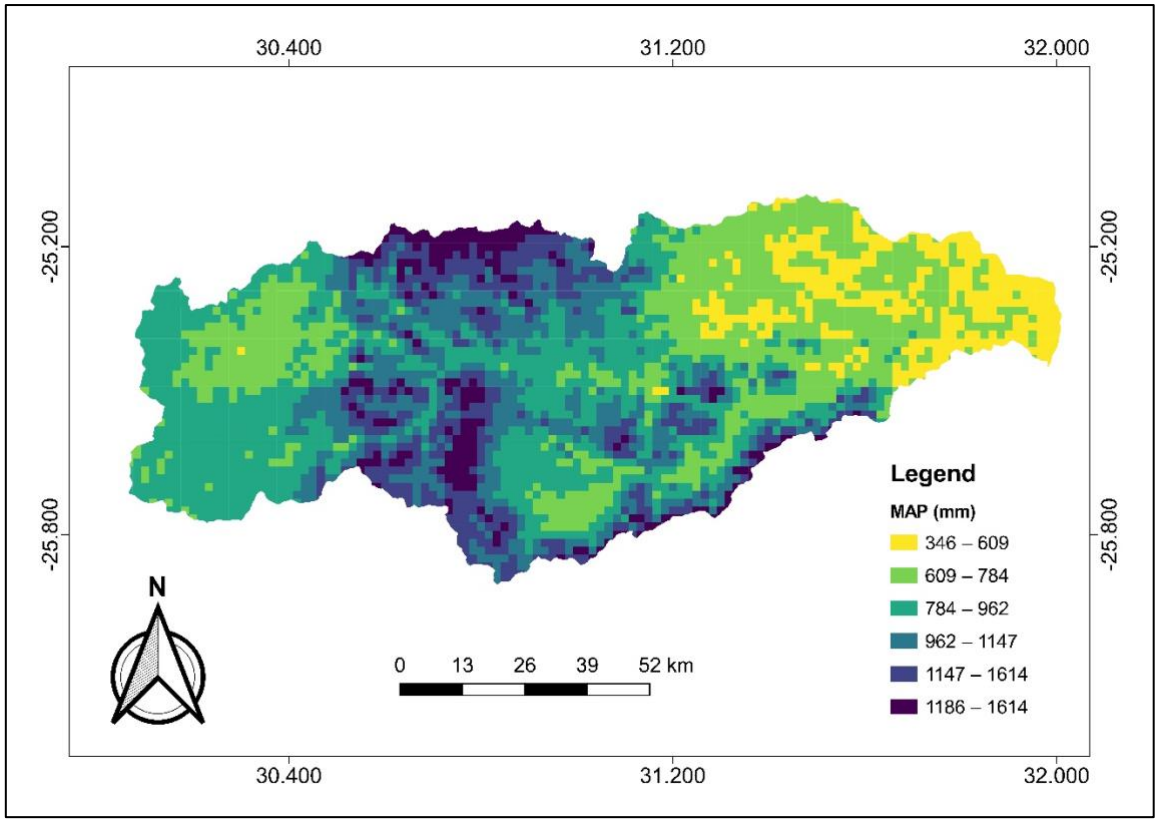

(Source: WR2012)

Figure 1.3: Catchment distribution of the Mean Annual Precipitation.

1.6.3 Temperature and Evaporation

Similar to the rainfall patterns, temperatures also vary with altitude and relief. The catchment usually experiences hot summer temperatures with maximum temperatures being in January and mild winters with minimum temperatures being in June. The highveld regions experience temperatures between 10–18^{o}C and the escarpment varies between 10–12^{o}C and 20–22^{o}C (Sauka, 2016). The lowveld area experiences more warmer temperatures with an annual average of 22^{o}C. Evaporation is generally high, and it is highly influenced by the high and dry temperatures of the catchment. The potential evaporation decreases from low altitudes to the high altitudes with a mean of 1 600 mm south-west and 2 000 mm in the east. Just like the temperatures, the highest evaporation rates are in January with amounts approximating 203 mm and a 101 mm in June ((Source: WR2012)

Figure1.4:).

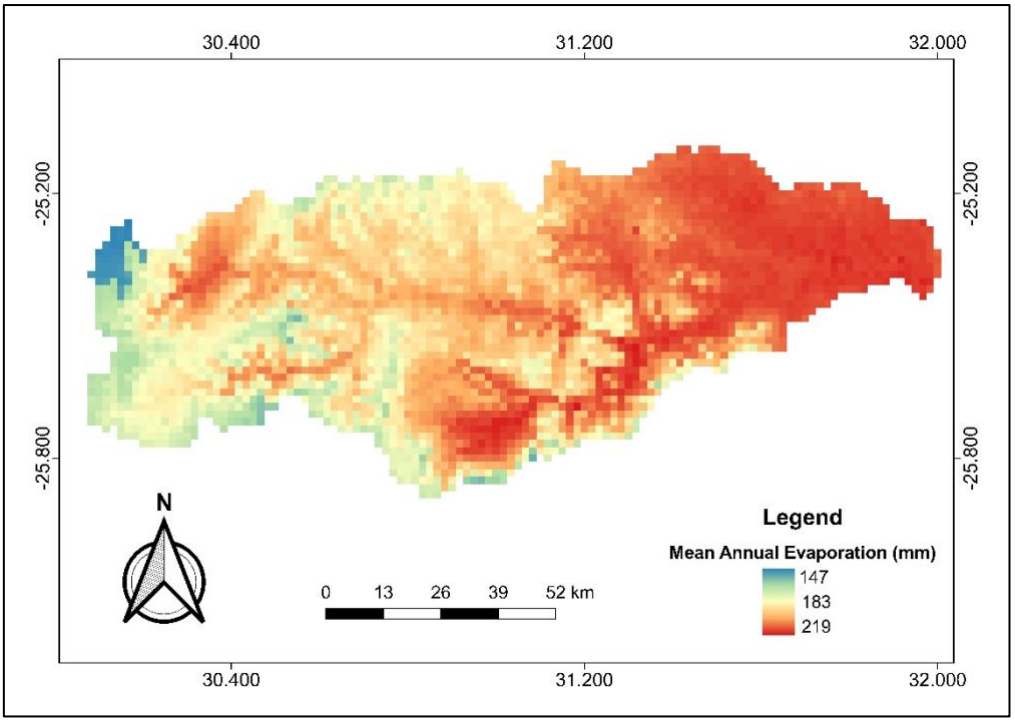

(Source: WR2012)

Figure1.4: Catchment evaporation distribution.

1.6.4 Major Land use and Land cover

There are three major recognised biomes in the Crocodile River Catchment - grassland, savanna (bushveld) and forest ((Source: WR2012)

Figure 1.4). The study area is made up of mostly a Savannah-type vegetation with dense thickets and large trees found along the drainage line and wetlands. The dominating Bushveld vegetation cover at 200 m elevation is *Acacia, Combretum, Sclerocarya and Termibalia* trees (Kleynhans *et al*., 2013). The grassland vegetation is found dominating at high altitude and the western part of the catchment is mostly made of exotic plantations while Afromontane Forests are found on the Drakensberg Escarpment. The Afromontane forests contain tree species, such as the Yellowwoods, Cape Beach, Lemon Wood and Forest Waterwood (Mbombela SoER, 2003), while the riverine forests are made of large Matumi and Sycamore fig trees; other noted vegetation cover includes reeds (*Phragmites*).

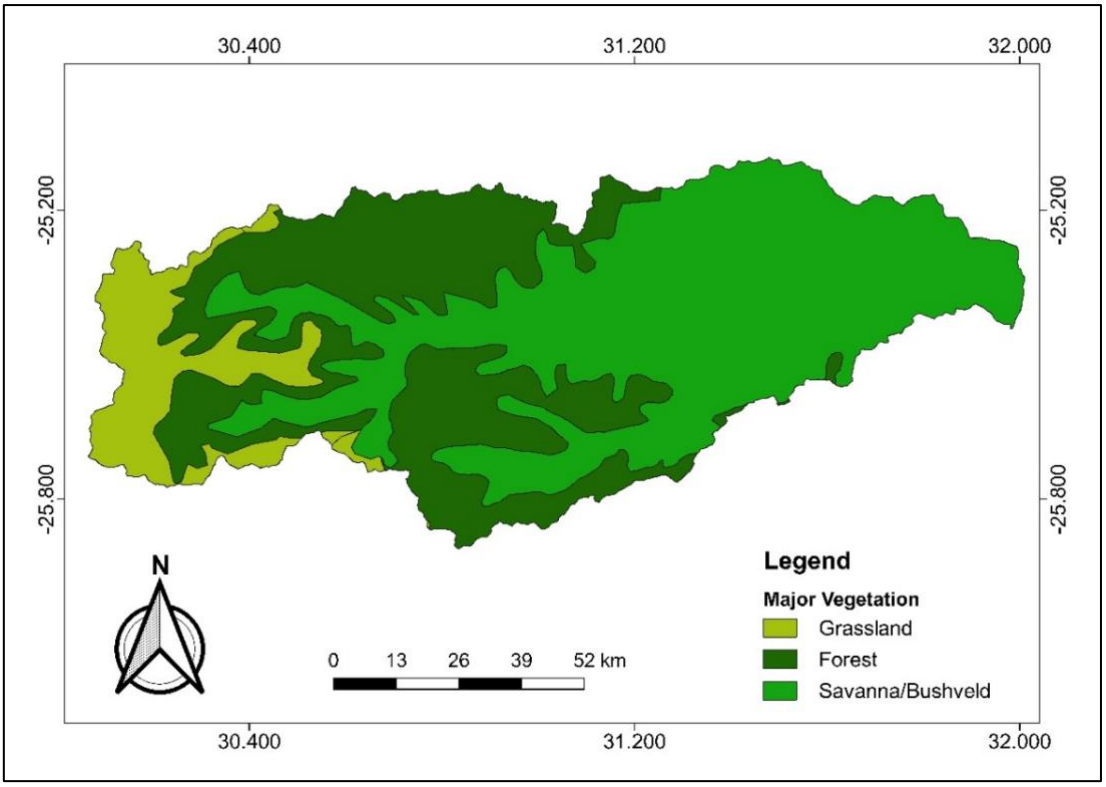

(Source: WR2012)

Figure 1.4: Major vegetation cover.

According to Sauka (2016), most of the catchment has been transformed from its natural vegetation to other land-uses, such as settlement, cultivation and commercial forest. Agriculture (pasture, dryland or irrigated) is the dominating land use and together with commercial forestry and settlements are major water-users, especially, in the upper and middle parts of the catchment. The lower part of the catchment consists of conservation sites, such as the Kruger National Park.

1.6.5 Soil Cover

(Source: WR2012)

Figure 1.*5* depicts the dominating soil textures in the catchment - sandy loam to loamy sand (LmSa – SaLm), sandy clay to clay (SaCl-Cl) and Sandy Clay loam (SaClLM). Saraiva-Okello *et al*. (2015) stated that the soil texture varies from clayey loam in the west to sandy loam in the middle area and moderately deep clayey soils. Sauka (2016), further indicated that the highveld grassland is on deep red to yellow sandy soils.

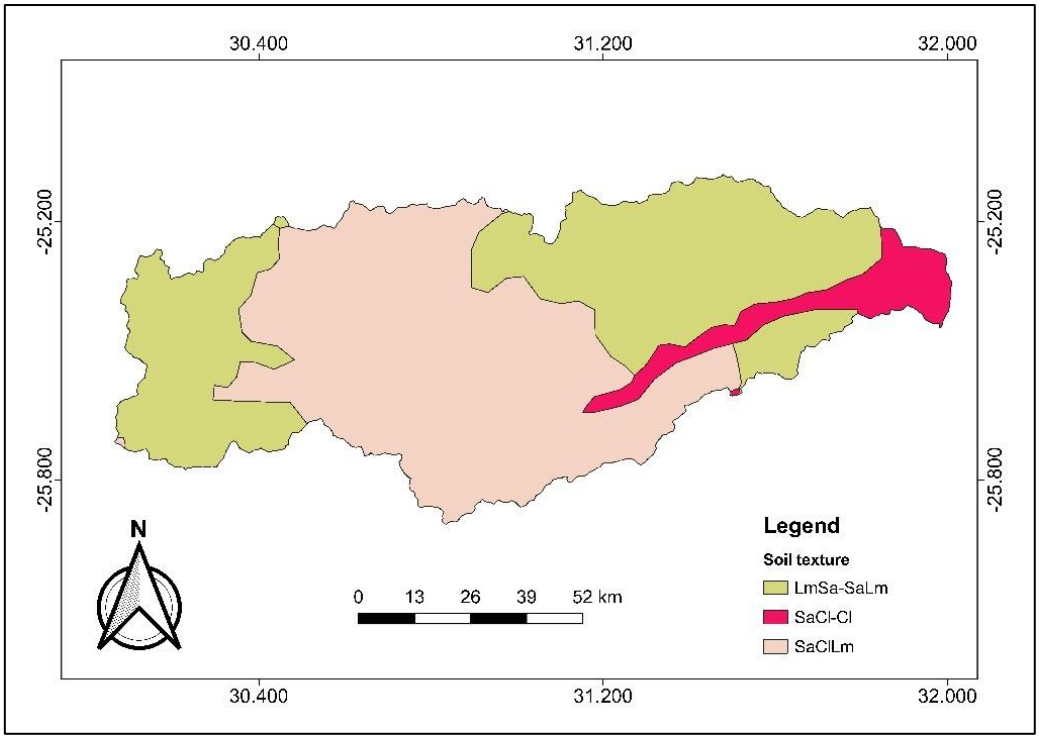

(Source: WR2012)

Figure 1.5: Catchment Soil texture.

1.7 Structure of the Dissertation

Chapter 1 provided the background of the study, the problem statement, research motivation, research questions, objectives of the study, and the structure of this study. This chapter also contains a detailed description of the characteristics of the study area.

Chapter 2 details the state of water resources and land management in the country. It provides the literature review of similar studies that have been done around the topic at both local and international scale. It further explores the application of GIS and RS on water resources, land management and hydrological modelling.

Chapter 3 presents the methodology of the study, the type of data requirements, types, and sources of the data. It also details the techniques and software used for data analysis. The steps followed in analysing the data are also presented in this chapter.

Chapter 4 shows the LULC results as classifiedhotspots and the NDVI results. It presents the changes in land-use between 1980 and 2020 and the accuracy assessment results for the classified LULC.

Chapter 5 provides the QSWAT results (hydrological response). The hydrological response results were also correlated with changes in LULC. This chapter further discusses the results and provides evidence from literature to support the study findings.

Chapter 6 presents the overall conclusion drawn from this study as well as recommendations based on the study findings. This chapter further summarises the research findings and study limitations.

CHAPTER 2: LITERATURE REVIEW

2.1 Preamble

This chapter presents an overview of similar studies that have been done on the subject; it presents both local and international coverage. It also presents what other studies have published with regards to the application of GIS, hydrological modelling and RS in land management and water resources, thereby, demonstrating the competency of these tools in water management and planning. It is also an overview of the interaction between LULC and catchment areas and to shed some light on that relationship, while taking into consideration the study area. This chapter also looked at how land management is linked with the hydrological cycle, thus, projects the essential aspects of the subject matter covered by this research.

2.2 Status overview of water resources in South Africa

Water is a natural resource that is both socially and economically valuable, and its quantity and quality affect the nature of its utilisation. Water is very special such that if it is properly managed, it becomes a renewable resource. Water has been highlighted by Mkheibir and Sparks (2003) as the main limiting source for development in southern Africa because of the direct impact it has on sectors such as agriculture. Baker and Miller (2013) stated that the lack of access to water resources in Africa may not be due to water scarcity alone, but also lack of investments in water infrastructure and management.

Muller *et al*. (2009) classified South Africa as water-scarce and estimated it to be the 29th driest country in the world with an estimated water availability of 1100 m^3/ person per year. Steven and van Koppen (2015) indicated climate as the major influencer of the distribution of water resources throughout the country; it varies from desert to semi-desert in the west and sub-humid in the eastern coastal area. South Africa's rainfall is strongly seasonal, and it spatially varies across the country with the eastern part receiving more rainfall than the western part. It receives an average rainfall of 450 mm which is below the world's average of 860 mm and almost 62% of this rainfall is used for agriculture, only 10% of the country receives more than 750 mm (Steven and Koppen, 2015; Worldwide Fund for Nature-South Africa (WWF-SA), 2016). Molobela and Sinha (2011) estimated that only 9% of the rainfall gets converted into runoff which is considered the lowest in the world.

Surface water resources in SA are highly developed with 350 major dams and many small dams (Steven and van Koppen, 2015). From the total of 12 871 km^3/year, approximately 9 500 km^3/year of the total is extracted from the surface water resources and the remaining is supplied by groundwater resources (Steven and van Koppen, 2015). Steven and van Koppen (2015) added that the occurrence of groundwater is influenced by the geological structure, soil conditions, rainfall patterns and anthropogenic activities. Out of the estimated groundwater use of 10 343 million m^3/year and 7 500 million m^3 in a drought year, South Africa is only using 2 000 million m^3 – 4 000 million m^3 (Masindi and Dunker, 2016). Much as there has been some efforts made to rectify unjust water supply to previously disadvantaged areas, WWF-SA (2016) indicated that, the country has challenges with supplying water to remote rural areas and the fast-growing informal settlements.

There is statistical evidence suggesting that South Africa has been getting hotter over the past four decades due to climate change, and there have been reported changes in rainfall patterns (Department of Environmental Affairs (DEA), 2017). The latter and temperature are inversely proportional, hence, the increase in temperatures has also resulted in high evaporation putting the country's reservoirs at risk (Mukheibir and Sparks, 2009; DEA, 2017). Water resource management promotes proper planning of water resources and sustainable water use while taking into consideration the hydrological cycle and water availability (Berjak, 2003). It ensures the sustainable rate of resource withdrawal or consumption without exceeding the rate of replenishment. Some of the country's catchments and management areas are water-stressed coupled with an uneven distribution of rainfall, population growth and urban or semi-urban development, thus, intensifying the already existing problem of water supply inadequacy. As stated by Jackson (2014), the CRC is considered as closing due to high demand, variability, and seasonality of water availability. A river catchment is considered 'closing' when "the supply of water falls short of commitments to fulfil demand in terms of water quality and quantity with the catchment and at the river mouth, for part or all of the year" (Jackson, 2014).

South Africa's water resources are governed by Water Service Act of 1997 and the National Water Act of 1998. Both these Acts work together to ensure that water is properly regulated; they provide equal right of access to basic water supply and sanitation while securing sufficient water for the ecosystem. The Integrated Water

Resource Management (IWRM) approach taken by the country ensures the holistic management of water resources as it is inclusive of the land, air and ecological resources, therefore it is in line with the mentioned Acts (Berjak, 2003). Muller *et al*. (2009) outlined pricing, limited terms of allocation, licensing and other administrative mechanisms, as other used methods to ensure that supply and requirements/demand are in balance. Masindi and Dunker (2016) pointed out that catchment management areas (CMA) are ways to ensure that water is used sustainably and efficiently at a catchment level.

CRC is managed by the Inkomati-Usuthu Catchment Management Area (IUCMA); the main responsibility of the CMA is to develop catchment management strategies, advise on the protection, development, use and conservation of water in the catchment. The Crocodile River is dominated by runoff water, which is sometimes supplemented from the Kwena Dam. CRC is also a tributary to one of the transboundary catchments in South Africa, the Inkomati River Catchment, and by law, according to Jackson (2014), it is obligated to fulfil the international transboundary agreement with regards to water allocation and management. Mbombela Municipality was identified as one of the municipalities that needed comprehensive strategy for reconciliation of water availability for future water requirements (DWA, 2014).

2.3 Land management in South Africa

Land in simple terms is defined as the solid surface on earth that is not completely covered by water and this is where most development takes place. Land consists mainly of soil, water, and biological resources, together with their diversity and their connection with the atmosphere and geology. The Food and Agriculture Organisation (FAO) (2017) further explained that the benefits derived from the interaction of the above-mentioned elements and the atmosphere plays a crucial role in livelihoods, as well as social and economic wellbeing. Dabrowski *et al*., (2013) defined land cover as the biophysical or vesical cover such as vegetation that can be detected by remote sensing. Land use is defined as the maintenance or modification of land by human arrangement or activities and unlike land cover, it cannot be mapped but rather be determined through socio-economic market force (Pretorius, 2009). It deals with modification of land surface and its biotic cover (Meyer and Turner II, 1992). The latter study continued that land-use changes add to global changes such as biodiversity loss, soil degradation and hydrological changes. The most recognised LULC classes

are cultivation land, forest, grassland, settlement, and waterbodies (Meyer and Turner, 1992; Lidzhengu, 2012; Aghsaei *et al.,* 2019; Tahiru *et al*., 2020).

Land management is a broad concept that is inclusive of the policies and regulations that govern the access and use of the land. South Africa covers approximately an area of 121.9 million ha, and it was reported that 4.47% of the country's natural land has been degraded, 80% turned to agriculture, 1.51% considered urban land use with only 1.41% forestry (National Department of Agriculture (NDA), 2005). Access to land is one of the most sensitive issues in this country, both socially and politically; Nel (2009) reported that South Africa's land use requires a holistic and integrated programme to achieve sustainable management of the land. Policies and laws currently active in guiding land use management include but not limited to the 1995 Development Facilitation Act 67, 2001 White Paper on Spatial Planning and Land use management, 1998 National Environmental Management (NEMA) Act 107 and legislations such as IDPs and zoning schemes (Ovens *et al*. 2007; Charlton, 2008).

2.4 Drivers of LULC changes

2.4.1 Population and Development

The LULC changes are the main effects of the increasing human pressures on natural resources directly affecting water resources (Boschet and Rambonilaza, 2015; Liu *et al*., 2017). Human activities (such as, agriculture, urbanisation, energy infrastructure development) are the primary sources of land use and land cover changes (Northeast Climate Science Centre (NECASC), 2021). Kaushal *et al*., (2017) and Liu *et al*. (2017) stated that LULC forms the link between human activities and ecological processes, and for a millennial, humans have affected over 75% of the earth's surface land and leaving a trail on water resources. NECASC (2021) adds that these activities are reported to directly modify land cover through loss of habitat, degradation, and fragmentation. Changes induced on LULC include the conversion and clearance of forest to another cover. According to Lidzhegu (2012), population growth has led to an increase in the conversion of forest and woodlands to agriculture. Rimba *et al*., (2019) reported that built-up areas have increased by almost 52% from 2000 to 2016 because of rapid conversion of agriculture to non-agricultural land uses, such as tourism infrastructure in places, like Bali. Other land management activities affecting LULC

changes as mentioned by Azanga *et al*., (2016) are inappropriate farming without conservation measures, inadequate land tenure and changing forest cultivation.

2.4.2 Climate change

Climate influences the distribution and type of land cover, according to Skyles (2009), it generally controls a broad-scale distribution of plants and vegetation species. In this view, climate change might influence current and future vegetation patterns due to its influence on temperature, rainfall, and climate patterns, therefore, affecting land cover (Ali, 2013; Gao *et al*., 2016). For example, increased salinity due to increased temperatures can reduce vegetation cover or agriculture. Climate also controls other factors such as soil communities (Pugnaire *et al*., 2019). Willis and Bhagwat (2009) associated the loss of the southern African Miombo savanna woodland to climate change; these changes intensify the global hydrological cycle thus increasing the frequency and variability of climate extremes (Saraiva Okello *et al*., 2015). Climate extremes refers to floods and droughts events; and they are said to have increased due to climate change. Changes in LULC can intensify the impacts from these extremes. LULC can modify the climate system by changing the atmospheric state and its functions through the modification of the biophysical characteristic of land surface, for example, albedo, roughness, soil-moisture among others (Sy and Quesada, 2020), therefore, as much as climate affects the distribution of LULC, changes in LULC also affect climate dynamics.

2.4.3 Land reform program

A land reform program is also one of the drivers of LULC changes. According to Lidzhengu (2012), land reform refers to the process of giving the land back to those who were denied ownership of the land at some point by a government in power. It was also indicated that the land reform process takes place at a time of independency from a dictatorial rule (Bullard, 2001; Lidzhengu, 2012). In South Africa, some of the objectives of land redistribution are to increase access to agricultural land by previously-disadvantaged black people, however, due to the abandonment of some agricultural lands in South Africa, LULC has been modified in some of the areas (Fourie *et al*., 2014). For example, the latter for study noted that some croplands have been converted to grasslands with lower species richness than natural grasslands. Chemura *et al*. (2020) indicated that in Zimbabwe, the population growth, coupled with the land reform program are expected to lead to more urban and agricultural

development in the upper Buzi basin. In another case, the increase in new farmlands under the land reform programme resulted in deforestation in Zimbabwe (Lidzhengu, 2012).

2.5 Land management and water resources

2.5.1 Hydrological cycle

The hydrological cycle presents the movement of water in the atmosphere, on the surface and, in the sub-surface. Water in the atmosphere moves in the form of gas i.e., vapor (evaporation/evapotranspiration) and liquid/solid (rain and snow) (see Figure 2.1). On the earth surface, water moves in the form of runoff/streamflow and on the sub-surface water moves in the form of infiltration, percolation, and aquifer recharge (Easton and Bock, 2015). Basically, the hydrological cycle is a complex system driven by solar radiation and gravitation (Brannstrom, 2019).

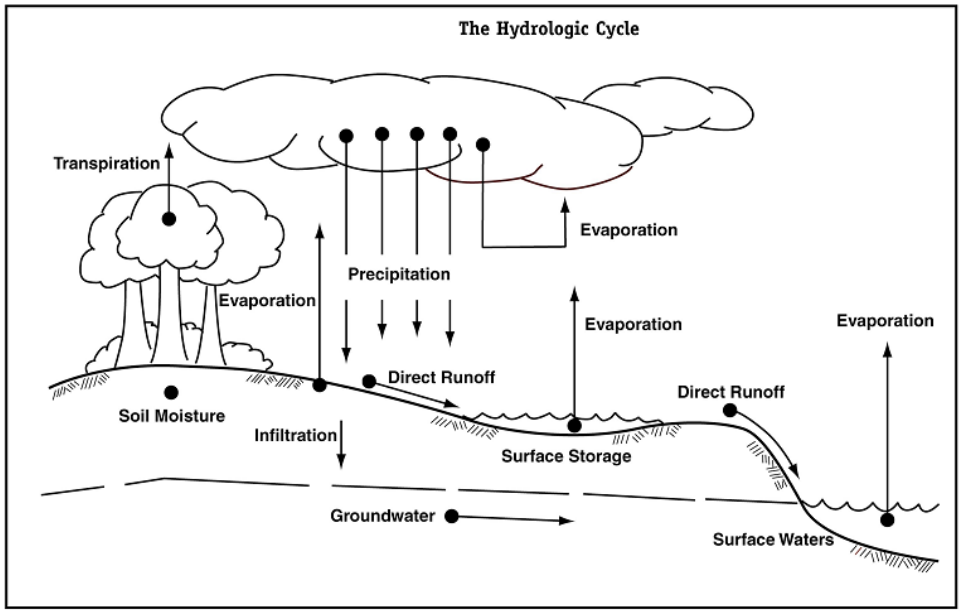

(Source: Ques10, 2020)

Figure 2.1: The hydrological Cycle.

The hydrological cycle, LULC and climate are interlinked (Brannstrom, 2019); for example, an increase in temperature will increase evaporation rates and it can modify vegetation, and changes in the vegetation can modify the components of the hydrological cycle and consequently, the climate. Uncertainties over water set into motion, uncertainties over biomass (Sheil, 2018), thus, it is vital to understand the components of the hydrological cycle and their interaction with the LULC. For this

study, only four processes of the hydrological cycle were focused upon - precipitation, evapotranspiration, surface runoff and infiltration - as these are relevant to the study.

2.5.1.1 Precipitation

Precipitation is condensed atmospheric water vapor that falls to the ground under the influence of gravity and can be in the form of hail, rain, snow, sleet, or fog (Shei, 2018). Precipitation is formed when water evaporates from the earth's surface and plants; when water falls back onto the earth's surface, some of it is intercepted by plants while some touch the ground - this is the water that is referred to as 'rainfall' (Easton and Bock, 2015). The availability of freshwater resources depends on precipitation and the intensity of the process is dependent on how the catchment areas have been modified.

2.5.1.2 Evapotranspiration

Evapotranspiration is a combination of evaporation and transpiration; water moves in a form of gas due to these two processes. Evaporation is the movement of water directly from the earth surface and waterbodies while transpiration refers to water from vegetation, such as trees and grass, (Chemura *et al*., 2020). Evaporation is greatly influenced by wind, solar radiation, heat and humidity, therefore, more water is likely to evaporates in very hot and windy conditions, while high humidity greatly decreases evaporation rate (Easton and Bock, 2015); usually, half of the solar energy that makes it to land is converted to evaporation, therefore, cooling the land surface (Sheil, 2018). Terrestrial precipitation has been reported to depend on the moisture from plants, however, LULC changes have reduced about 6% of the global moisture (Sterling *et al*., 2013). The reduction of global moisture could reduce precipitation, thus, affecting water resources' availability (Konapala *et al*., 2020).

2.5.1.3 Runoff

Runoff is described as the portion of precipitation that flows on the earth surface through channels and is associated with excess stormwater (Luo *et al*., 2020). Runoff is greatly influenced by the soil conditions, vegetation cover as well as the intensity and amount of rainfall; for example, it is higher in previously saturated soils, in compacted soils and during intense rainfalls (Easton and Bock, 2015). Runoff is an essential part of the water cycle, thus, its modification affects the hydrological dynamics of a catchment (Luo *et al*., 2020). Land-use/land-cover changes can modify the way in which water moves through the environment, either enhance it or decrease it, depending on the changes imposed on the catchment (New Jersey Stormwater, 2016).

2.5.1.4 Infiltration

Some of the precipitation that reaches the ground moves downwards to the ground in a form of infiltration. The amount of water that can infiltrate the ground greatly depends on the soil properties, such as the moisture content, texture, bulk density, permeability, and porosity. Infiltration is much higher in porous soils and water retained in soil pores is referred to as 'soil storage'; this water is mostly used by plants during transpiration. The water that manages to infiltrate the ground, past the root zone and make it to the water table, however, plays an important role in recharging groundwater resources (New Jersey Stormwater, 2016), therefore, LULC changes may have major impacts on this component. The increase in deep-rooted vegetation, such as forests can, for example, increase the amount of water that transpires before reaching the water table (Gee *et al*., 1992), while activities that compact the soil may reduce infiltration, thereby decreasing groundwater recharge (Owuor *et al*., 2016).

2.5.2 Land management impacts on water resources studies

Land use management is one of the major drivers of catchment change as they affect ecology, sociology, geomorphology, hydrological processes, and soil properties on a local, regional, and global scale (Albhaisi *et al*., 2013; Singo, 2014; Namugizea *et al*., 2018). LULC directly interacts with water resources through vegetation interception, evapotranspiration, surface runoff, infiltration, and soil moisture status, hence, it can modify the processes taking place in the catchment's hydrology and water resource cycle (Liu *et al*., 2017); for example, Easton and Bock, (2015) mentioned that the presence of vegetation promotes infiltration by increasing permeability.

Dabrowski *et al*., (2013) reported that due to a small dam construction, a decrease in flow volumes was observed at Mngeni River. From a study by Zhou *et al*., (2013), it was reported that urbanisation led to 11.3% increase in surface runoff and baseflow decreased by 11.2%. Baker and Miller (2013) reported a similar case with reduced groundwater recharge due to the conversion of dense natural forests to agricultural land in the Kenya's rift valley. Changing forests to cattle grazing area has been linked with soil compaction and increased soil water storage, thus diminishing soil infiltration, and enhancing quick lateral flows and stream flow response to precipitation in the Amazon lowlands (Chaves *et al*., 2008). Another study revealed that an increase of shallow-rooted items, such as agricultural crops in previously dominated deep-rooted catchments increased groundwater recharge in southern high plains in US (Scanlon

et al., 2007). A decrease of 6.6 million m^3 in annual pre-development runoff (48.5%) was observed due to agricultural abstraction at Duiwe River in southern Cape, South Africa (Petersen *et al*., 2017). Van der Laan *et al*. (2012) recorded similar findings in the CRC and its tributaries due to irrigation abstraction and afforestation. Some mentioned impacts include an increase in urban heat islands and their roles in rising river temperatures, thus, affecting water quality and quantity (Kaushal *et al*., 2017).

LULC changes coupled with hydrological turbulences are some of the common explanations for land degradation (Zacharias *et al*., 2009; Kumar *et al*., 2017; Wagner *et al*., 2013). Before 2000, human activities were reported to have extensively altered the Heihe River Basin resulting in the deterioration of the ecosystem (Jin *et al*., 2019). Large-scale deforestation due to rapid development of irrigation farming was observed in the Crocodile River rising from the Witwatersrand, Johannesburg (Hobbs *et al*., 1985). Dabrowski *et al*. (2013) reported that Umngeni Catchment in KwaZulu-Natal has been converted to 19% cultivated land and 17% forestry, while 8% of the catchment has been transformed to urban area. Water resources (catchments, rivers, aquifers, and wetlands) are the building blocks of water supply, if these sources are overexploited, downstream investments and ecological infrastructure tend to collapse. Water sources generate about 50% of river flows, therefore it is important to ensure their maintenance and protection (WWF, 2016). In South Africa, from the total Mean Annual Runoff (MAR) of 49 040 m^3/a, 6% is lost through land use (Muller *et al*., 2009).

Some changes in land cover have positive impacts, as a study done in Lake Malawi depicted what could be a positive impact of LULC change on water resources. Calder *et al*. (1995) reported an increase in streamflow and surface runoff, consequently raising the water level in lake Malawi due to conversion of forest cover to agricultural land. The latter study showed that, in turn, the lake sustained activities such as hydropower, water transport and livelihoods, during the 1992 drought. There is, hence, a need to optimise the use of land in South Africa to ensure livelihood support and improve environmental conditions.

2.6 Remote sensing

Remote Sensing (RS) has been one of the most used tools since the 1970s. It is defined as an art of retrieving information about an area without coming into physical contact with it (Masud and Bastiaanssen, 2017). It uses electromagnetic spectrum to

show images of land, ocean, and atmosphere by measuring their electromagnetic radiation (EMR) (Campbell and Wynne, 2011). RS first came into existence in 1800 when Sir William Herschel discovered infrared, then in 1850–1860 photographs could be taken using balloons. In 1909, Wilbur Wright used an aeroplane to take photographs of the Italian landscape; these were considered the first aerial photographs (Campbell and Wynne, 2011). In 1999, the National Aeronautics and Space Administration (NASA) launched Terra-1, a satellite that can monitor changes in nature and the earth's ecosystem at a global scale. The spatial, spectral, radiometric, and temporal data produced was said to make RS techniques preferable over traditional methods (Thankur *et al*., 2017). Recently, it has been indicated that satellite (and sensors) for earth observations have been used to monitor environmental changes at regional and global scales, through large dataset provided by remotely-sensed images and indices (Mancino *et al*., 2020).

2.6.1 **Common remote sensors for land covers**

2.6.1.1 Landsat

The first Landsat satellite was launched under the name Earth Resources Technology Satellites (ERTS-1) in 1972. The name was changed to Landsat-1; this is a multispectral earth-orbiting satellite designed to observe the earth surface (Skidmore *et al.*, 1997; Campbell and Wynne, 2011); before 1982, the spatial resolution was at 79 m. More multi spectral scanner (MSS) Landsat satellites (Landsat-2 to Landsat-5) were launched in the 1970s and 1980s, followed by the Landsat-7 in 1999 with an Enhanced Thematic Mapper Plus (ETM+) sensor that provides an image with 30-m resolution (USGS, 2016). Data was collected in 6 spectral bands with different wavelength, and it was reported to be more comparable with Landsat 4-5 Thematic Mapper (TM) due to the similarities in bandwidth (Mancino *et al*., 2020). Landsat-8 was launched in 2013 containing two new sensors - the operational Land Imager (OLI) and the Thermal Infrared Sensor (TIRS) - to make it operate with TM and ETM+. Landsat-8 contains new enhanced bands and collect images in more push-broom scanner mode, unlike the previous sensors which used a whiskbroom scanner-based sensor (Mancino *et al*., 2020). It can also highlight an earth surface variability while reducing saturation of high reflective surfaces. Landsat 9 was expected to be launched in 2021; Landsat 7 data was made free to the public in October 2008 and in 2009, all Landsat data was free to download.

2.6.1.2 Sentinel-2

The Sentinel-2 multispectral instrument (MSI) contains 13 spectral bands ranging from Visible and Near-Infrared (VNIR) to Shortwave Infrared (SWIR) wavelengths (USGS, 2021). The Sentinel-2A satellite was launched in 2015 and the second Sentinal-2B was launched in 2017, with no historical data. According to the Satellite Imaging Corporation (2021), Sentinel-2A supports generic land cover, land use and change detection maps and it has a spatial resolution of 10 m to 60 m. Sentinel-2A has been applied in the LULC classification by several researchers Cavur *et al*., (2019); Baamonde *et al*., (2019) and Isbaex and Coelho, 2021).

2.6.1.3 ASTER

The Advance Spaceborne Thermal Emission and Reflection Radiometer (ASTER) was recently developed to provide accurate satellite images with high spatial and spectral resolution (Yuksel *et al*., 2008); it was launched in December 1999. In addition, the sensor operates in 3 different spectral regions, - VNIR, SWIR and thermal infrared (TIR); it has a 15 m spatial resolution, and can retrieve vegetation information (Yuksel *et al*., 2008). ASTER has been regularly applied in the classification of LULC (Franklin *et al*., 2009; Wilson, 2005; Aynekulu *et al*., 2008).

2.6.2 Land use hotspots

In simple dictionary explanation, a ‘hotspot’ refers to a place of significant activities (Oxford Dictionary, 2020) and in this context, it describes the intensity and pattern changes of land use (Kuemmerle *et al*., 2016). In other words, it can be concluded that hotspots are areas of high concentration of LULC activities. It is crucial to demarcate such areas when developing relevant mitigating and management strategies and policies (Kuemmerle *et al*., 2016). According to Guay *et al*., (2014), LULC hotspots can be determined from analysing significant trends in the greenness and brownness of vegetation. The intensity of the impact of land-cover changes on hydrological processes or response, depends on the vegetation type (Singo, 2014).

2.6.3 Vegetation indices (VI)

Vegetation index is the spectral measurement parameter in remote sensing used to indicate the amount of earth surface vegetation covers and growth status (Gandi *et al*., 2015). Most VIs are developed according to different spectral bands and different satellite sensors (Yeom *et al*., 2019). Some of these satellites’ sensors are Sentinel-

2, MODIS, Landsat 4-5 TM, Landsat 7 ETM+ and Landsat 8 OLI/TIR, AVHRR/GIMMS and SPOT/PROBA-V (Sheffield *et al*., 2018). Vegetation cover plays an important role in the hydrological cycle and partitioning of surface energy through albedo, while RS plays an important role in differentiating between managed and unmanaged vegetation (Sheffield *et al*., 2018). Using characteristic reflectance pattern of green vegetation, VIs can delineate the disruption of vegetation and soils. Different plants have different emissivity rates and different reflectance of light. According to Xue and Sue (2017), the application of remote sensing on vegetation is done through the ultraviolet region (UV) spectra, the visible spectra (red, green, and blue wavelength regions) and the near and mid-infrared bands, however, UV spectra are not commonly used. Most VIs are based on the Visible Red and near-infrared spectral range (Yue *et al*., 2007). As much as VIs are sensitive to the greenness and amount of leaf material, known as the green leaf area index (LAI), canopy chlorophyll density (CCD) and biomass, they are also sensitive to other factors such as the spectral quality of the soil, atmospheric composition, and view illumination geometry among other things (Broge *et al*., 2003). VIs, therefore, come in different forms and can be used for different functions, and have different limitations. Presented below are the potential VIs considered for this study.

2.6.3.1 Difference vegetation Index (DVI)

It is considered the simplest vegetation index (Equation 1). Susantoro *et al*. (2018), explained that the index was designed to optimise vegetation in the regions of LAI and more sensitive to the amount of vegetation and changes in the underlying soil (Xue and Su, 2017). It can differentiate between soil and vegetation, but it does not depict the difference between reflectance and radiance caused by the atmosphere or shadows. It is also shown to be sensitive to photosynthetically active vegetation (Tucker, 1979) It is used to monitor vegetation ecological environment, hence, it is sometimes called, Environmental Vegetation Index (Xue and Su, 2017). Studies that have used this index includes Tucker (1979).

$$\mathrm{DVI} = \mathrm{NIR} - \mathrm{RED} \quad (1)$$

where, NIR is near-infrared and RED is red band reflectance.

2.6.3.2 Normalised Difference Vegetation Index (NDVI)

It is considered a good index and widely used; it calculates the ratio difference between reflectance of the measured canopy in the visible red and NIR (Equation 2) (Ghanghi *et al*., 2015). NDVI was developed in the 1970s, and is used to quantify vegetation greenness and assess changes in vegetation density and health because it correlates with the photosynthetic activities of vegetation (Xue and Sue, 2017). According to Lo *et al*. (1997), NDVI serves as a good indicator of surface radiant temperatures. The index values vary between -1.0 and 1.0; the lowest values (0.1 and below) present barren areas of rock, sand or snow, moderate values (0.2 to 0.3) present shrubs and grassland and (0.6 to 0.8) values indicate rainforests. The index is sensitive towards soil colour, soil brightness, atmospheric effects, cloud cover, cloud shadow and leaf canopy shadow (Xue and Su, 2017); many researchers prefer it due to its simplicity (Livelethu, 2013; Wagner *et al*., 2013; Kumar *et al*., 2017).

$$NDVI = \frac{NIR-RED}{NIR+RED} \quad (2)$$

where, NIR is near-infrared and RED is red band reflectance.

2.6.3.3 Ratio-based Vegetation Indices (RVI)

The ratio-based index was developed in 1969, and is sometimes referred to as, Simple Ratio (SR) (Equation 3). It is one of the first proposed indices and is based on the principle that leaves absorb more red than infrared light. The index is used mostly to estimate and monitor green biomass and on the usefulness of the index in estimating biomass (Colwell, 1973), however, when vegetation cover is below 50% (sparse), it tends to give poor representation of the biomass (Xue and Sue, 2017). In addition, bushy plants were reported to have low reflectance on the red band (Quan *et al*., 2011); it has been used, extensively, to assess crop growth and development during the past decade (Broge *et al*. (2003). This latter study indicated that while the vegetation index has been noted to depend on the position of the sun and the structure of the canopy, however, some studies have questioned its ability to estimate both LAI and CCD in the absence of atmospheric noise, as the index is sensitive to atmospheric effects (Broge *et al*., 2003). The highest value represents vegetation, while its lowest is for soil, ice and water. Studies that have successfully applied this model include, Tucker 1979); Broge and Mortensen (2002); Broge *et al*., (2003) and Din *et al*., (2017). The process is represented as:

$$RVI = \frac{NIR}{RED} \quad (3)$$

where, NIR is near-infrared and RED is red band reflectance. Table 2.1 summarises the advantages and disadvantages of the selected VIs reviewed in this study.

Table 2.1: Advantages and disadvantages of the selected VIs.

Vegetation Index	Advantages	Disadvantages	References
DVI	• Can differentiate between the soil and vegetation	• Cannot depicts the radiance from the shadow and atmospheric effects	Richardson and Weigand, 1977
NDVI	• Can explain the density of vegetation • Sensitive towards soil and Clouds • Simplicity • It can offer information on vegetation species	• Saturate high levels of LAI	Rouse Jr. et al., 1974
RVI	• Can reduce atmospheric effects and topography • Simplicity	• Low for soil, ice, water	Jordan, 1969

2.6.4 Application of remote sensing in land management and water resources

The spectral radiation being emitted at all wavelengths can be interpreted to give out quantitative information on hydrological processes, making RS an ideal technique to use in areas with lack of data (Skidmore *et al.*, 1997; Thankur *et al*., 2017). Monitoring of large atmospheric-oceanic anomalies, deforestation, climate and weather prediction, vegetation and soil mapping, natural disaster and LULC maps are some of the capabilities of RS (Skidmore *et al.,* 1997; Marwa *et al*., 2011). Landsat Thematic Mapper (TM) images of 1987 and 1999 were used to analyse LULC changes in the city of Addis Ababa and surrounding areas (Tadasse *et al.*, 2001); results showed the loss of forests from urban and residential sprawls. High resolution satellite data

enables interpretation of finer scale variations in energy balance of human-dominated watersheds and changes in regional water balance; for example, RS was used to evaluate the relationship between land surface temperatures due to urban growth and NDVI in the city of Shanghai (Yue *et al*., 2007). NDVI was also applied in the identification of hotspots in LULC changes in India; the study used data from 1982-2015 to map hotspots with significant positive and negative changes (Duraisamy *et al*., 2018).

In water resources, satellite sensor can directly and indirectly measure most of the components of the hydrological cycle such as evaporation, precipitation, soil moisture and total water storage (Sheffield *et al*., 2018). RS is suggested for exploring, evaluating, analysing, monitoring, and managing groundwater because of its efficiency (Thankur *et al*., 2017). It can easily uncover unknown information about water resources, LULC changes and climate changes and the consequences of those changes on the hydrologic cycle (Kaushal *et al*., 2017). RS techniques can monitor water colour and temperature, thereby providing information about the presence of nutrients in the water; for example, it was used to assess water quality at Dikgathong Dam in Botswana (Mosimanegape, 2016). It can also be used to analyse water quality and the situation of a dam, considering aspects, such as land cover dynamics and evolution at catchment scale (Giardino *et al.*, 2010). Different plants reflect light at different spectra, thus, RS can be applied in the analysis and measure of vegetation cover (Xue and Su, 2017).

2.7 GIS

GIS is a computer application that can store, manipulate and analyse spatial data (Tsihrintzis *et al.,* 1996). It is formally defined as “a system of hardware, software and procedures to facilitate the management, manipulation, analysis, modelling, representation and display of georeferenced data to solve complex problems regarding planning and management of resources” (Escobar *et al*., 2008). GIS was historically developed to capture and store map contents and produce statistics on the size of the area mapped and specific themes, although it has limited functionalities (Goodchild, 2011). Currently, it has so many applications, such as, land use planning, market analysis, ecosystems modelling, tax assessments, utilities management and visual impact analysis (Escobar *et al*., 2008). The major GIS functions include data entry, data display, data management, information retrieval and analysis. Data can

either be in a vector format (points, polygons, or lines) or raster format (in the form of grid or pixels). Data sources for this tool can be field surveys or remote sensing, digitised and scanned data, GPS field sampling co-ordinates (X, Y), GIS brings together this remotely sensed data into one frame. Currently, there are many GIS software products with advance functions, all capable of doing any operation on any type of recognised type of geographic information, particularly, Esri ArcGIS, QGIS and Grass GIS.

2.7.1 QGIS

Quantum GIS (QGIS) is the most well-known and mostly used open-source GIS programming framework (Khan and Mohiuddin, 2018). It is made of 4 components - QGIS Desktop, QGIS Browser/Mobile, QGIS Web Client and QGIS Server. GIS supports vector, tabular and Raster data. LULC classification is done via a plug-in called 'Semi-Classification automatic plug-in' (SCP).

2.7.2 ArcGIS

ArcGIS is a software produced by the Environmental Systems Research Institute (ESRI). It is accessible as ArcGIS online, ArcGIS for Desktop, either to create maps, or "it can further perform spatial investigation on vector and raster information, alter and geocode information" (Khan and Mohiuddin, 2018). The disadvantage of the software includes the cost of the licenses (Sipe and Dale, 2003). Land use classification is done through the ArcGIS Spatial Analyst extension through the Image Classification toolbar (Ismail *et al*., 2020). A study was conducted to investigate Land use/ Land cover analysis using QGIS and ArcGIS and results showed that ArcGIS has an overall high accuracy compared to QGIS, however the study further indicated that QGIS showed a better producer's accuracy when it comes to classifying water and built-up areas (Ismail *et al*., 2020).

2.7.3 GIS application in water resources

GIS is a powerful tool that has been applied locally, regionally, nationally, and globally to address a wide range of water-resources problems, namely, water quality, groundwater movement and contamination, river restoration and flood prediction (Khathami and Khazaei, 2014). GIS can be used to overlay different maps to better analyse land use changes and to plan resources optimally (Trung *et al*., 2006). Not

only can it overlay maps, but this tool can also be used in integration with other tools such as RS and hydrological models, making it a flexible tool.

Tsihrintzis *et al.* (1996) used GIS tools to predict and monitor non-point sources of water pollution and flow of pollutants in storm sewer networks. It was also applied in groundwater quality studies in Khartoum State of Sudan (Shakak, 2015). Studies such as those of He(2003); Sing *et al*., (2014) and Singo (2014) have applied GIS in conjunction with different tools in water resources assessment studies; For example, it was used in conjunction with Agricultural Nonpoint Source Pollution (AGNSP) model to analyse the effects of land use changes on non-point pollution at a watershed (He, 2003). It was also applied with groundwater flow model (Ashraf and Ahmad, 2012). It has also been used in combination with RS to investigate the sensitivity of hydrogeological factors to infiltration patterns and to further map potential zones of semi-arid watershed in Karnataka (Sing *et al.*, 2014). Furthermore, it was used to evaluate the impacts of land cover changes on hydrology and water resources in Luvuvhu River Catchment (Singo, 2014).

2.8 Hydrological modelling in water resource management

Hydrological models can be used in integration with RS and GIS or as a stand-alone. Thankur *et al*. (2017) maintains that RS provides the most reliable spatially-distributed data for calibration and model inputs. Hydrological models can enhance the understanding of the environment system behaviour and give solutions to long-term water resources management problems (Cuceloglu and Ozturk, 2019). In addition, it enables the user to manipulate a system's variables and parameters to promote an understanding of the interaction between variables that make up a complex system (Mengistu *et al*., 2019).

Hydrological models are divided into three categories: Statistical models, Conceptual hydrological models and distributed hydrological models (Liu *et al*., 2017). Statistical models are based on the relationship between runoff, rainfall and air temperature but cannot project future resources, while conceptual models are based on hydrological scenarios, but the challenge is that a river basin is assumed to be an integral component. These group of models do not account for spatial heterogeneity resulting from the difference in topography and vegetation. Distributed models are described as those that need spatial and temporal data to simulate the hydrologic behaviour of a

watershed (Cuceloglu and Ozturk, 2019). With distributed models, input variable can be obtained easily; they are large scale basin models with high computational efficiency (Liu *et al*., 2017). Physical-based models play a significant role in predicting the effects of LULC changes on the hydrology of a river system (Jin *et al*. 2019). A hydrological model should be able to accurately depict the interaction between hydrological processes, sensitivity to land use and give a satisfactory representation of climate change (Warburton *et al*., 2010). Some commonly-used hydrological models outlined by Rowe (2015); Warbuton *et al*. (2010); Yamagata *et al*., (2012; Graham and Butts (2005) and Herpertz, (1994) are discussed below.

2.8.1 Soil and Water Assessment Tool (SWAT)

Soil and Water Assessment tool (SWAT) is classified as a semi-distributed model (Liu *et al*., 2017; Cuceloglu and Ozturk, 2019 and Gabiri *et al*., 2019) and a continuous-time model (Mengistu *et al*., 2019). Physically-based semi-distributed hydrological models can give a detailed presentation of the hydrologic process' fundamentals (Gabiri *et al*., 2019); it uses a daily time-step and can produce long-term simulations (Ang and Oerng, 2018). The model subdivides the watershed into multiple sub-watersheds which are further subdivided into hydrologic response units (HRUs) (Dechmi *et al*., 2012). Each unit is made of a specific soil/land-use characteristic and the water balance for each unit is presented by four storage volumes - snow, soil profile, shallow aquifer, and deep aquifer (Dechmi *et al*., 2012). The soil profile is also subdivided into multiple layers that take into consideration soil water processes such as infiltration, evaporation, plant uptake, lateral flow, and percolation. Due to this ability, the model can be applied in even big catchment sizes, such as the Yellow River in China with a catchment size of 121 972 km^2 (Wu *et al*., 2019). Calibration and validation of the model can either be done manually or can be done automatically using SWAT-CUP. Thavhana (2018) explains that auto-calibration can minimise labour, frustration and the uncertainties that come with manual calibration, however, a study by Mengistu *et al.,* (2019) found that manual calibration improved a simulated annual runoff volume by 23% and annual evapotranspiration by16%. SWAT can also be linked with other models such as MODFLOW and MODSIM (Brannstrom, 2019). The model is driven by the water balance, and it assumes that all processes in the catchment are driven by the water balance (Equation 4) (Thavhani, 2018). The equation is as follows (Ang and Oeurng, 2018):

$$SW_t = SW_0 + \sum_{i=1}^{t}(R_{day} - Q_{surf} - E_a - w_{seep} - Q_{gw} \quad (4)$$

where, SW_t is the final soil water content (mm H2O), SW_0 is the initial water content on day i (mm H2O), R_{day} is the amount of rainfall on day i (mm H2O), Q_{surf} is the surface runoff on day i (mm H2O), w_{seep} is the amount of water entering the vadose zone from soil profile on day i (mm H2O) and Q_{gw} is the amount groundwater flow on day i (mm H2O). SWAT is one of the widely-used model to assess or analyse the impact of land management and climate on hydrology and water resources (Sead 2009; Liu *et al*., 2017); it also allows the simulation of conservation and land-use management. SWAT was used to analyse the response between hydrological cycle and land use (Utamahadi, 2018). Some studies have successfully applied it in simulating streamflow due to LULC changes ((Zhou *et al*., 2013; Baker and Miller, 2013; Shafiei *et al*., 2018). In addition, it was used to determine sediments and nutrients hotspots in Lake Tanganyika (Azanga *et al*., 2016).

2.8.2 MIKE-SHE

MIKE-SHE is a physically-based and integrated model that simulates surface and groundwater flow (Singo, 2014); it is also classified as a deterministic and fully-distributed model. The model uses extensive physical parameters, and it accounts for the variability in the hydrological cycle processes such as precipitation, runoff, evapotranspiration (Devi *et al*., 2015). Not only does it simulate surface and groundwater movement, but it also simulates the interconnection, sediments and nutrients and various water quality problems, and it can be applied to large catchments (Devi *et al*. (2015). It can capture processes at various temporal and spatial scales, and can be applied with any catchment size including those with complex hydrogeology (Refsgaard and Abbott, 1996; Ma *et al*., 2016; Thavhana, 2018). Mike-SHE divides the catchment into a large number of discrete grids in three dimensions' order to account and reflect the spatial variation of catchment properties (Ma *et al*., 2016). These grids are divided according to land-use, soil type and precipitation and rely on finite difference equations to solve equations at each cell (Golmohammadi *et al*., 2014 and Brannstrom, 2019).

Mike-SHE is data intensive and requires data involving factors affecting hydrological data, which can be obtained through field investigations (Feyen *et al*., 2000; Ma *et al*., 2016). According to Golmohammadi *et al*., (2014), it is rare to find a watershed with

all the measured input data required for the model, therefore, conducting such field investigations can be costly (Feyen *et al*., 2000). It was also indicated that the model for integrated catchment modelling requires an experience in modelling and skills in disciplines, such as hydrology because of the complexity of the task (Ma *et al*., 2016). Due to the numerous parameters and complex structure, the process often leads to over-paramaterisation. Mike-SHE is not freely available online as its usage requires a licence, making it not easily accessible. Mike-SHE has been successfully applied in a simulation of streamflow, overland flow and groundwater flow under the influence of climate and LULC (Zhang *et al*., 2008, Zhang *et al*., 2019, Tian *et al*., 2016, McMichael *et al*., 2007, Golmohammadi *et al*., 2014).

2.8.3 HEC-HMS

Hydrologic Engineering Center-Hydrologic Modelling System (HEC-HMS) was developed by the United State (US) Army Corps of Engineering; it simulates runoff from rainfall over a dendritic watershed and used to analyse urban flooding, flood frequency and flood warning (Halwatura and Najim, 2013). It is an open-source, physically based, rainfall-runoff model. The model can also analyse hydrological events, such as event infiltration, unit hydrographs and hydrological routing; the simulated results can be stored in HEC-DSS (data storage systems) (Hameed, 2018). Furthermore, it has components that can process rainfall loss, direct runoffs, and routing (Hamdan *et al*., 2021). The latter can be used in integration with other software that deal with water availability, urban drainage, flow forecasting and reservoir. The model is much favoured for its simplicity and use of common methods, and can also be used with ArcGIS through the Geospatial Hydrological modelling extension (Hec-GeoHMS) (Tassew *et al*., 2019). Data preparation for the model includes the preparation of curve numbers for the related LULC. Studies have successfully applied HEC-HMS in the simulation of rainfall-runoff processes and flooding (Oleyiblo *et al*., 2010; Saeedrashed *et al*. 2021; Hamdan *et al*., 2021; Tassew *et al*., 2019).

2.8.4 Agricultural Catchments Research Unit (ACRU)

ACRU is a physical-conceptual, daily time-step, multi-level, multi-purpose model that was developed around the 1970s (Warburton *et al*., 2010). The model's sensitivity to hydrological processes, land use and climate change drivers makes it one of the most recommended models to use in such studies (Schulze, 2010; Choi and Deal, 2008 and Chang, 2003). ACRU is an agrohydrological model that can simulate a wide range

of climatic settings and land use using complex methods of configuration. It was originally designed for the application of design hydrology, crop yield modelling and reservoir yield simulations. In places where there is lack of data, the model uses national data set and previous experience-based default parameters. In addition, the model can simulate the main processes of the hydrological cycle that are linked to the soil-water budget, such as streamflow volume, peak discharge, and hydrograph (Smithers *et al*., 1997). It can divide the catchment into sub-catchment of less than 30 km^2 in catchments where physical characteristics and processes are more complex, thus it can also be referred to as a 'distributed model' (Smithers *et al*., 1997). The model does not require calibration because it not a parameter-fitting model; optimised parameters are derived from the physically-based characteristics of the catchment (Schulze and Smithers, 2004). One of the major limitations of the model is that it is not user-friendly, hence, it requires an expert to run it (Thavhana, 2018). The model has been successfully applied a lot in flood estimation studies and climate change, due to its sensitivity to climate, LULC and soil (Smither *et al*., 1997; Smithers *et al*., 2013; Aduah *et al*., 2017, Kusangaya *et al*., 2017). Table 2.2 summarises the advantages and disadvantages of the above-mentioned models.

Table 2.2: advantages and disadvantages of SWAT, MIKE-SHE, HEC-HMS and ACRU.

Model	Advantages	Disadvantages
SWAT	• It can simulate missing weather information • It provides auto-calibration option • It can be used in QGIS interfaces • It accounts for soil, land-use and climate change • Open source	• It assumes the catchment dimensions remains static
MIKE-SHE	• It is applicable in any catchment size • It can produce a water budget for the hydrological cycle	• High computational demand • Large input data • Needs a licence • Overparamaterisation
HEC-HMS	• Simplicity • Use of common methods • Open source	• HEC-GeoHMS requires the Spatial Analyst Extension from ArcGIS • It can only be applied in Dendritic catchments • Requires terrain pre-processing

ACRU	• It accounts for climate, land use and soil changes • It does not require calibration and validation • Open source	• Least user friendly

2.9 Model performance

Model performance is measured by comparing calculated values with observed data. It ensures and validates the simulated results, thus, showing the importance of evaluating model performance. It was reported that for the model to successfully simulate environmental variables and reduce uncertainty, an objective model calibration and verification is required (Ritter and Munoz-Carpenza, 2013); it is also recommended to combine the absolute value error statistics and a normalised goodness-of-fit instead of using a single indicator.

2.9.1 The Nash-sutcliffe coefficient (NSE)

NSE is a normalised statistic, it compares the variance of a simulated data with the observed data variance (Equation 5) and it is dimensionless. It shows how well a plot of observed versus simulated value fits the 1:1 line. NSE values range from -1 to 1, where the value of 1 means a perfect model performance, observed streamflow corresponds with simulated streamflow (Sead, 2009; Ridwansya, 2010; Zang and Mao, 2019; Cuceloglu and Ozturk, 2019). NSE is sensitive to flow peaks and timing of flows, therefore it is not recommended when it comes to evaluating a model's fit to low flows because it could lead to errors in the high flow. In cases where low flow performance is important, the NSE log (equation 6) is the preferred option because it decreases the sensitivity of the metric high flows and increases sensitivity towards low-mid range flow (Parra *et al.*, 2019). Both NSE and NSE log values range between -1 to 1. The recommended values for good model performance are between 0.65 and 0.75, for a very good model performance, they should be above 0.75 (Morán-Tejeda *et al*., 2015). NSE values that are equal to or less than 0 indicate that the prediction is not acceptable (Zhu and Li, 2014). NSE is calculated as follows:

$$NSE = 1 - \left[\frac{\sum_{i=1}^{n}(S_i - O_i)^2}{\sum_{i=1}^{n}(O_i - \bar{O})^2}\right] \quad (5)$$

where, O_i is the observed data, $\bar{O}$ is the mean of the observed data, S_i is the simulated data and n is the number of observations

$$NSE_{log} = 1 - \left[\frac{\sum_{i=1}^{n}(ln(S_i + \varepsilon) - ln(O_i + \varepsilon))^2}{\sum_{i=1}^{n}(\ ln(O_i + \varepsilon) - ln(\bar{O} + \varepsilon))^2}\right] \quad (6)$$

where, ε is a small value to avoid problems caused bu observed and simulated streamflows equalling zero; it must be chosen as small fraction of the mean interannual discharge (Parra *et al*., 2019).

2.9.2 RMSE-observation standard deviation ratio (RSR)

RSR is the ratio of the RMSE to the standard deviation of the simulated data (Equation 7). It incorporates the benefits of error index statistics and scaling/normalisation factor (Moriasi *et al.*, 2007); it further standardises the root mean square error using the standard deviation of the observation (Ang and Oeurng, 2018). The ideal values range between 0 and +1; lower values indicate good model performance while zero indicates a perfect model simulation (Gyamfi *et al*., 2015; Ang and Oeurng, 2018), however, RSR larger positive RSR values, indicate a poor model performance. RSR is given by:

$$RSR = \frac{RMSE}{STDEV_{obs}} = \frac{\sqrt{\sum_{i=1}^{n}(O_i - S_i)^2}}{\sqrt{\sum_{i=1}^{n}(O_i - \bar{O})^2}} \quad (7)$$

where, O_i is the observed data, $\bar{O}$ is the mean observation, S_i is the simulated data, n is the number of observations.

2.9.3 Percent bias (PBIAS)

PBIAS is known as an error index and it measures the average tendency of the simulated data to be bigger or smaller than the observed data (Equation 8) (Ang and Oeurng, 2018). The optimal value is 0, and it depicts the exact simulation of the observed values. If the values are negative, it means that the model is overestimating while positive values is for an underestimation (Dechmi *et al*. 2012; Jin *et al*. 2019), although, a lower value of PBIAS generally shows accurate model simulation. The values are computed as follows:

$$PBIAS = \frac{\sum_{i=1}^{n}(O_i - S_i) \times 100}{\sum_{i=1}^{n} O_i} \quad (8)$$

where, O_i is Observed variable, S_i is Simulated variable, $\bar{O}$ is Mean observed variable and n = Number of observations under consideration.

2.9.4 Mean Absolute Error (MAE)

This is another widely and longest used dimensioned error index model evaluation measure (Chai and Draxler, 2014) and it expresses average prediction error in units of the variance (Equation 9). MAE can describe uniformly-distributed error; it was reported by Morias *et al*., (2007) that the value zero indicates a perfect fit and values below half of the calculated standard deviation may be considered low and recommended for model evaluation.

$$MAE = \frac{1}{n}\sum_{i=1}^{n}|e_i| \quad (9)$$

where, n is sample size and e_i is the error index

2.9.5 Coefficient of determination

The coefficient of determination (R^2) shows the fraction of data that is close to the line of best fit and it can measure the certainty of the prediction (Thavhana, 2018). According to Krause *et al*., (2005), it is the squared value of the correlation (Equation 10). R^2 ranges between 0 to 1 and values less than 0.5 are considered unsatisfactory, values; those between 0.5 to 0.75 mean that the results are acceptable, and values greater than 0.75 indicates a good model simulation. R^2 values indicate the percentage of variability of the observed data explained by the model; for example, if R^2 is equal to 0.5, it means that 50% of the variance in the observed data is explained by the model (Krause *et al*., 2005; Rahbeh *et al*., 2011). Both NSE and R^2 can be used as probability measures because of the comparison between observed and predicted streamflow (Thavhana, 2018). NSE has the tendency to overestimate large values and underestimate or neglect lower values, although, the coefficient of determination was said to be limited and it can provide the correlation measure for the linear relationship between simulated and observed data (Rahbeh *et al*., 2015). It was also noted that through the manipulation of the intercept and the slope, the results of the R^2 can be manipulated (Krause *et al*., 2005), however, for this study those two variables were not manipulated.

$$R^2 = \left(\frac{\sum_{i=1}^{n}(O_i - \bar{O})(S_i - \bar{S})}{\sqrt{\sum_{i=1}^{n}(O_i - \bar{O})^2}\sqrt{\sum_{i=1}^{n}(S_i - \bar{S})^2}} \right)^2 \quad (10)$$

where, O_i is the observed data, $\bar{O}$ is the mean observation, S_i is the simulated data, $\bar{S}$ is the mean of the simulated and n is the number of observations

2.10 Chapter summary

LULC changes are inevitable, while some changes are due to natural occurring events, some are induced by the growing population which is one of the main drivers as indicated in section 2.4.1. South Africa is a water-scarce country with high seasonal and variable rainfall (Nkosi *et al*., 2021). The latter study reported a decrease in water availability per annum from 1100 m^3/person/annum in 2005 to 905 m^3/person/annum in 2017, thus, both the growing pressure from the increased population and the change in climate will exert more strain on this already scarce resource. The interaction between land management and water resources is a delicate one, whatever is done on the land has an impact on the processes taking place on the hydrological cycle and this also affects the functions of the catchments. To support this, Kaushal *et al*. (2017) highlighted some of the hydrologic processes that have been strongly influenced by human interaction with the land, such as altered rainfall regimes through climate change, enhanced runoff and overland flow, less infiltration due to the compaction of land and modifications in the evapotranspiration. In response to those changes induced on the land, water systems tend to evolve overtime; this includes changes in river flow pattern and tributaries distribution.

Studies conducted on South African catchments (Dabrowski *et al*., 2013; Hobbs *et al*., 1985, Petersen *et al*., 2017, van der Laan *et al*., 2012) have confirmed an increase in human-driven LULC activities, such as forest plantations, urban areas and cultivated areas among others and such activities have been proven to alter the hydrological response regimes of a catchment, such as runoff, evapotranspiration and infiltration. South Africa loses about 6% of its MAR through land-use (Muller *et al*., 2009). The Crocodile River Catchment in Mpumalanga is one of the important rivers in terms of biodiversity, however, it is also one of the most stressed rivers, experiencing spatial variability in rainfall. Given the current status of water resources in the country and the

threats posed by climate change, it is important that such studies be done in order to promote the sustainable use, protection and management of water resources (Nkosi *et al*., 2021).

With the advancement in Remote Sensors, Masud and Bastiaanssen (2017) described how RS and GIS can be applied in water resource management. RS can be used as an alternate, to obtain “spatially and temporally consistent information that would be used in water resource analysis and management”. In addition, hydrological models can simulate a phenomenon, or a physical process of the hydrological cycle (Khatami and Khazaei, 2014). GIS and RS are tools that have been applied to water and land management, successfully for over a decade. QGIS is chosen as the GIS interface for the study because it does not require a licence and the LULC classification plug-in, SCP, furthermore, Landsat data are selected for all LULC classification related activities. This study chose the NDVI due to its ability to depict vegetation density and is one of the widely used vegetation index in the world. The SWAT model is adopted because it can be used with QGIS, it can simulate missing weather information and has been used in over 100 countries, including semi-arid regions like the CRC. Furthermore, it has been applied in bigger catchments than the CRC and gave satisfactory results; the model was manually calibrated. Due to its integration with QGIS, it will be referred to as QSWAT henceforth.

CHAPTER 3: METHODOLOGY

3.1 Preamble

To achieve the objective of the study, certain steps had to be followed and that is the purpose of this chapter. The chapter details the data requirement of this study and the respective data sources and the reasons for the data choices. This section provides the details of the methodology followed to obtain the result, the techniques (QSWAT and SCP) for data analysis and other forms of analysis employed.

3.2 Data requirement, sources, and collection

This study made use of streamflow data, climate data and geospatial data - Satellite, soil data, LULC maps and DEM. LULC maps, DEM, soil data and climate data were used as input data for the QSWAT model while the Landsat data was used for LULC classification and NDVI mapping. The study period covers a period of 40 years (1980–2020), which was further divided into 3 periods taking into account data availability. The period from 1980–1990 represent the base period, 1995–2005 is the transitioning period while the period from 2010–2020 represents the post-change period. Table 3.1 summarises the data, their sources and the period covered by each dataset.

Table 3.1: Data type and the respective data sources.

Data type	Source	Period covered	Online repository
Streamflow	DWS	1981–2020	https://www.dws.gov.za/Hydrology/Verified/hymain.aspx
Landsat data STRM DEM	USGS	1980, 2000 and 2020	www.earthexplorer.usgs.gov
Climate data: Temperature, wind speed, solar radiation, and humidity	ARC	2010–020	-
Climate data: Rainfall	SAWS	2010–2020	-
Classified national land cover images (NLC)	DEA	1980 – 2018	-
Soil data	FAO		https://data.isric.org/geonetwork/srv/eng/catalog.search#/metadata/c3f7cfd5-1f25-4da1-bce9-cdcdd8c1a9a9

3.2.1 LULC changes

LULC was classified for every 20 years (1980, 2000 and 2020) due to the slow rate of change in some of the LULC in the study area. The data required to assess LULC changes were obtained from USGS in the form of Landsat images. Landsat 1-3 MSS was used to classify 1980, Landsat 4-5 TM was used to classify 2000 and Landsat 8 OLI was used to classify 2020 (see Table 3.2). Due to factors, such as differences in sensor technologies, orbital parameters, and atmospheric correction schemes, the process required cross-validation (Verstraete, 2015). For the scope of this study, the NDVI values were calculated from the acquired Landsat images for only the post transition period, 2020. Landsat imageries with low to no cloud coverages images were chosen for this study, mostly during the winter months (May, June, and July); in cases where images were not available, images, preceding or prior to the target year and in winter months were used.

Table 3.2: Landsat data details.

Period	Satellite	Sensor ID	Path/row	Date of acquisition	Grid Cell size (m)
1980	Landsat 1-3	MSS	180/078	7 July 1979	72
			181/077	16 June 1978	
			181/078	14 November 1980	
2000	Landsat 4-5	TM	169/078	29 July 2000	30
			169/077		
			168/078	6 May 2001	
			168/077		
2020	Landsat 8	OLI_TIRS	169/078	2 June 2020	30
			169/077		
			168/078	29 July 2020	

3.2.2 QSWAT data

Table 3.2 shows the QSWAT model data used in this data. These included classified LULC, soil data, DEM, climate (temperatures, rainfall, humidity, wind speed and solar radiation) and the streamflow data and Table 3.3 gives a thorough description of the data. For the 1980 classified LULC, the climate data from 1980–1990 used was obtained from ARC and SAWS; for the 2000 classified LULC map, climate data for 1995–2005 was obtained from SAWS, data from 2010–2020 was obtained from SAWS and ARC while streamflow data from 1980–2020 was obtained from DWS. Due to the lack of continuous climate data, different sources had to be used. Weather data

was used for the simulation of the model and streamflow data was used for calibrating and validating the simulations.

Table 3.3: Details of the climate and streamflow station data.

ARC					
Station ID	Latitude	Longitude	Elevation	Period	Data type
Krokodilbrug	-25.3566	31.89542	170	2007–2020	Temperature (Max, Min), Humidity, Solar Radiation, Wind speed
Mhlati	-25.4843	31.51994	313	2007–2020	Temperature (Max, Min), Humidity, Solar Radiation, Wind speed
Nelspruit	-25.4546	30.97157	673	2007–2020	Temperature (Max, Min), Humidity, Solar Radiation, Wind speed
SAWS					
Station ID	Latitude	Longitude	Elevation	Period	Data type
Malelane	-25.471	31.507	346	2007–2020	Rainfall
Alkmaar	-25.444	30.819	776	1993–2005	Rainfall
Mayfern	-25.468	31.043	610	1978–1990 2009–2020	Rainfall
Nelspruit-B	-25.503	30.911	883	1993–2005	Temperature, Humidity, wind speed
Friedenheim	-25.433	30.983	671	1978–1990	Temperature, Humidity, wind speed
Krokodilbrug	-25.356	31.895	172	2007–2020	Rainfall
Streamflow station					
				Period	Data type
Station ID	Latitude	Longitude	Elevation	1980–2020	Streamflow
X2H032	-25.514	31.2245	-		

3.2.2.1 Climate data

Figure 3.1 presents all the weather stations obtained from ARC and SAWS. As shown in Table 3.3, a single station does not have all the five weather parameters - rainfall, temperature, solar radiation, wind speed and humidity. For example, the Mhlati weather station lacks rainfall data, therefore, the missing weather parameters were

then supplemented using the nearest station within the same quaternary catchment - Malelane station (Table 3.4). This was applied in all the stations with incomplete data.

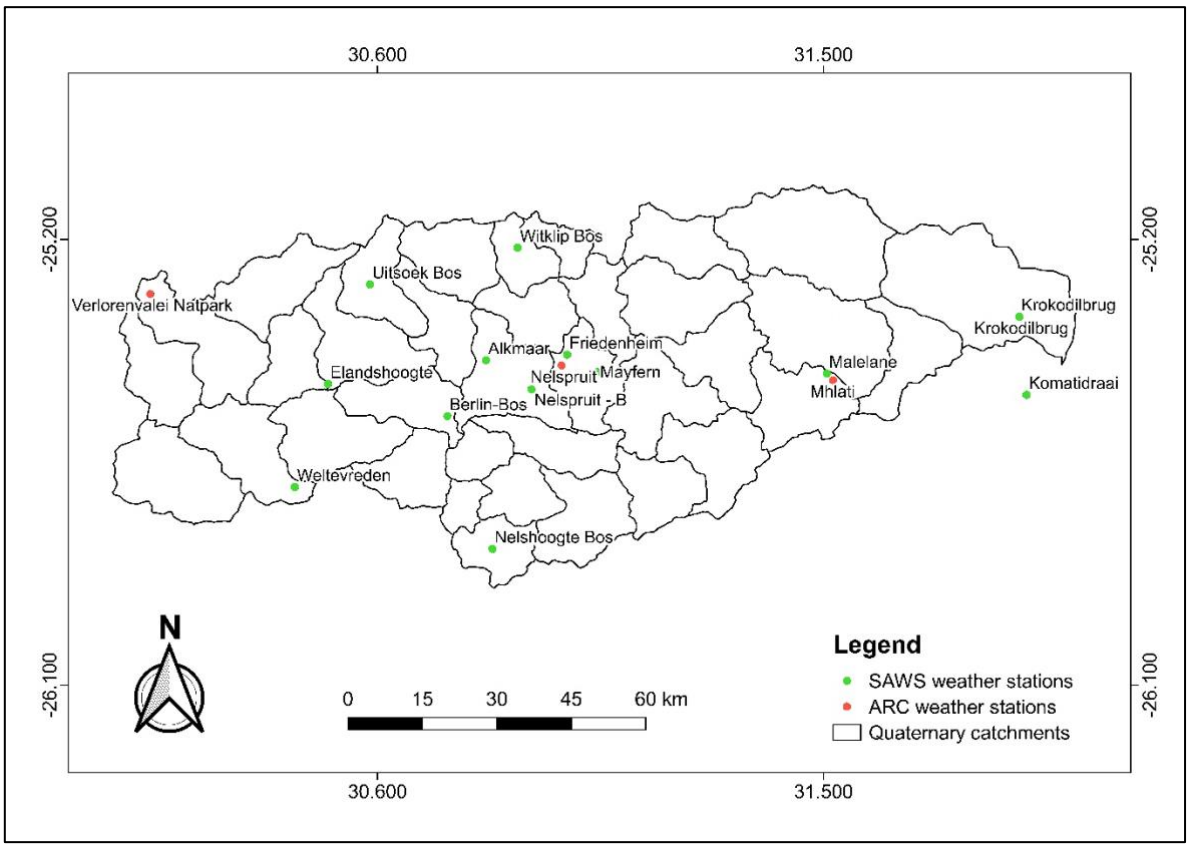

Figure 3.1: Location of the weather stations.

Table 3.4: The paired weather stations.

Rainfall stations	Temperature, solar radiation, wind, humidity stations
Krokodilburg	Krokodilburg
Malelane	Mhlati
Mayfern	Nelspruit and Friedenheim
Alkmaar	Nelspruit-B

3.2.2.2 Streamflow data

Figure 3.2 shows the active streamflow stations used for calibrating and validating the simulation from 1980 to 2020. Given the size of the catchment, four streamflow stations were chosen, X2H014, X2H032, X2H046 and X2H036. However, X2H046 and X2H036 had missing data. X2H036 had data from 1982 until recent with most gaps observed in the year 2000 while X2H046 had data from 1985 until recent.

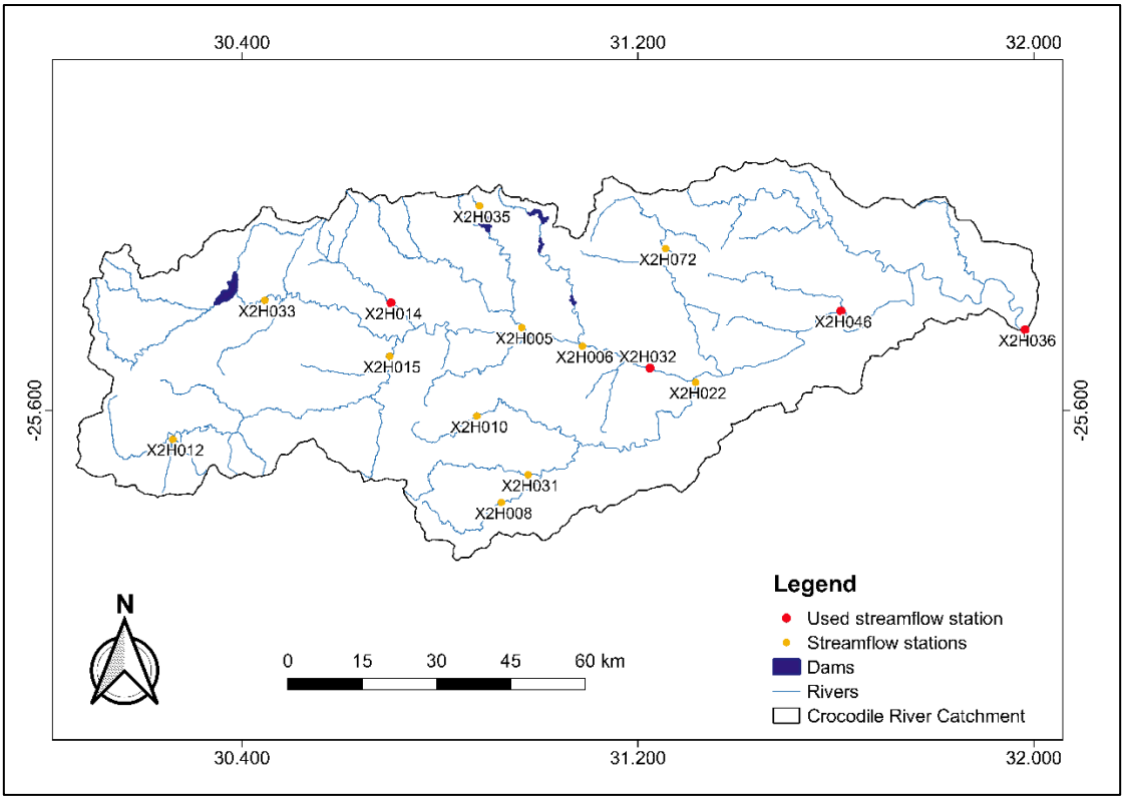

Figure 3.2: Location of streamflow stations.

3.2.2.3 Spatial Data

Spatial data is another form of input data required for the QSWAT model, these include DEM, LULC maps and soil maps. Table 3.5 shows the LULC classes used in QSWAT and Figure 3.3 shows the soil data that was used as input in the form of Geotiff.

Table 3.5: Land-use classes and SWAT codes.

LULC	Description	SWAT Code
1. Cultivation	Crop lands, irrigated, dry crops, rotational crops, pastures	AGRR
2. Forest plantation	Alpines, evergreen, deciduous forests	FRSE
3. Waterbodies	Dams, ponds, rivers	WATR
4. Grassland	All grass range	GRAS
5. Built-up	All urban areas and settlements, commercial, mines, manmade structures	URBN
6. Bushland/Savanah	Bush, thickets, shrubs,	SAVA
7. Bare	No or little vegetation and exposed areas in cultivation areas, rocks, burnt areas, quarries areas	BSVR
8. Natural forest	Mixed indigenous forest and woodland	FRST

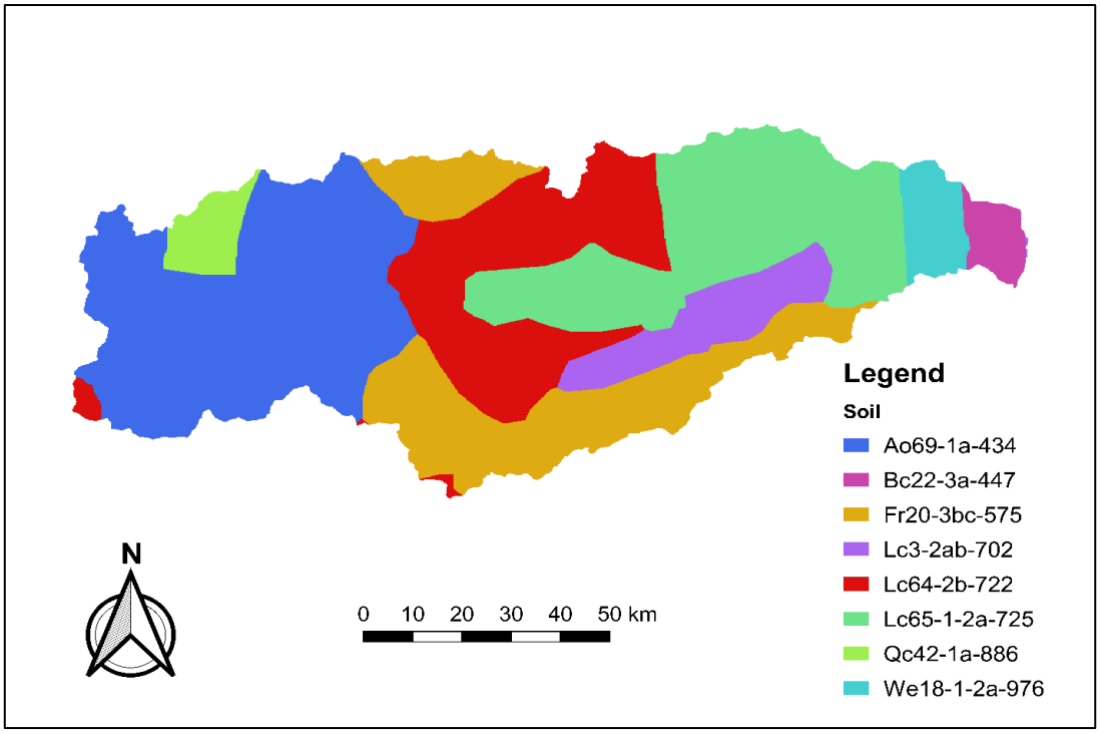

(source: FAO)

Figure 3.3: Soil map used in QSWAT.

3.3 Data analysis

3.3.1 LULC classification

QGIS interface was used for LULC classification and analysis and to calculate the NDVI value. The GIS software comes with a plug-in called 'semi-automatic classification' (SCP). The SCP plug-in within QGIS has been widely used for the classification of land-use and other remote-sensing analysis. For this study, SCP was used for pre-processing, band processing and post-processing of the Landsat data. Figure 3.4 shows the steps involved in land classification using SCP.

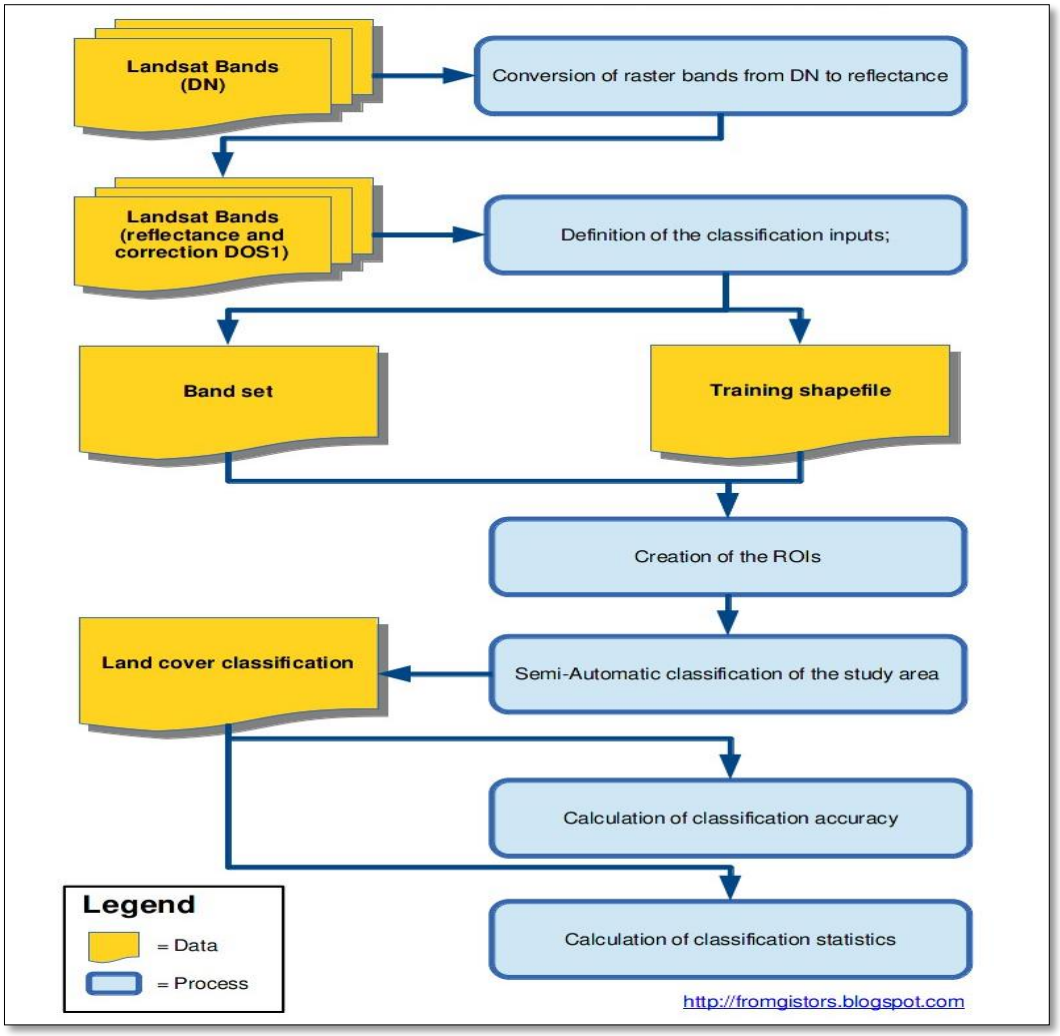

(Cogendo, 2014)

Figure 3.4: Schematic representation of the semi-automatic classification workflow.

i. Images Pre-Processing

Pre-processing of the satellite band involves conversion of the bands from digital number (DN) to reflectance, atmospheric correction, projections and clipping. For this study, the images were pre-processed using the SCP plug-in. The bands were loaded into SCP, first stacked and mosaicked, then clipped to mask the study area.

ii. Band Processing

After pre-processing, the correct band combination (RGB) was then selected. For this study the RGB combination values used for Landsat 1-3 MSS were 1-3-4, for Landsat 4-5 TM were 1-7-4 and for Landsat 8 OLI/TIR were 2-3-4. In addition, the regions of interest (ROI)s were created by drawing a polygon instead of using the ROI pointer. Land use classification can either be unsupervised or supervised; supervised classification is when the user develops spectral signatures of the known category

(built-up, forest, and others) and unsupervised classification is when the software assigns the pixel corresponding to that signature (Rwanga and Ndambuki, 2017). For this study, classification was done under supervision; LULC was classified into 8 major classes - built-up, grassland, savannah/bushlands, bareland, waterbodies, cultivation land, forest plantation and natural forest - as shown in Table 3.5.

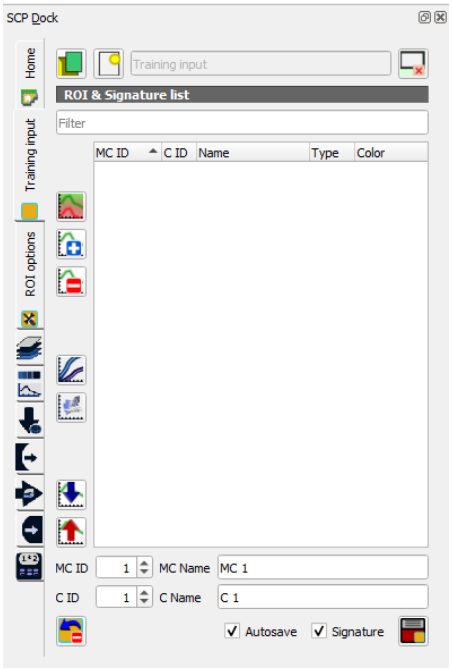

Figure 3.5: Training input on SCP.

iii. Post Processing: Accuracy Assessment

Accuracy assessment is one of the important steps in LULC classification and is used to validate the classified LULC, as well as quantitatively assess that the sampled pixels are assigned to the correct LULC class. For this study, the accuracy assessment was done using Landsat images with high resolution, Google Earth and NLC images. The NLC images used in this study, that is, 1980, 2000 and 2018 as the closest to 2020 the time of this study, were classified from Landsat 1-3, Landsat 4-5, Landsat 7 and Landsat 8 images. The error matrix (Table 3.6), Kappa coefficient, standard error (SE), user accuracy (UA), producer accuracy (PA) and overall accuracy were used to measure the accuracy of the classified land-use. After accuracy assessment, a LULC report, the statistics of land cover, was then generated for each period of classification. The kappa coefficient was calculated using Equation 11.

$$x = \frac{\text{Observed accuracy} - \text{change agreement}}{\text{Sum of product of row and column totals for each class}} \quad (11)$$

$$\text{UA} = \frac{\text{Correctly classified}}{\text{Total classified}} x\ 100 \quad (12)$$

$$\text{PA} = \frac{\text{Correctly classified}}{\text{Total number of reference sites}} x\ 100 \quad (13)$$

The Kappa Coefficient ranges from -1 to 1. Values that are less than a zero are considered poor or the agreement is not perfect, fair accuracy is between 0.2 and 0.4, moderate accuracy is between 0.4 and 0.6, good accuracy is between 0.6 and 0.8, while values closer to 1 are considered substantial to almost perfect (Lekha and Kumar, 2018). The columns of the error matrix table show the class validation pixels, while the rows of the table show the classes in which the validation pixels have been assigned to during classification (Table 3.6). According to Rwanga and Ndabuki (2017), the diagonal shows the pixels that have been classified correctly. Furthermore, the User accuracy accounts for when a pixel belonging to one class is included in a class being evaluated (Lekha and Kumar, 2018).

Table 3.6: An example of an error matrix table

Land-use class	**Class 1**	**Class 2**	**Class 3**	**Total**
Class 1	3	0	2	**5**
Class 2	1	2	4	**7**
Class 3	0	8	2	**10**
Total	**4**	**10**	**8**	**22**

3.3.2 Determination of hotspot Areas

Using LULC classification, the land-use activities with major impacts on the catchment cover were identified. The hotspots of those identified land-uses were then mapped based on the CRC quaternary catchments; an NDVI map was also generated based on those mapped hotspots. The NDVI values were used to account for the hotspot land-use activities. NDVI was generated on QGIS using Equation 2 in section 2.6.3.2 and the band combination are shown in Table 3.7. To compare the long-term changes in the hotspots activities as identified in this study, Landsat 1-3 MSS images were closely compared with those of Landsat 8 OLI/TIR.

3.3.3 Hydrological Modelling

QSWAT was used to simulate the changes in the streamflow before and after LULC changes. Figure 3.6 shows the set-up of SWAT as used in this study and the steps involved. SWAT is made up of 3 steps - step 1 is the delineation of catchment, HRUs were created in step 2 (Figure 3.6). After the creation of the HRUs, step 3 was enabled, and the SWAT2012 editor was activated.

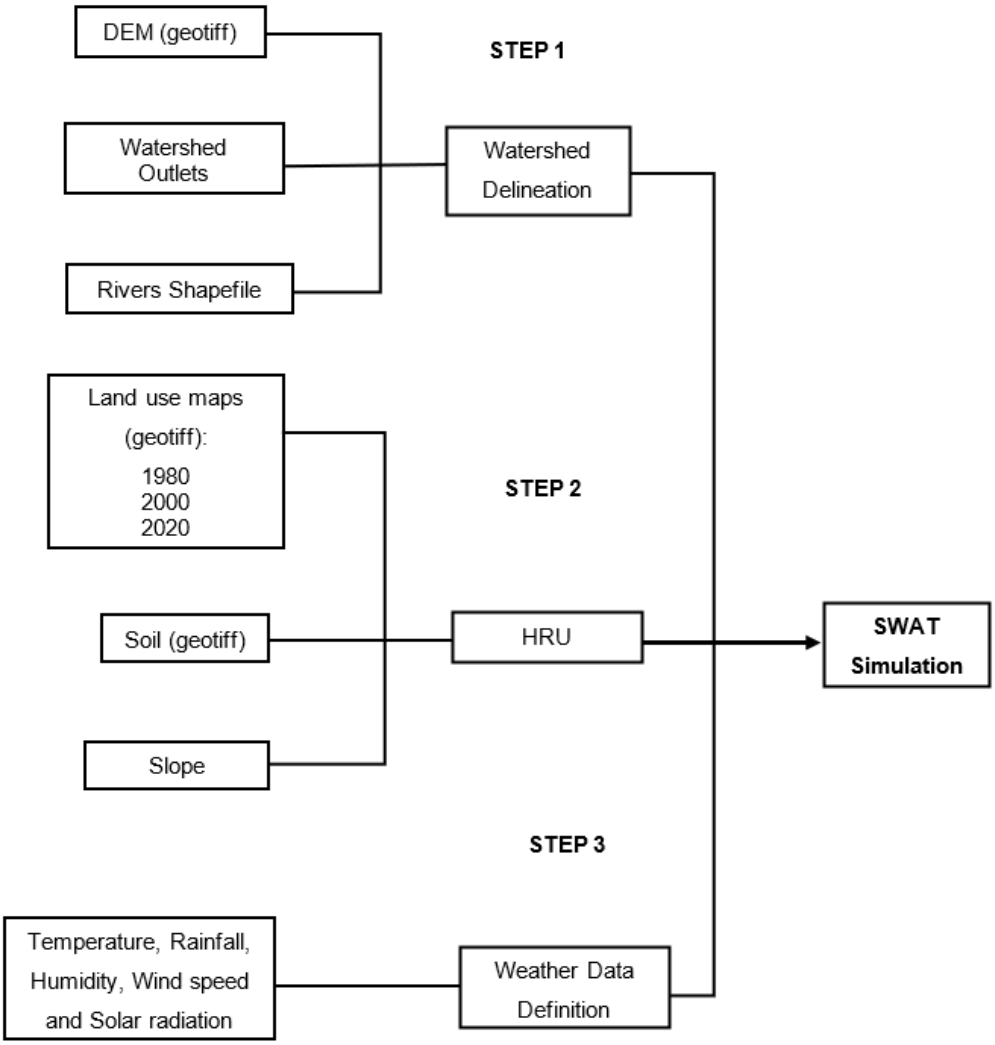

(Source: Phukoetphin et al., 2015)

Figure 3. 6 : Schematic representation of the SWAT model.

The SWAT2012 editor also had several steps to complete before the simulation of the model. This includes the creation of a weather generation station and batch files and importing the databases into the editor. The weather generation *csv* file contained statistics of the climate data, station names, elevation, and the location; it was imported to the QSWAT2012 reference database. The simulation step was involved in the selection of years to be simulated and selecting the warm-up period. A warm-

up period is the number of years to be skipped by the model; for this study, a warm-up period of 2 to 3 years was used depending on the availability of data and the results were printed per month. The results from the model can be read in the project databases through importing the results to the project database or it can be viewed on QSWAT through the visualise option. For this study, the output files chosen were output.rch (for streamflow) and output.sub (for the water balance components - surface runoff and evapotranspiration).

i) Streamflow

Streamflow consists of the total flows from all HRUs to the subwater level and can be re-routed via the variable-rate storage method or the Muskingum method; both methods were indicated as variations of kinetic wave approach (Gassman *et al*., 2007). For this study, the Muskingum routing method was used because it calculates the outflow hydrograph downstream based on the inflow hydrograph upstream (Tassew *et al*., 2019).

ii) Surface runoff

Surface runoff is estimated from daily or sub-hourly rainfall, and it can be estimated through the modified soil conservation service (SCS) curve number (CN) or Green and Ampt infiltration method (Gassman *et al.*, 2007; Jamil, 2020). The SCS-CN is modified based on the antecedent soil moisture content and LULC; the SWAT equation is given as shown by Equation 14 (Jamil, 2020).

$$Q_{surf} = \frac{(R_{day} - 0.2S)^2}{(R_{day} - 0.8S)} \quad (14)$$

Runoff will occur when $R_{day} > I_a$

where Q_{surf} is the collected runoff (mm H_2O), R_{day} is the rainfall depth for the day (mm H_2O), I_a is the initial abstractions (including surface storage, interception) prior to runoff (mm H_2O) and S is the retention parameter (mm H_2O).

iii) Evapotranspiration

SWAT has three methods for the estimation of evapotranspiration and these are: Penman-Monteith, Priestly-Taylor and Hargreaves (Gassman, *et al*., 2007). For the period of 1980–2005, ET was simulated using Hargreaves because there was no solar

radiation data for this period, and the method only requires Temperature (Maximum and Minimum) data (Jung *et al*., 2016). For the 2010–2020 period, ET was simulated using the Penman-Monteith evapotranspiration method because there was solar radiation for this period.

3.3.3.1 Calibration and Validation

Model calibration is achieved by modifying parameter values and further comparing the model outputs with the observed data (Ang and Oeurng, 2018). The latter study further explained that model validation is done in order to ascertain whether the calibrated model can predict streamflow based on the adjusted parameters. Model validation is usually done using later time periods. Calibration and Validation were done manually on the SWAT2012 editor window. The calibration and validation periods for this study were chosen as follows (Table 3.8).

Table 3.7: Calibration and validation period.

Period	**Calibration**	**Validation**
Base period: 1981–1990	1980–1985	1986–1990
Transitioning: 1995–2005	1995–2000	2001–2005
Post transition: 2010–2020	2010–2015	2016–2020

SWAT2012 editor contains 39 parameters; sensitivity analysis was done to determine the parameters to be adjusted. The NSE, RSR, PBIAS and R^2 were used for model performance and the trendline was used to indicate the corelation between the observed and simulated data for the calibration and validation periods.

3.4 Chapter Summary

The study is assessing the impact of LULC on water resources over a 40-year period (1980–2020), however, due to the lack of weather parameters in some weather stations, multiple weather databases had to be used. Most data obtained from SAWS did not have solar radiation, humidity, wind speed and temperature, while the data obtained from ARC did not have rainfall, therefore, to account for the missing data parameters either from ARC or SAWS, stations were paired with those found within the same quaternary catchment. Landsat images were used for LULC classification, Landsat-1-3 MSS was used to classify the year 1980 (the base period), Landsat 4-5 TM was used to classify the year 2000 (transition period) and Landsat 8 OLI/TIR was

used to classify the year 2020 (the post-change). All LULC classification analysis (including Landsat processing and accuracy assessments) were done using the SCP plug-in in QGIS. The NDVI was used to account for the hotspot areas. QSWAT was simulated 3 times, based on the LULC maps; for LULC 1980, the simulation was between 1980–1990; for LULC 2000, the simulation was between 1995–2005 and for LULC 2020, the simulation was between 2010–2020. Streamflow station X2H032 was used for calibration and validation of the model and the measures of performances were NSE, PBIAS, RSR and R^2. All data analysis for this study were carried out on QGIS.

CHAPTER 4: RESULTS AND DISCUSSION

LAND USE/LAND COVER CHANGES

4.1 Preamble

This chapter presents and discusses the results of the land use / land cover classification as analysed with the SCP plug-in in QGIS. It also discusses the accuracy results for 1980, 2000 and 2020 followed by the changes in LULC for these same time periods. In addition, the hotspots and NDVI results for the identified main land uses (cultivation land, urban areas, and forestry) for 1980 and 2020 periods (the pre- and post-change periods only) were outlined.

4.2 Land use/Land cover classification

4.2.1 Land-use classification

igure 4.1 shows the land use/land cover classification between 1980 and 2020 while Table 4.1 presents the LULC classification report, which details the percentage of change in LULC between 1980 and 2020.

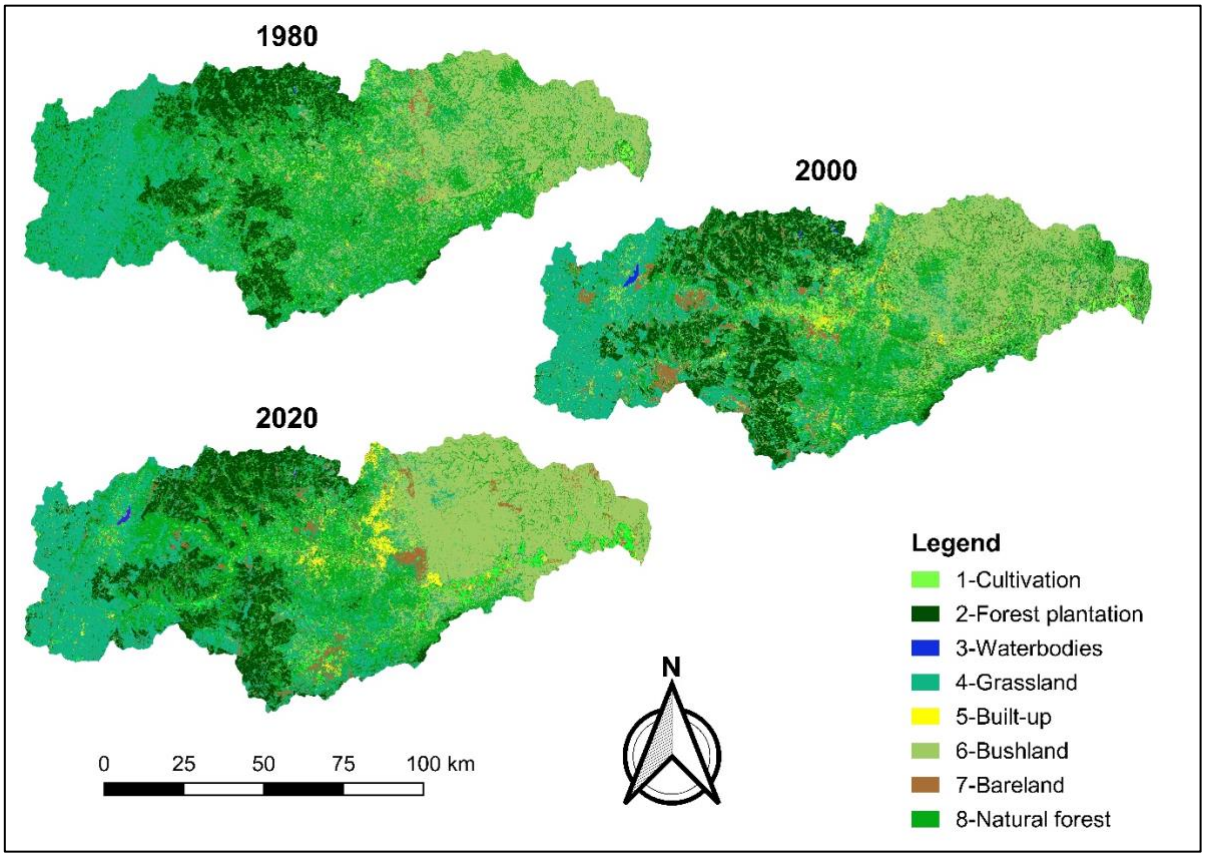

Figure 4.1 :Classified land-use from 1980–2020.

Table 4.1: Land-use report.

Land-use	1980	2000	2020	% of change from 1980–2020
1- Cultivation	2.59	5.05	5.06	2.47
2- Forest plantation	12.29	14.43	15.38	3.09
3- Water	0.04	0.26	0.13	0.09
4- Grassland	27.01	27.04	26.01	-1.00
5- Built-up	0.47	1.31	2.81	2.34
6- Bushland/Savana	23.78	23.02	25.87	2.09
7- Bareland	1.29	5.55	4.99	3.70
8- Natural Forest	32.54	23.33	19.74	-12.80

4.2.1.1 Cultivation

Cultivation increased by 2.5% between 1980 and 2020, from 2.6% to 5.1%, however, there was no change in cultivation land-use between the years 2000 and 2020. The increase in cultivation land could be due to increased population and the economic sector of Mpumalanga. The agricultural sector plays an important role in food security in the Province, and MPCOGTA (2018) reported that it is responsible for providing food security through subsistence farming and employment to unskilled workers. The main crops in the study area are sugarcane and citrus which are estimated to be occupying about 44.32% and 20% of the total irrigated area, respectively, especially in the lower catchment (Mussa *et al*., 2015). The latter study indicated that maize occupies about 5% and is mostly cultivated in the upper catchment.

4.2.1.2 Forest plantation

Forest plantation increased by 3.1% from 1980–2020; it was occupying an area of 12.3% in 1980 and this increased to 15.4% in 2020. Afforestation was reported to have occupied about 40% of Sabie/Graskop and 76% of the area east of Barberton (MMDC, 1998). The forestry industry is a major contributor to the South Africa's economy, thus the increase in this land-use cover. About 39 of the 148 primary processing plants are found in the Mpumalanga Province, and the biggest paper mill in the Southern hemisphere, the Ngodwana Sappi Kraft pulp and paper mill are located within the Crocodile River Catchment and the other driver of the commercial forest is wood demand. The most dominating forest trees are pines and *Eucalyptus* (Bate *et al*., 1999); these were also classified as alien vegetation in a report by the Mbombela SoER (2003).

4.2.1.3 Water

The results also showed major changes in waterbodies from 1980 to 2000 with an increase of approximately 0.3%, however this decreased by 0.2% in 2020. The increase between 1980 and 2000 can be attributed to construction of the Kwena Dam in 1984 and the Ngodwana Dam, as well as seven more medium dams on the catchment and over 200 small farm dams (Deksissa *et al*. (2003). The construction of dams was driven by the need to meet the water demand from different sectors; for example, the Ngodwana Dam was constructed to supply water to the Sappi Kraft (pty) Ltd pulp and paper mill and for domestic supply to the village of the Ngodwana (DWA, 2013). The latter report stated that the Kwena Dam was constructed for irrigation purposes. The decrease in waterbodies between 2000 and 2020 can be due to the difficulty that came with separating waterbodies from the surrounding land-cover. High spectral and spatial diversity of the waterbodies and inhomogeneity of the surrounding surfaces were shown to affect the extraction or classification of waterbodies (Wei *et al*., 2020). The latter study added that the urban surfaces, building and mountain shadows can obstruct the accuracy of waterbody classification. Furthermore, most waterbodies, including some of the major rivers were more visible in 2000 and this can be attributed to the Intense Tropical Cyclone Leon–Eline that occurred in 2000 over southern Africa. In 2020, however, water levels were low in some dams and not as visible in some rivers which may have led to the misclassification of some waterbodies, thus, Wei *et al*. (2020), suggest that climate is also another aspect to consider when classifying waterbodies.

4.2.1.4 Grassland

There has been an overall decrease of grassland between the year 1980 and 2020, it has decreased by 1% since 1980, it covered 27% of the area in 1980 and in 2020 it only covered about 26% of the area. Grassland covers most of the Mpumalanga Province. The latter has been transformed by 44% and 45% nationally (South Africa) and provincially (Mpumalanga) respectively, if not transformed, they are reported to have been degraded or severely invaded by alien plants (Fourie *et al.*, 2014). This latter study concluded that grasslands are mostly affected by grazing and crop production, urban development, and forest plantation. This could explain the decrease in grassland from 1980 with the increase of the mentioned activities, as shown in this

study. In addition, in Mpumalanga, most grasslands are found in fertile soils which are used for crop production (Ferrar and Lotter, 2007; MPCOGTA, 2018).

4.2.1.5 Built-up

Built-up areas account for anthropogenic impervious surface such as settlement areas, towns, roads, commercial areas and railways. Figure 4.1 and Table 4.1 show an increase of 2.3% in built-up areas from the year 1980 to the year 2020. One of the major drivers of built-up areas is population growth and development (Kumar *et al*, 2017). The biggest settlement area within the catchment is the Nsikazi South, made up of Daantjie, Kanyamazane, Kabokweni and Thekwane (DWA, 2013). The population for Nsikazi South was estimated to be about 219 118 in 2009 and was estimated to be about 229 417 for low growth scenario and 231 981 for high growth scenario in the year 2020. In addition, it is estimated to reach 237 660 in 2030 for low growth scenario and 255 605 for high growth scenario (DWA, 2013). The city of Mbombela is the economic hub of Mpumalanga and is fast growing, therefore, the increase in built-up areas, since 1980, may be due to the growing population. It was estimated to be about 49 907 in 2009 and it is estimated to be about 62 777 in 2020 for low growth scenario and 66 239 for a high case scenario (DWA, 2013). Other major recognised fast-growing settlements include Plaston/Karino located 15 km from the city, White River located 20 km from the city, Matsulu located 40 km from the city and the Nsikazi/Daantjie located about 25 km from the city (MEGDP, 2011).

4.2.1.6 Bushland/Savannah

Savannah/Bushland are made of a mixture of trees, shrubs, and grass, and it further varies between tall dense woodland, open woodland, and dense thickets. Figure (4.1) and Table (4.1) indicate an increase of about 2.1% in 2020 from 1980; it covered an area of 23.8% in 1980 and this increased to about 25.9% in 2020. Based on igure 4.1, there is more bushland cover in the lower catchment, especially in the Kruger National Park, which MPCOGTA (2018) stated as providing the ideal landscape for wildlife.

4.2.1.7 Bareland

The results indicate a high number of bare areas between 2000 and 2020, as there was an increase of about 3.7% from 1980 to 2020. Burnt areas, exposed cultivation land, and cleared forest plantation land account for most of the bare area classes in this study. It was noted that veld fires are natural events and they are used as

management tools (Mucina and Rutherford, 2006), however, the frequency of fires within the catchment is “far greater than natural burning regimes” (Mbombela SoER, 2003). Wildfire results in landscape degradation, thus affecting the vegetation and soil properties (Moran-Tejeda *et al.*, 2015).

4.2.1.8 Natural Forest

Natural forests only refer to indigenous forests, and the results indicated a decrease of about 12.8% since 1980 (from 32.7% in 1998 to 19.5% in 2020). Natural forests have a significant cultural value as they are a source of many traditional medicinal herbs. Other factors affecting natural forests include land-uses such as cultivation, forest plantation and urban sprawl, thus an increase in those land-use activities could have been one of the reasons for the reduced natural forests. About 25% of South Africa’s natural forest are conserved within timber plantations and provide shade and moisture-conserving leaf litter that affects the growth of ground-layer vegetation such as grass and shrubs (MPCOGTA, 2018). This could explain the increase in bushland with the decrease in forest cover on the lower Crocodile catchment, thus, the overall increase of bushland in the year 2020.

Mbombela SoER (2003) indicated that due to land use activities in Mbombela, only a few habitats remain in their natural state and have become “islands” or patches. These includes natural forests, wetland, riparian zones and natural grasslands, the latter are also considered ecologically sensitive. Agricultural expansion, housing development, urban sprawling, poor fire management and bush encroachment are some of the major drivers of natural vegetation changes (Mbombela SoER, 2003), however, changes in natural vegetation can also be attributed to climate (Sheil, 2018). There was less rainfall observed in 2020 than 2000 and this could also explain the decrease in natural forests downstream.

4.2.2 Accuracy Assessment

Table 4.2a presents the error matrix results; for the year 1980, UA ranged between 46.7% to 93.3% while PA ranged between 61.9% to 100%. The confusion was mostly due to the built-up areas and barelands, especially exposed rocks. For the year 2002, UA ranged between 40 % and 100% while PA ranged between 61.5% to 100%; like in 1980, confusion was mostly between built-up areas and bareland (see Table 4.2b). In 2020, from Table 4.2c, UA ranged between 70% and 100% and PA ranged between

66.8% and 100%. PA indicates the accuracy of a prediction while the UA indicates the reliability of the classification (Rwanga and Ndambuki, 2017), therefore, UA was indicated to be a more relevant measure of classification. The matrix error table (Table 4c) also showed the standard error, for the year 1980; the SE ranged between 0-0.039, between 0-0.0406 for the year 2000 and 0-0.0407 for the year 2020.

Table 4.2: Error Matrix table for the years (a) 1980, (b) 2000 and (c) 2020.

a. 1980									
Classified Land use	**Cultivation**	**Forest plantation**	**Waterbodies**	**Grasslands**	**Bareland**	**Savanah**	**Built-up**	**Natural Forest**	**Total**
Cultivation	**12**	3	0	1	2	0	0	2	20
Forest Plantation	0	**14**	0	0	0	0	0	1	15
Waterbodies	0	0	**13**	0	0	0	0	2	15
Grassland	3	0	0	**9**	0	1	0	2	15
Bareland	2	0	0	1	**9**	1	2	0	15
Savanah	0	0	0	0	3	**12**	0	0	15
Built-up	1	2	0	0	0	4	**7**	1	15
Natural Forest	0	0	0	0	0	1	1	**13**	15
Total	18	19	13	11	14	19	10	21	125
SE	0.029	0.0085	0	0.0354	0.0255	0.038	0.0218	0.0393	
PA (%)	66.7	73.7	100	81.8	64.3	63.2	70.0	61.9	
UA (%)	60	93.3	86.7	60	60	80	46.7	86.7	

a. 2000									
Classified Land use	**Cultivation**	**Forest plantation**	**Waterbodies**	**Grasslands**	**Bareland**	**Savanah**	**Built-up**	**Natural Forest**	**Total**
Cultivation	**9**	1	0	1	4	0	0	0	15
Forest Plantation	0	**15**	0	0	0	0	0	0	15
Waterbodies	0	0	**10**	0	0	0	0	0	10
Grassland	1	1	0	**12**	0	0	0	1	15
Bareland	1	0	0	0	**7**	0	0	2	10
Savanah	0	0	0	0	0	**9**	0	1	10
Built-up	1	2	0	2	0	0	**4**	1	10

Natural Forest	0	1	0	1	0	0	0	**8**	10
Total	12	20	10	16	11	9	4	13	95
SE	0.0206	0.029	0	0.0373	0.0066	0.0221	0.0086	0.0405	
PA (%)	75.0	75	100	75.0	63.6	100	100	61.5	
UA (%)	60	100	100	80	70	90	40	80	

a. 2020

Classified Land use	Cultivation	Forest Plantation	Waterbodies	Grassland	Bareland	Savanah	Built-up	Natural Forest	Total
Cultivation	**14**	1	0	2	0	1	1	1	20
Forest Plantation	0	**13**	0	1	0	0	0	1	15
Waterbodies	0	0	**15**	0	0	0	0	0	15
Grassland	0	0	0	**14**	1	0	0	5	20
Bareland	0	0	0	1	**13**	0	1	0	15
Savanah	0	0	0	1	2	**16**	1	0	20
Built-up	3	0	0	0	0	0	**12**	0	15
Natural Forest	1	4	0	0	0	0	0	**15**	20
Total	18	18	15	19	16	17	15	22	140
SE	0.0121	0.0236	0	0.0321	0.0221	0.0232	0.0136	0.0347	
PA (%)	77.8	73.6	100	75.0	81.3	94.1	80	66.8	
UA (%)	70	86.7	100	70	86.7	80	80	75	

The overall accuracy for land use classification ranged between 77.2 % and 82.3% and the kappa statistics ranged between 0.71 – 0.78 (Table 4.3). According to the criteria presented by Lekha and Kumar (2018), the results depict good accuracy and are within the acceptable range, thus the classification is acceptable.

Table 4.3: The overall performance and Kappa statistics for the classified land-use.

Period	Overall accuracy	Kappa statistics
1980	71.2	0,71
2000	77.9	0.78
2020	80.0	0.72

4.3 NDVI analysis for hotspots area for major land-uses

From the classified land use maps, the recognised land-uses were commercial forest plantation, built-up areas and cultivation lands; these were recognised as the major drivers to the changes on natural land cover in the catchment. These results are consisted with findings by Saraiva-Okello *et al*. (2015), which indicated an increase of over 4 times in areas under commercial forest and agriculture. From this view, the hotspot areas of interest were demarcated based on quaternary catchments as shown in Figure 4.2. From the Figure, the lower and upper parts of the catchments seem to be the major hotspots for agriculture, while the middle reach of the catchment is shared between built-up and forest plantation. Based on the land use classification (igure 4.1), forest plantation further extends toward the upper reaches.

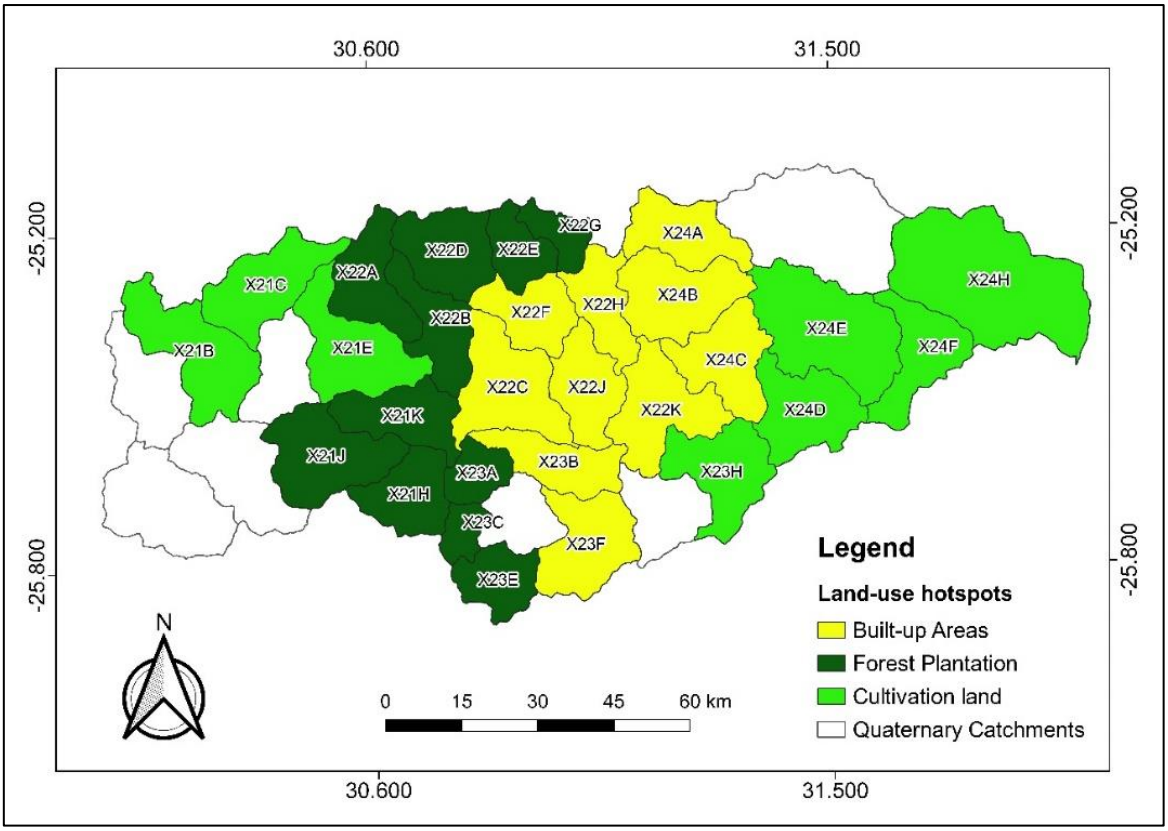

Figure 4.2: Land-use hotspots.

4.3.1 **Built- up Areas**

Ten quaternary catchments were recognised as the major hotspots for built-up changes - X22C, X22F, X22H, X22J, X22K, X23B, X23F, X24B, X24A and X24C as shown in Figure 4.2. The NDVI value for the extracted quaternary catchment where built-up areas are dominant was 0.1 (see Figure 4.3). This is supported by a study by Akbar *et al*. (2019), where the values presenting built-up areas were found to be between 0.015–0.14.

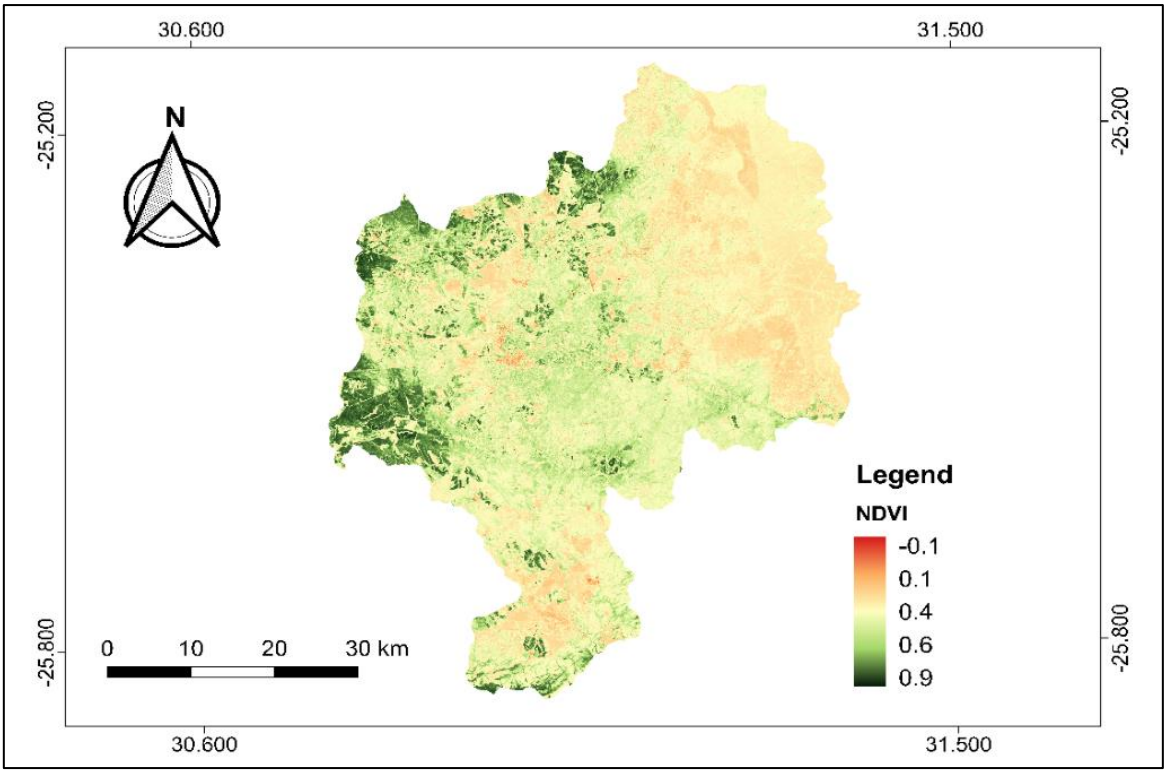

Figure 4.3: The NDVI for built-up hotspots

The increase in built-up areas not only affect natural vegetation - natural forests, grasslands, and bushland - but also existing land-use classes being converted to built-up areas. An example is provided in the X22F and X22H the areas marked A in Figure 4.4. As depicted, point A was an agricultural area in 1980 and was converted to a settlement in 2020. It should be noted that most of the Karino area was previously a cultivation area. Zubair *et al*. (2019) mentioned that urban expansion presents a problem to agricultural land use within the vicinities of large urban areas. Point B indicates the City of Mbombela (X22J; X22C), the capital city of the Mpumalanga Province and the major economic hub within the catchment as previously indicated. Increase in built-up areas, therefore, can also be attributed to the increase in rural-urban migration and new developments such as the construction of malls in the settlement area for the growing population.

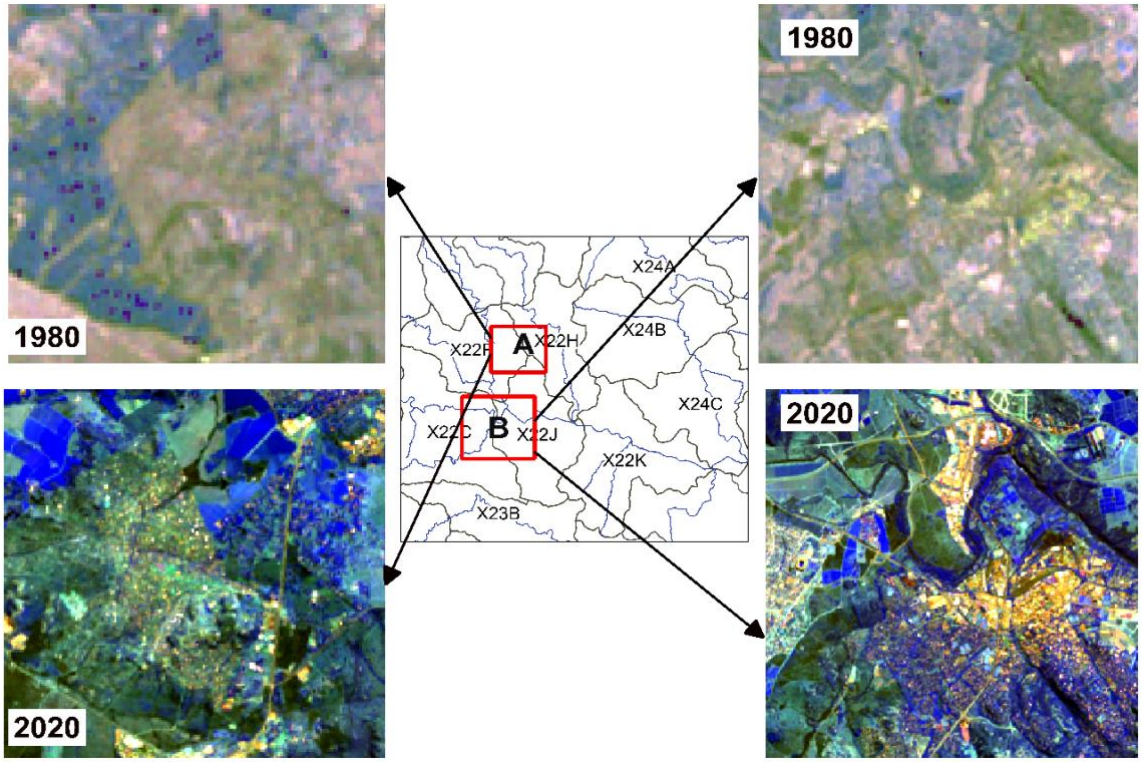

Figure 4.4: Changes in land-use between 1980 and 2020.

4.3.2 **Cultivated Lands**

Eight quaternary catchments were recognised as the cultivation hotspots and these are: X21B, X21C, X21E, X23H, X24D, X24E, X24H and X24H (Figure 4.2). These were found in the upper and lower reaches of the catchment (Figure 4.5). It has been reported that most irrigated crops are found on the lower catchment while dry crops are found on the upper catchment (Mussa *et al*., 2015; MEGDP, 2011). The NDVI value for the irrigated crops varies between 0.6 and 0.7 while the NDVI value for dry crops vary between 0.0 and 0.4, especially, closer to the Kwena Dam. On average, the NDVI values for the croplands in the lower catchment were higher than that of the upper reaches, thus, it indicates that the crop vegetation in this part of the catchment is greener (X24H) than upstream, especially in X21B and X21C (Figure 4.5). It should be noted that the croplands were located within other major LULC classes, for example, the upper reaches crop is found within commercial forest plantation.

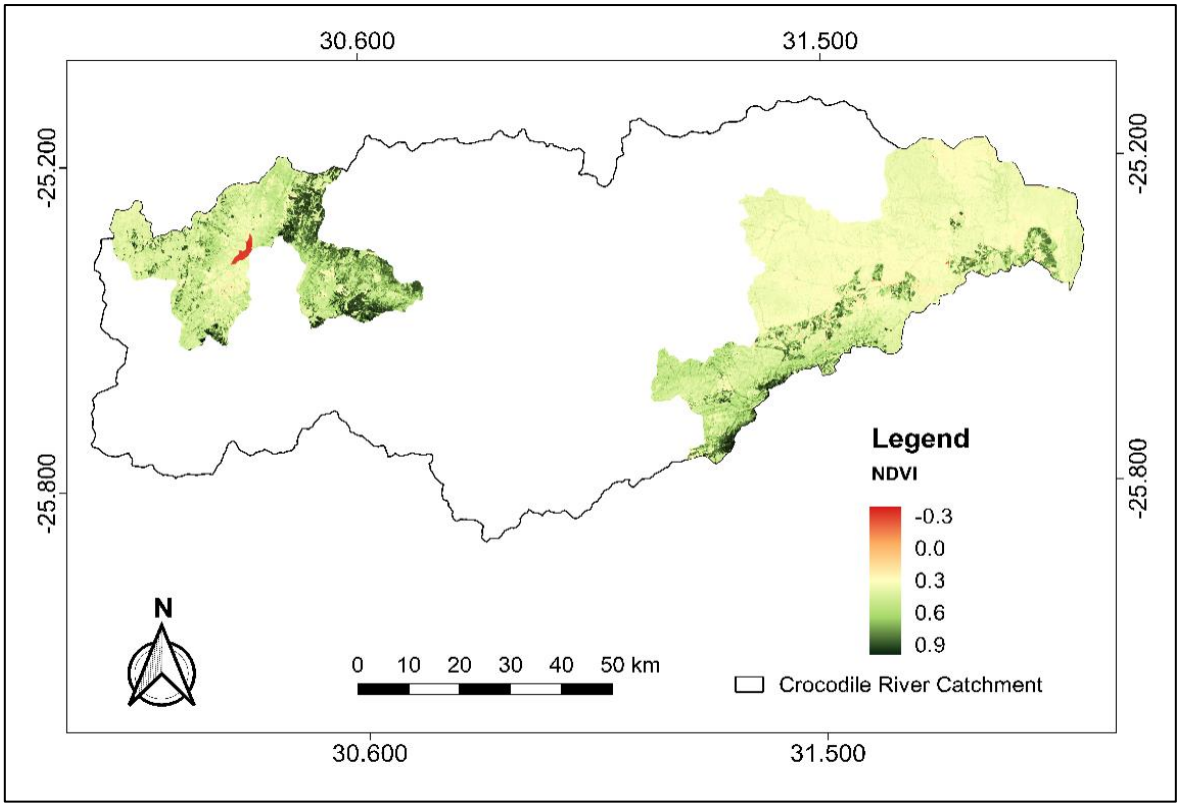

Figure 4.5: NDVI for cultivated lands.

Cultivated lands have also been indicated to have increased since 1980 in LULC classification results. Figure 4.6 shows the changes that have occurred from 1980 to 2020, there were more cultivation plots in 2020 than 1980. Due to the competition between agricultural land (that is, grazing land and cultivation land) and other land-uses such as mining and urban expansion, MEGDP (2011) highlighted the need for protecting high potential and productive agricultural land. In addition, it was reported that agriculture is the economic backbone of the Mpumalanga Province (MEGDP, 2011)

4.3.3 Commercial plantation Forest

Eleven quaternary catchments were identified as being the hotspots areas for commercial forest land-use - X21H, X21J, X21K, X22A, X22B, X22D, X22E, X22G, X23A, X23C and X23E (see Figure 4.2). The NDVI value for forest plantation varied between 0.8 and 0.9 as shown in Figure 4.7 and these were highest in the quaternary catchments containing only forest plantation such as X22D. These findings are comparable with those obtained by Hadebe (2001).

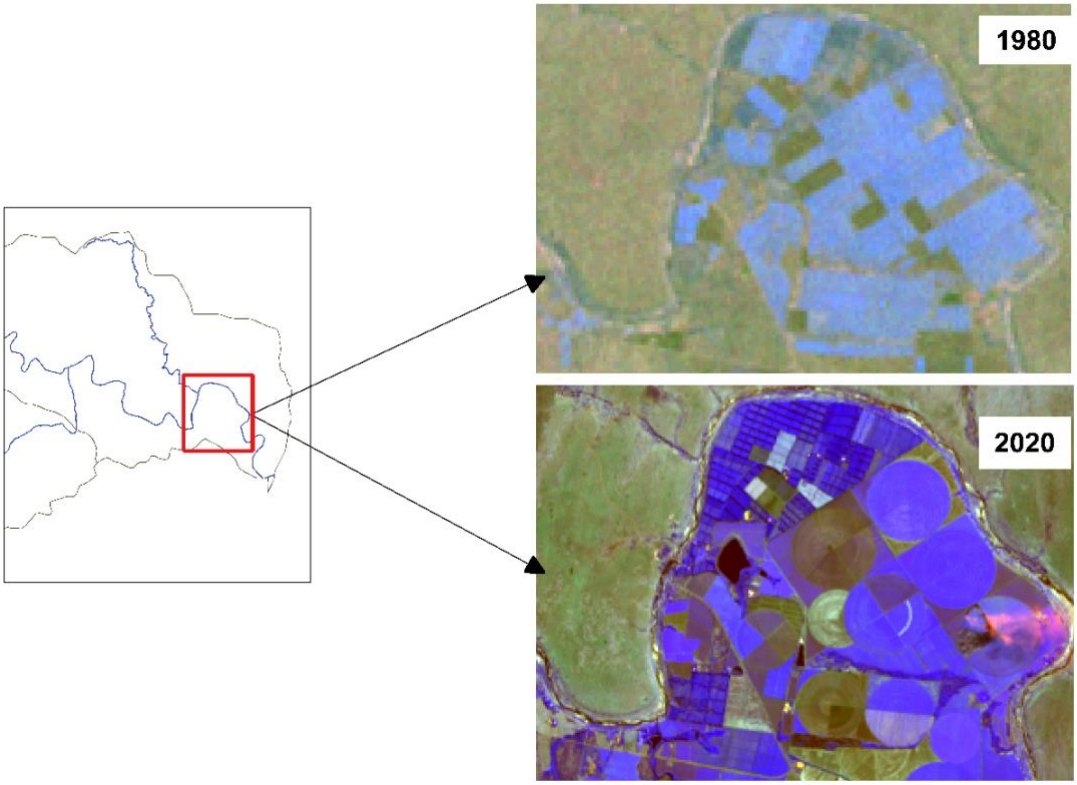

Figure 4.6: Cultivated land changes between 1980 and 2020.

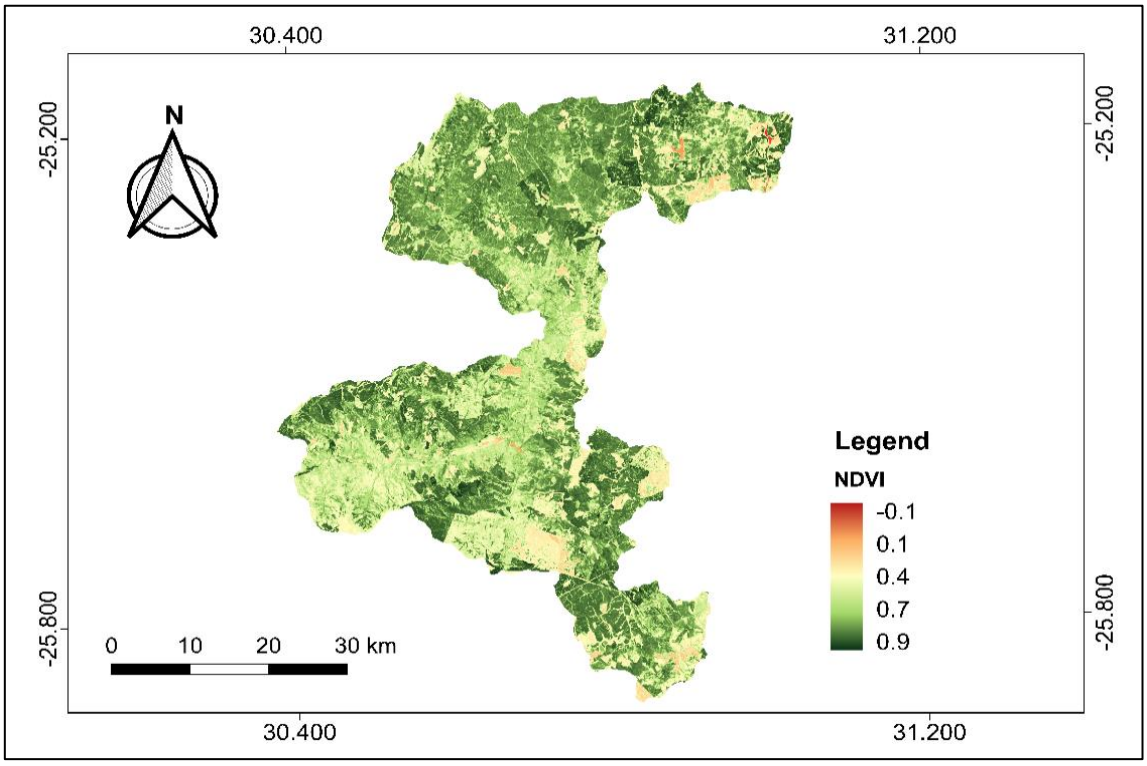

Figure 4.7: NDVI for Forest plantation hotspots.

As can be seen from the LULC results analysis, forest plantation is the major land-use activity in the Crocodile Catchment and in Mpumalanga; it accounts for 22.8% of the country's forestry Gross Value Added (GVA) (MEGDP, 2011). The land-use results analysis marked an increase of 3.1% in forest plantation from 1980 – 2021, examples of these changes are presented in Figure 4.8 (quaternary catchment X21J). Moreover, Mkhondo, parts of Msukaligwa local municipalities and Mbombela were noted as areas of high forest plantation capabilities within the catchment, thus, suggesting the potential for more forest plantations within the catchment (MPCOGTA, 2018).

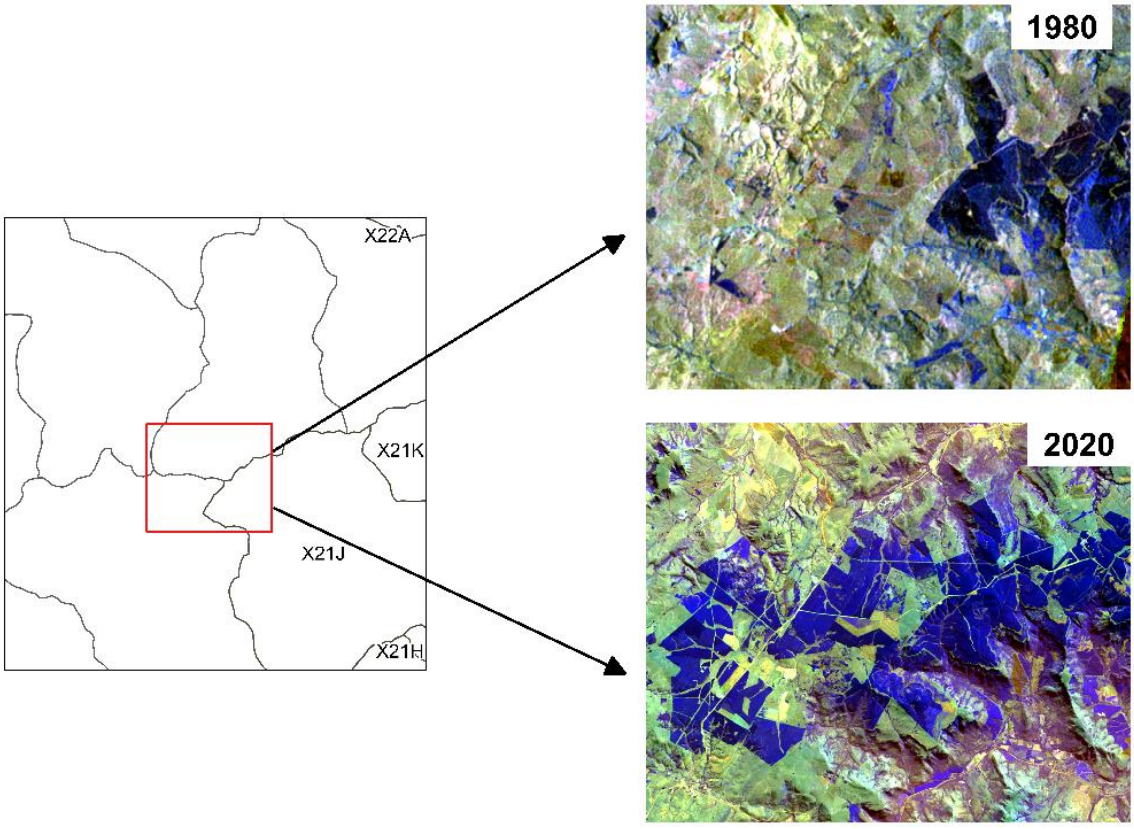

Figure 4.8: Changes between 1980 and 2020.

4.4 Chapter Summary

The chapter aimed at presenting the changes in LULC from 1980–2020 and to map the land-uses (hotspots) with major impacts on natural cover. The classification results' analysis indicated a positive change in most LULC classes from 1980 to the year 2020, however, a negative change was marked in grassland and natural forest cover vegetation. The negative changes were attributed to the increase in other LULC classes; for example, the decrease in grassland was attributed to the increase in cultivated areas, built-up areas, and forest plantation. Increase in cultivated areas, built-up areas and forest plantation were driven by population demand and the areas

economic contribution, thus, making them the hotspot activities with major impacts on the catchment land cover. The upper and lower catchments were found to be the hotspots for irrigated crops and dry crops, respectively, with NDVI values ranging between 0.0–0.7. The middle-catchment was found to be the hotspot for built-up areas and forest plantation, with an NDVI value of 0.1 for built-up areas and NDVI values ranging between 0.8 to 0.9 for forest plantation. The closer the NDVI value is to 1, the more densely the vegetated area is (USGS, 2021). It should be noted that the land-use activities are not limited to the mapped areas, however, this is where they are mostly concentrated. The increase in these land-use activities - cultivation, built-up area and forest plantation - resulted in an increase for water demand which in turn led to the construction of dams - Kwena Dam and Ngodwana Dam - for water supply. Other recognised major dams are Primkop Dam, Da Gama Dam, Witklip Dam and Klipkopjes Dam augmented with more than 200 farm dams (DWA, 2013). The study also observed a trend in the distribution of some LULC (that is, forest plantation) and the distribution of the rainfall ((Source: WR2012)

Figure 1.*3*). As indicated, the highest amount of precipitation (1071–1614 mm) is received in the western mountainous area; this is the area in which most afforestation activities were concentrated. It was also noted that the bushland/savannah is distributed in areas with rainfall ranging between 527 and 708 mm/year, thus, showing that climate also plays a role in the distribution of LULC.

CHAPTER 5: RESULTS

HYDROLOGICAL RESPONSE

5.1 Preamble

This chapter presents the hydrological simulation-analysis findings from the SWAT model. It provides the calibration and validating of the simulations with model performance measures (NSE, PBIAS, RSR and R^2). It further presents the streamflow trends from 1980–2020 and details impacts of LULC on the catchment hydrological response - surface runoff and evapotranspiration – thus, the effects on water resources.

5.2 SWAT results

5.2.1 Watershed results

There were 27 sub-basins and 377 HRUs created from the 1980 simulation, 2000 and 2020 had 29 sub-basins with 380 HRUs for the year 2000 and 373 HRUs for the year 2020 as shown in Figure 5.1. The sub-basins and HRUs were created based on soil, land-use, and slope data, thus giving rise to difference in the number of sub-basins created as shown in Figure 5.1. The choice of the sub-basins was based on their correspondence with the observed station.

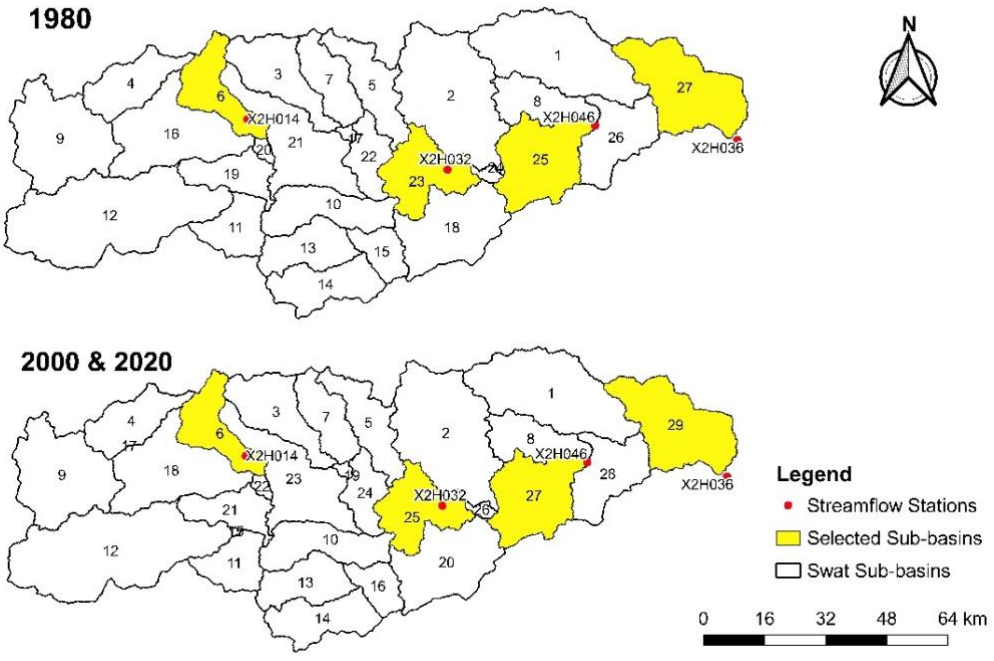

Figure 5.1: Simulated QSWAT Sub-basins.

5.2.2 Model Calibration and Validation

The SWAT model has 14 flow parameters (El-Sadek and Irvem, 2014), and the listed parameters in Table 5.1 were found to have more influence on the model during sensitivity analysis, in this study. The most sensitive parameters for this study were ALPHA-BF, CN2 and SOL_K. **Error! Reference source not found.** shows the fitted values for each period.

Table 5.1: SWAT model calibrated parameters for the CRC.

Parameters	Description	Calibration range		Fitted value		
		Max	min	1980-1990	1995-2005	2010-2020
1. SOL_K	Saturated hydraulic conductivity	100	0	0.05	5	0.95
2. CN2	The initial SCS Curve Number II value (%)	98	35	0.5	0.05	1.2
3. SOL_AWC	Available water capacity	1	0			0.9
4. SOL_Z	Soil depth	3000	0	0.01	0.3	
5. GW_DELAY	Groundwater delay time	50	0	5	8	0.5
6. GWQMN	Threshold depth of water in the shallow aquifer required for return flow to occur (mm)	5000	0	2	0.95	2
7. ALPHA_BF	Baseflow alpha factor (days)	1	0	0	0.03	0
8. GW_REVAP	Groundwater revap coefficient	0.2	0.02	0.15		0.15
9. REVAPMN	Threshold depth of water in the shallow aquifer required for revap to occur (mm)	500	0			50

For the 1980 LULC, the period between 1980–1985 was used as the calibration and the period between 1986–1990 was used for validation. For 2000 LULC, the period between 1995 –2000 was used for calibration and the period between 2001–2005 was used for validation. Then, the period between 2010–2015 was used for calibration while 2016–2020 was used for validation for 2020 LULC.

5.2.2.1 Base period: 1980–1990

Figure 5.2 shows the calibration and validation runs for the period between 1980 and 1990 for stations X2H014, X2H032, X2H046 and X2H036. For the calibration period, the hydrograph for simulated and observed streamflow followed the same trend, especially, while simulating low flows. The hydrographs for both the simulated and observed streamflow for the validation period depict the same trend, especially for X2H032 (Figure 5.2c). The model however, underestimated most of the peak flows, especially the 1989 peak flow. The simulation was more pronounced for the X2H014 station (Figure 5.2a).

The highest simulated peak flow was in February 1985 equalling 86.7 m3/s and an observed streamflow of 79 m3/s; this high streamflow was also shown to have been a flood (Masereka *et al.,* 2018). The lowest streamflow was observed between March 1982 and October 1983. It should be noted that between October to March is naturally a high-flow period, in correspondence with the high rainfall season over the study area (Riddell *et al.,* 2014). The low flow is between April – September, however, the low flow simulated between March 1982 and October 1983 was during a high flow period, but coincided with an ENSO event (Riddell *et al.,* 2014; Roualt *et al.,* 2019).

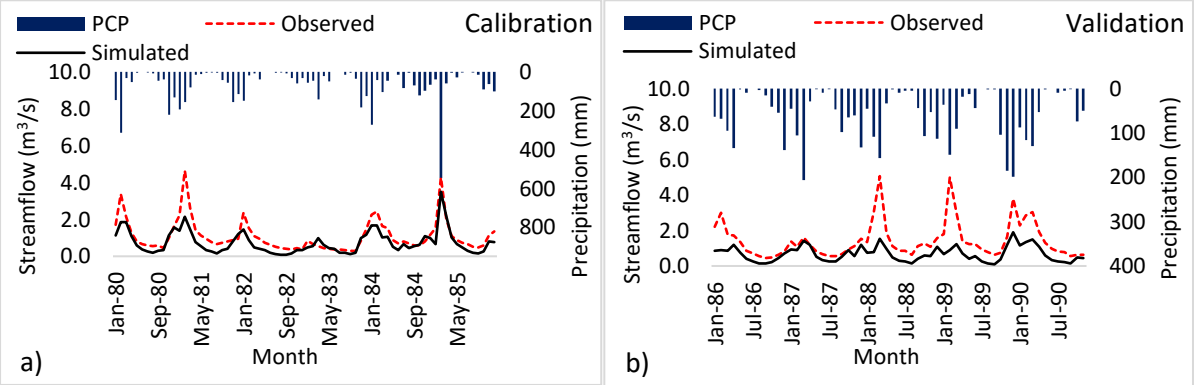

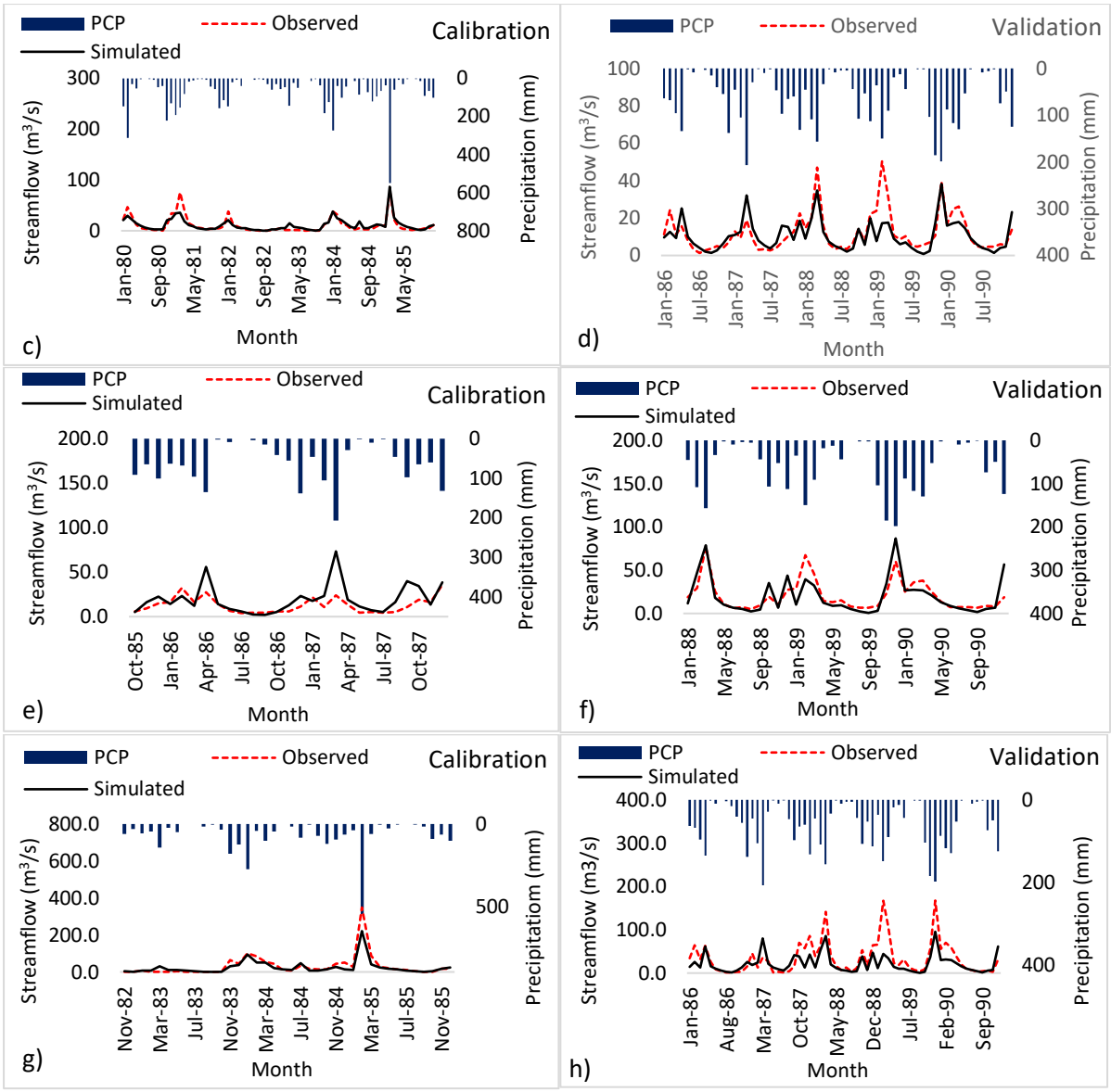

Figure 5.2: Simulated and observation hydrographs for 1980 (a) calibration and (b) validation for station X2H014, (c) calibration and (d) validation for X2H032, (e) calibration and (f) validation for station X2H046 and (g) calibration and (h) validation for station X2H036

5.2.2.2 Transitioning: 1995–2005

For calibration, the simulated and observed hydrographs showed an almost perfect similar trend as can be seen in Figure 5.3 for all the stations. The model was able to simulate the high peaks, however, it slightly underestimated the peak flow in February 1999, especially, for stations X2H014 and X2H036 (Figure 5.3a and Figure 5.3g), and slightly underestimated the January and December 2000 peak flows. The simulated hydrograph for the validation period depicted by Figure 5.3 underestimated the

December 2001 peak flow in all the stations, however, the underestimation of streamflow was most evident at station X2H014 (Figure 5.3g). The model, however, overestimated the streamflow in January 2005 and December 2005 for stations X2H032, X2H046 and X2H036 (Figure 5.3d, f, and h).

The peak discharges observed in February 1996 and February 2000 amounted to a simulated value of 170 m^3/s and an observed value of 135 m^3/s for February 1996. For February 2000, the flow varied between an observed value of 193 m^3/s and 163 m^3/s for simulated. Both the mentioned peak flows were due to floods that took place in those periods (Smither *et al*., 2001; Masera *et al.*, 2018). The February 2000 flood can be attributed to tropical cyclone Eline that resulted in heavy rainfall over the study area, which resulted in a flood that exceeded the 100-year return period (Van Bladeren and Van der Spuy, 2000). The lowest flows recorded for the 1995–2005 period was in 1995, 1997–1998 and between 2002–2003. The catchment had a low flow below 20 m^3/s during those periods which is below the normal for the catchment. The identified low flows were attributed to a drought event (Mathieu and Yves, 2005); the drought for 1997–1998 was also associated to an ENSO event (Thomson *et al.,* 2003).

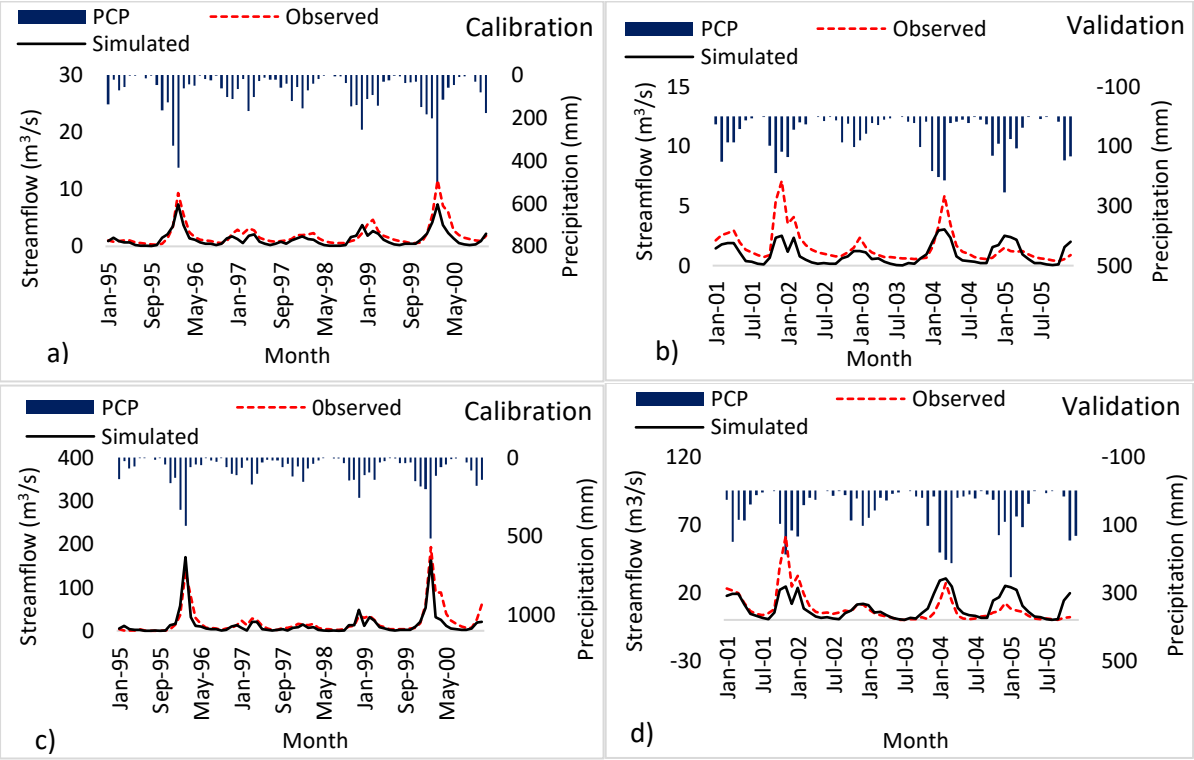

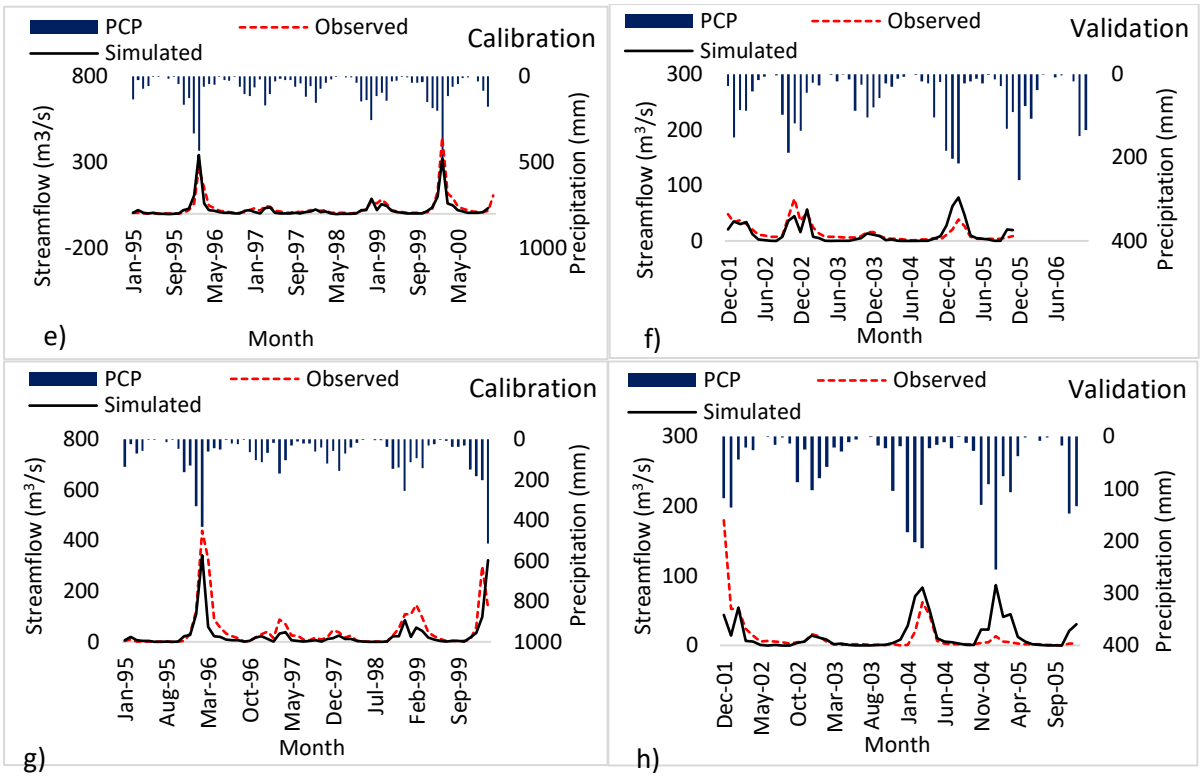

Figure 5.3: Simulated and observation hydrographs for 2000 (a) calibration and (b) validation for station X2H014, (c) calibration and (d) validation for X2H032, (e) calibration and (f) validation for X2H046 and (g) calibration and (h) validation for X2H036

5.2.2.3 Post transition: 2010–2020

For calibration, the simulation and observed hydrographs showed a very similar trend, the model was basically successful at simulating both the low flows and some of the high peaks. The model however overestimated the low flows for station X2H014 (Figure 5.4a). From Figure 5.4g, the model slightly overestimated the peak flow for January 2012 and February 2014 for X2H036. The model further underestimated the January 2011, 2012, 2013 and 2014 peak flows for stations X2H014, X2H032 and X2H046 (Figure 5.4a, c and e). The simulation for the validation hydrograph also shows the same trend as the observed and the model showed better simulation for station X2H032 and underestimated the streamflow for X2H014 (see Figure 5.4b and d). The model also underestimated the February 2019 peak flow for station X2H036 in Figure 5.4(h).

A fairly high streamflow was observed between 2010 and March 2014 with the highest recorded in January 2012 and March 2014, which was estimated to have been about 84.5 m^3/s and 51 m^3/s, respectively, from the simulated timeseries. The observed

streamflow ranged between 68 m^3/s for January 2012 and 93 m^3/s for March 2014. The high streamflow for January 2012 can be attributed to a flood event that occurred in that month (Sauka, 2016). From December 2014 to July 2020, streamflow started showing a decreasing trend. Based on the observed streamflow hydrograph, the catchment had a flow below 25 m^3/s between 2014–2016, and according to Nhamo *et al.,* (2019), between 2014–2015, South Africa was experiencing drought, and this was evident in the reduced streamflow. After the peak flow recorded in 2017, the low streamflow streak trend (below 25 m^3/s) continued until 2020.

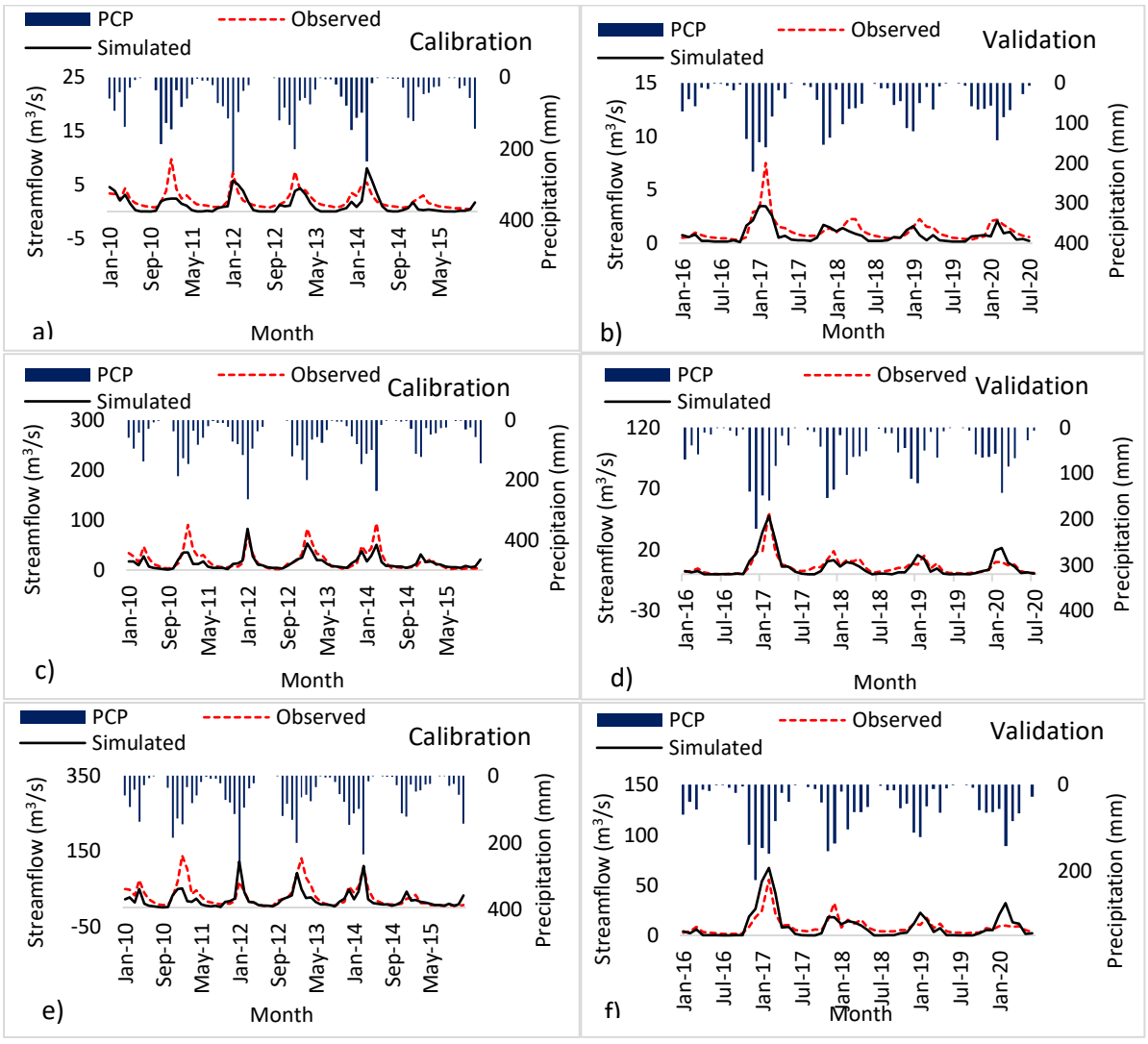

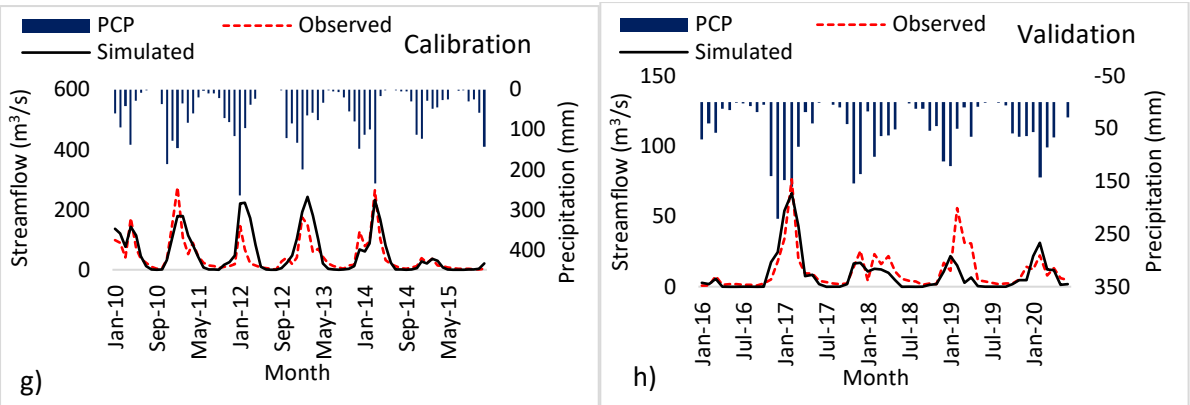

Figure 5.4: Simulated and observation hydrographs for 2020 (a) calibration and (b) validation for station X2H014, (c) calibration and (d) validation for station X2H032, (e) calibration and (f) validation for station X2H046 and (g) calibration and (h) validation for station X2H036

5.2.3 Test for model performance

Error! Reference source not found. shows the model performance for both calibration and validation periods. Station X2H014 had an acceptable NSE value for the 1980 and 2000 calibration periods with acceptable RSR values. The model gave a good performance for station X2H032 for the 2010–2020 period with an NSE value of 0.63 and 0.73, a PBIAS value of 22.3 and 5.7 as well as an RSR value of 0.60 and 0.52 for the calibration period and validation period, respectively. The model also performed well for the 1980-1990 validation period and calibration period of 1995–2005 for X2H032. Table 5.2 further shows that station X2H046 only performed well for the calibration period of 2000 with an NSE value of 0.83, PBIAS value of -23.7 and an RSR value of 0.41. Station X2H036 showed a better performance for 2020 calibration and validation periods with an NSE value above 0.5, however, the 1980 and 2000 validation periods were below 0.5.

Table 5.2: Model performance results for calibration and validation.

X2H014 Model performance			**1980**	**2000**	**2020**
NSE	1980 -1985	**Calibration**	**0.59**	**0.68**	0.2
	1986 - 1990	**Validation**	-0.1	0.31	**0.5**
PBIAS	1995 - 2000	**Calibration**	**-2.6**	32	38.07
	2000- 2005	**Validation**	53	37.9	33
RSR	2010 - 2015	**Calibration**	**0.47**	**0.57**	0.9
	2015 - 2020	**Validation**	1	0.8	**0.7**
X2H032 Model performance			**1980**	**2000**	**2020**
NSE	1980 -1985	**Calibration**	**0.78**	**0.76**	**0.63**
	1986 - 1990	**Validation**	**0.57**	0.41	**0.73**

PBIAS	1995 - 2000	**Calibration**	**-2.6**	27.9	**22.3**
	2000- 2005	**Validation**	**12**	**-5.9**	**5.7**
RSR	2010 - 2015	**Calibration**	**0.47**	**0.49**	**0.60**
	2015 - 2020	**Validation**	**0.66**	0.76	**0.52**
X2H046 Model performance			**1980**	**2000**	**2020**
NSE	1980 -1985	**Calibration**	-1.4	**0.83**	0.4
	1986 - 1990	**Validation**	**0.56**	-1.3	0.3
PBIAS	1995 - 2000	**Calibration**	-49	**-23.7**	29
	2000- 2005	**Validation**	**3.4**	-90	**-2.8**
RSR	2010 - 2015	**Calibration**	1.6	**0.41**	0.76
	2015 - 2020	**Validation**	**0.66**	1.5	0.83
X2H036 Model performance			**1980**	**2000**	**2020**
NSE	1980 -1985	**Calibration**	**0.80**	**0.51**	**0.5**
	1986 - 1990	**Validation**	0.4	0.10	**0.5**
PBIAS	1995 - 2000	**Calibration**	**23.6**	40.6	**-22.3**
	2000- 2005	**Validation**	36	**-24**	**20.3**
RSR	2010 - 2015	**Calibration**	**0.43**	**0.7**	0.72
	2015 - 2020	**Validation**	0.75	0.9	**0.70**

According to Nugroho *et al.,* (2013), NSE values ranging between 0.75 – 1 indicate a very good model performance, while values between 0.5 – 0.65 shows a satisfactory model performance and values less than 0.5 represents an unsatisfactory model performance. The PBIAS value for the calibration period varied between -2.3, -.2.6 and 27.9 for the year 2020, 1980 and 2000, ranging between -2.3 and 27.9, while for validation it varied between -5.9 and 41.9. Ang and Oeurn (2018) noted that a PBIAS value ≥ ±25 means the model gave an unsatisfactory performance while a PBIAS value between ±15 or less and < ±25 means the contrary. A good performance is achieved when the PBIAS is between ±10 and ±15 and very good performance is achieved when the PBIAS is below ±10. Generally, the models gave an unsatisfactory performance for station X2H014, a satisfactory performance for X2H032, an unsatisfactory performance for X2H046. Furthermore, according to Ang and Oeurn (2018), RSR values above 0.7 indicate poor performance. The model further gave a satisfactory performance for the 2020 period while giving an unsatisfactory performance for the other periods which indicates good model performance, especially for the calibration period.

Figure 5.5 presents the relationship between observed and the simulated flow for the study period with R^2 for X2H014 and the R^2 results for the other stations are presented in Appendix 1. The correlation showed a positive relationship between the simulated and observed flow for both the calibration and validation periods for all the stations.

The R^2 for the calibration period varies between 0.5 – 0.8 and 0.5 – 0.6 for the validation period for the X2H014 station. The R2 value for X2H032 varied between 0.6 – 0.8 for the calibration period and it further varied between 0.4 to 0.8 for the validation period, for station X2H046; the R2 value ranged between 0.5-0.9 for the calibration period and 0.4 to 0.7 for the validation period. The R2 value varied between 0.5-0.9 for the calibration period and 0.2 to 0.7 for the validation period. Based on the R2 results, the model's performances were satisfactory.

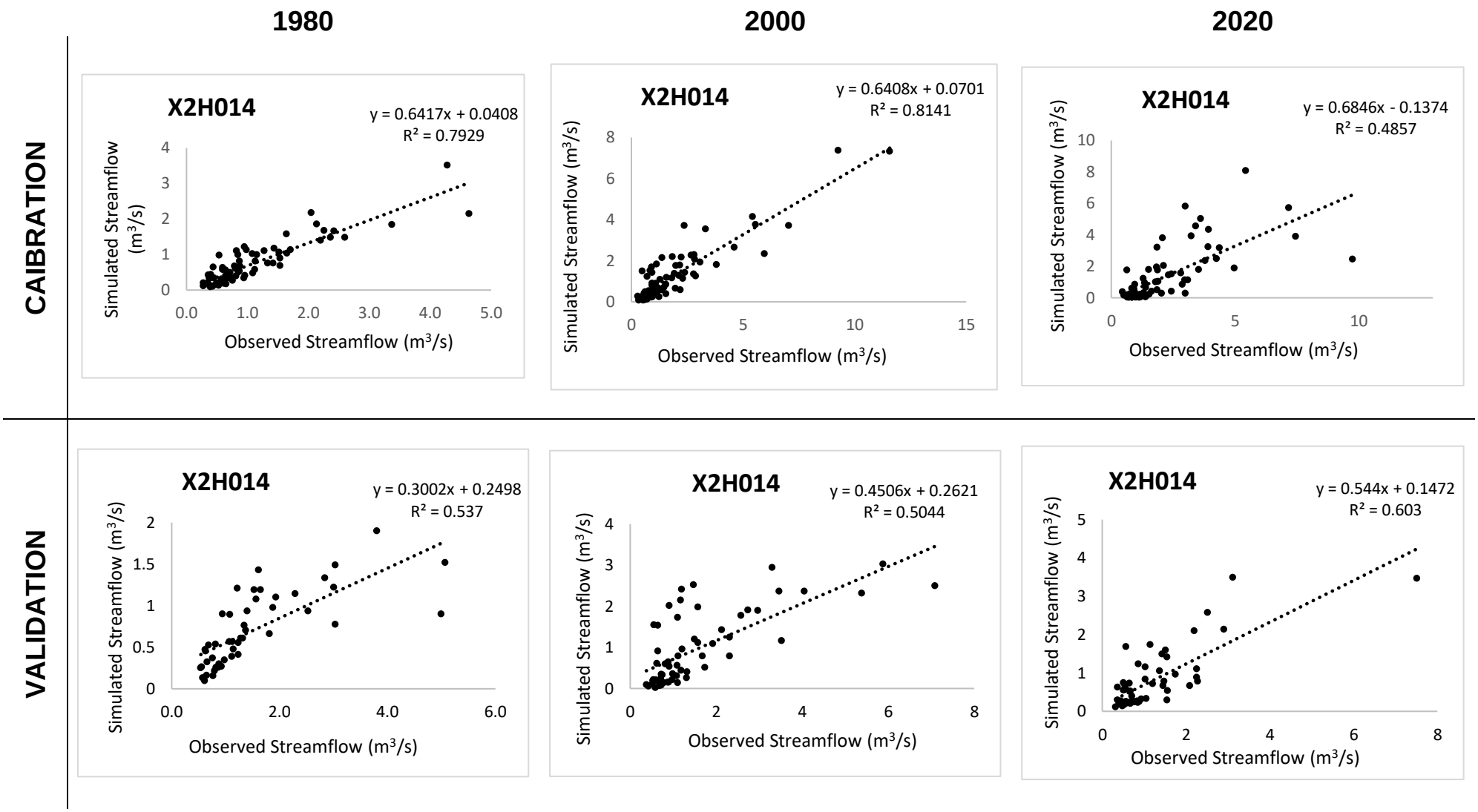

Figure 5.5: The correlation between simulated and observed streamflow.

Overall, the model performed very well in simulating the streamflow for stations X2H032 and X2H036 for the calibration period of 1980–1990 and further simulated streamflow for the calibration period in all the stations except for X2H014. For the validation period, the model was able to simulate the streamflow for the 2010–2020 period in all the stations, but it underestimated high peak for stations X2H014 and X2H036. The model also did not perform well in simulating the streamflow for the 1980–1990 and the 1995–2005 periods for all the stations. In some cases, this can be attributed to the heterogeneity of rainfall input data and its lack of accuracy (Rostamian *et al*., 2008; El-Sadek and Irvem 2014; Thavhana, 2018), the input data plays a major role in the accuracy of the model simulation. The rainfall distribution tends to vary with the size of the catchment, thus the gaging station used in the study may not be representative of the entire catchment (Yuan *et al*., 2015). Another explanation can lie in the high simulated streamflow during calibration period as noted in other studies (Stehr *et al*., 2008; Rahbeh *et al*. 2011); for example, the maximum simulated streamflow recorded for the 1980 period was 76 m^3/s, while for validation it was 38 m^3/s. Similar trends can be seen in both the 2000 and 2020 periods, where the calibration period recorded high discharge rates compared to validation. According to Rahbeh *et al*., (2011), SWAT can better simulate hydrological processes during wet conditions than dry conditions. This is proven in this study as the overall rainfall received during validation was much lower than that received during calibration.

Impacts of Land use on water resources**Error! Reference source not found.**The change in the water balance of the catchment for the year 1980 is shown in Figure 5.6 and Appendix B contains the catchment water balance for the years 2000 and 2020. Percolation from the surface and precipitation decreased from 1980 to 2020 while evapotranspiration increased. Based on Figure 5.7, evapotranspiration, and surface waterflow show an inverse relationship; and in areas with high evapotranspiration, surface waterflow seems low. The distribution pattern of evapotranspiration shows similar pattern for 1980 and 2000, there is more evapotranspiration in middle reaches and upper reaches of the catchment. The year 2020 show an increase in the rates of evapotranspiration in the middle reaches and decreased rates in the downstream parts of the catchment.

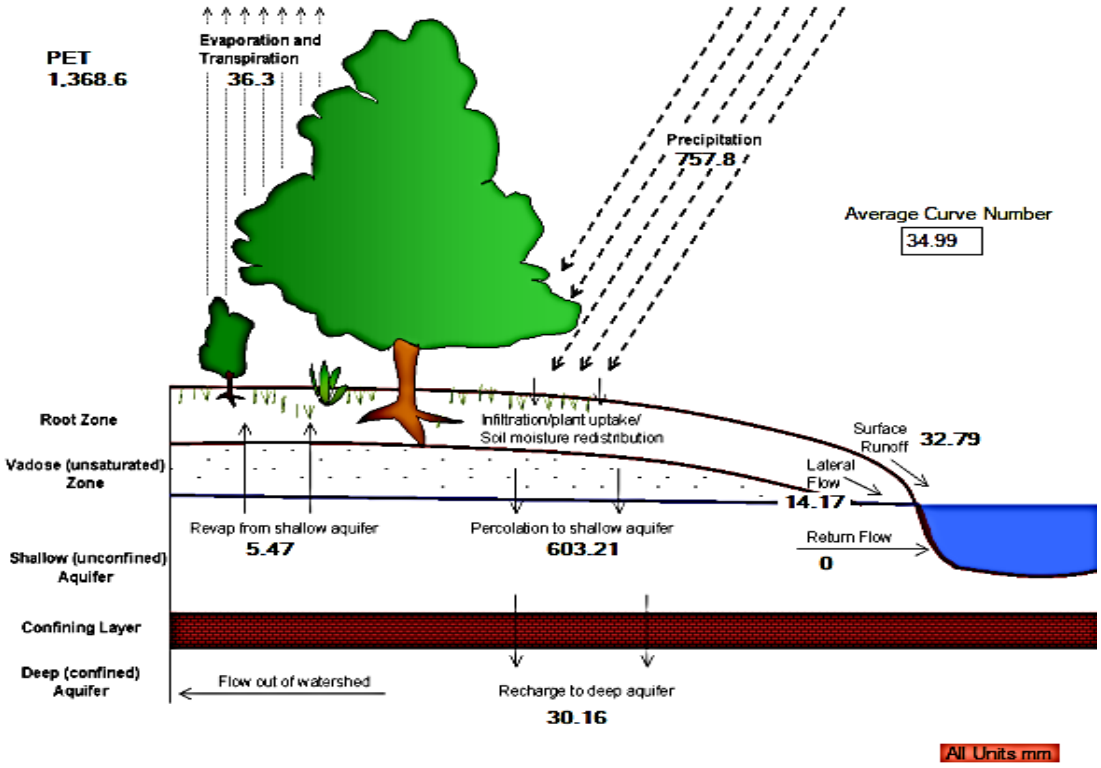

Figure 5.6: Water balance diagram for the CRC in the year 1980.

The evapotranspiration rates were higher in the upper catchment compared to 1980 and 2000. Evapotranspiration is higher in densely-vegetated areas and surface water flow is high in less-vegetated areas, thus, the increased evapotranspiration in the middle reaches can be attributed to forest plantations, as this part of the catchment was noted as a hotspot for forest plantation. Figure 5.7 also shows low surface runoff in areas with forest plantation cover than in areas with a different LULC. Vegetation cover is naturally known to reduce runoff, however, the extent of the reduction varies

with the vegetation type (Hosseini *et al*., 2017; Luo *et al*., 2020). Forests were noted to produce less runoff and high evapotranspiration rates when compared to grassland (Madani *et al*., 2018; Wang *et al*., 2019). The results of the study showed a similar pattern; the upper reaches where the dominating cover is grassland, less evapotranspiration was observed while, there was high surface runoff compared to the forested areas in the middle reaches of the catchment. Furthermore, studies have reported a decrease in runoff, especially during low flow period in the CRC. Hadebe (2001) reported that forest plantations have reduced the MAR of the primary catchment by 14.8% during high flows and by 24% during low flows, while Kleynhans *et al*. (2013) indicated that the flows have been reduced by 18% during the dry period.

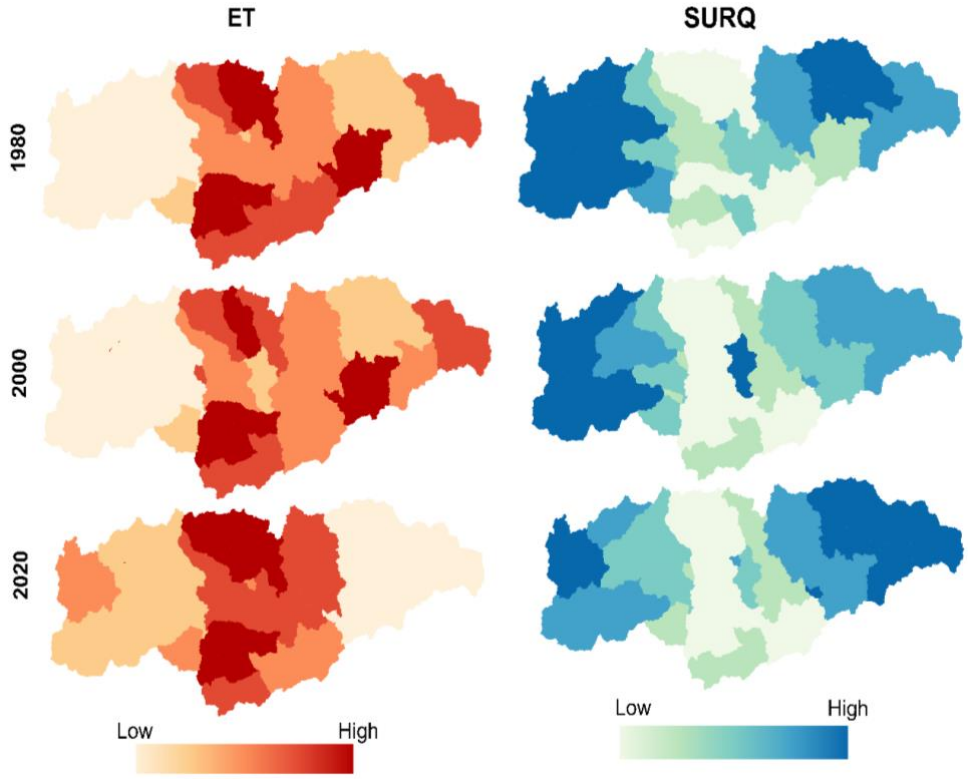

Figure 5.7: Evapotranspiration and Surface runoff from 1980 to 2020

Given the increase in forest plantation from 1980 to 2020, this could also be one of the reasons for the declining streamflow over the study period as observed in **Error! Reference source not found.**8 (a-c). The simulated and observed streamflow trends of the catchment from 1980 to 2020 is for the X2H032 station because it showed better performance than all the other stations. Based on Figure 5.7, both simulated and observed flows indicate a decreasing trend from 1980 to 2020, with an R^2 of 0.0002 and 8E-09 for simulated flow and observed flow, respectively, for the year 1980. For

the year 2000, an R^2 of 0.0046 for the simulated and R^2 of 0.0195 were for the observed flow and for the year 2020. The R^2 varies between 0.1503 for simulated streamflow and 0.1585 for observed streamflow.

a)

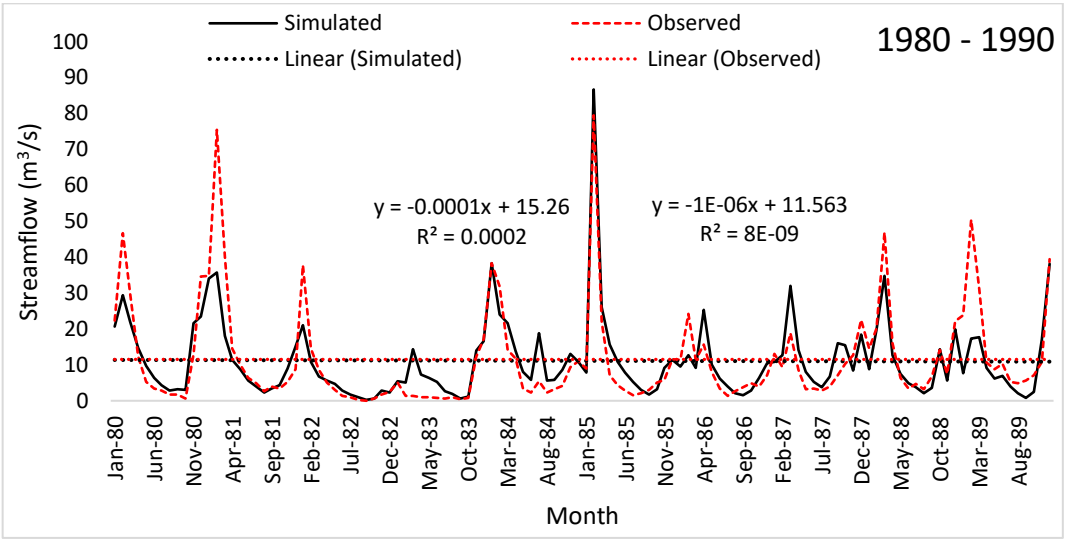

b)

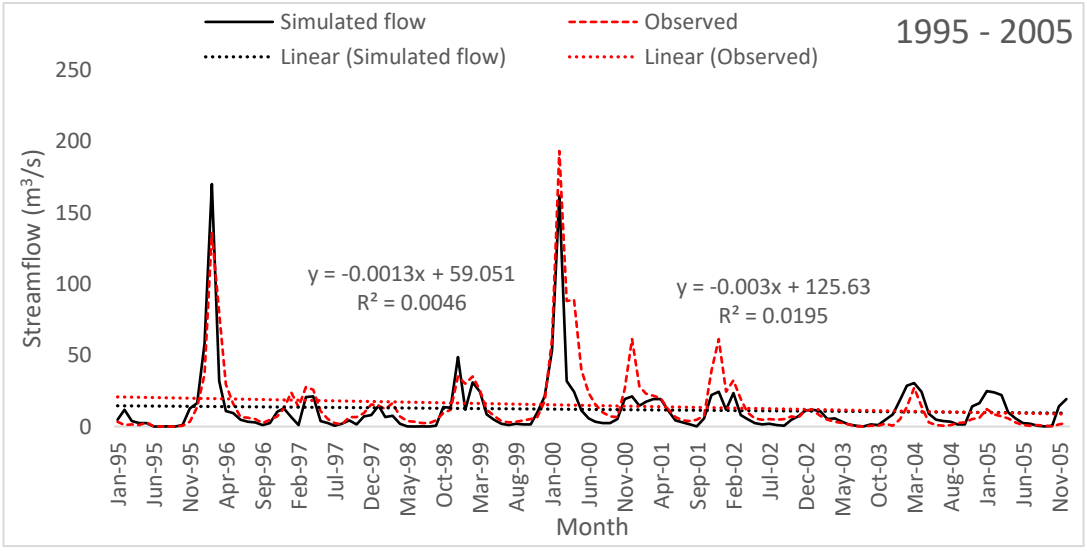

c)

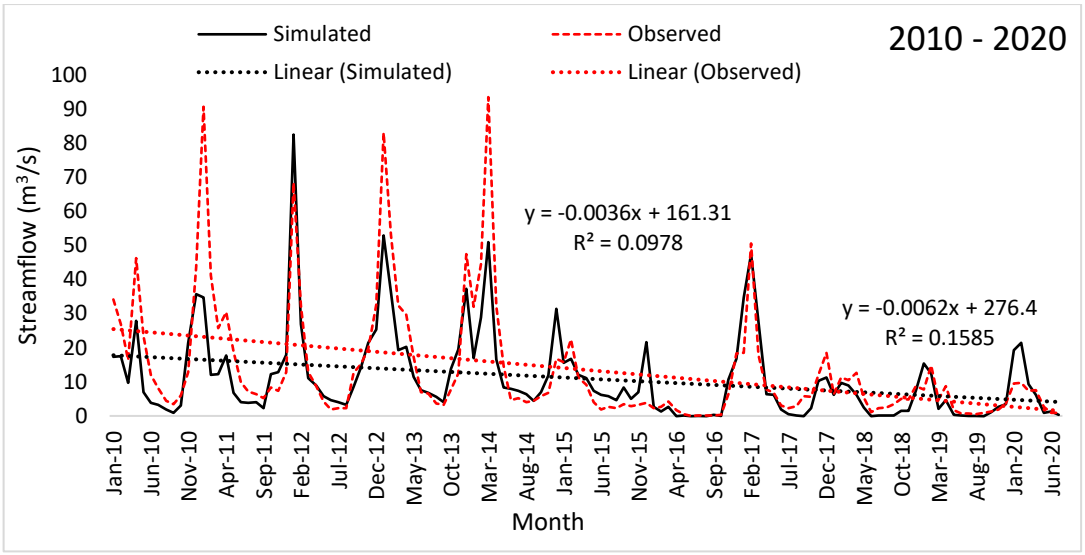

Figure 5.8: Streamflow trend (a) 1981-1990, (b) 2000 – 2005 and (c) 2010-2020.

Eucalyptus tree species were reported to show more effects on streamflow from their third year while pines start to respond from the 5th year onwards (Hadebe, 2001). The catchment is also host to other vegetations, such as guava, lantana, black mattle and syringa, and these were also classified as alien vegetation by Versveld (1998). Versveld (1998) added that these alien species reduce about 19% of MAR in the upper catchment, 10% in the middle catchment and the least affected were in the lower Crocodile River because these plants only reduced 2% of the MAR.

The middle catchment was not only noted as a hotspot for forest plantation, but also a hotspot for built-up areas. In 1987, Bate *et, al*., (1999) reported that water use for domestic, municipal, industrial, and mining purposes amounted to 20 million m^3 per year for the entire catchment and this was estimated to increase to 78 million m^3 in 2015. Approximately 14.6 million m^3/a has been allocated to the City of Mbombela from the CRC (Mbombela SoER, 2003). Due to built-up areas occupying a small portion of the catchment (2.8%), evapotranspiration rates in this part of the catchment may also be influenced by other LULC classes such as savannah, forest plantation, grassland, and cultivated area. In addition, the impacts on evapotranspiration, surface runoff and consequently, streamflow, are not as pronounce as the impacts from forest plantation and cultivation or any large land-use class. Built-up areas are known to increase runoff (Kumar *et al*., 2017), however, in highly-vegetated areas, changes in the streamflow by built-up areas are not as evident. It has been further highlighted that water allocated to this class is lower compared to irrigation and afforestation

requirements. Similar findings were noted in Little River found in Tennessee, where urban areas were occupying less than 12% of the catchment (Zhu and Li, 2014). This latter study demonstrated a reduction in the impact of the urban area on streamflow after a slight increase in forest resulted in low streamflow within the national park.

In the lower reaches, evapotranspiration showed a decreasing trend from 1980 to 2020; this can be attributed to the decrease of natural forest cover. The lower catchment was identified as a hotspot for irrigated crops and is mostly covered by savannah vegetation. It should also be noted that the distribution of vegetation is also influenced by the climate (Sheil, 2018). Dry regions usually do not have dense vegetation covers; low rainfall areas promote less plant growth (MPCOGTA, 2018). The decrease in the natural forest results in increased savannah/bushland cover, thus resulting in increased surface runoff (MOCOGTA, 2018), therefore, there was more surface water flow in 2020 compared to 1980. Mussa *et al*., (2015) reported that the lower Crocodile River is the driest part of the catchment, however it has the highest water demand. The high demand can be due to the high amounts of irrigation requirements resulting from the increasing crops production in the lower catchment since the 1980s. In addition, MEGDP (2011) indicated that most water from this catchment is used for irrigation with about 46% supplying irrigation requirements followed by afforestation. Water demand in the agriculture sector is higher between December and January and this was estimated to be about 570 million m^3 per year. Compared with the middle Crocodile River, the lower catchment was estimated to be the most stressed sub-catchment (Mussa *et al*., 2015). According to Deksissa *et al*., (2003), irrigation abstraction and the decreased inflows by afforestation have resulted in low flows during winter within the Crocodile River Catchment.

Burning was also noted as a problem in the catchment and most burning activities affect natural vegetation and forest plantation. Moran-Tejeda *et al*. (2015) stated that wildfires can modify hydrological dynamics because they affect vegetation and soil properties. Other major land-use changes in catchment include the construction of the Kwena Dam in 1984. As stated, Kwena Dam was constructed to regulate the flow of the Crocodile River and for irrigation purposes (van der Laan *et al*., 2012). It is used to maintain a minimum flow of 7 m^3/s for irrigation in the lower reaches of the catchment during dry month and to also assist in flushing out wastewater effluent discharges from towns such as Mbombela (van der Laan *et al*., 2012). The Kwena

Dam was reported to have negatively impacted streamflow immediately after its construction, such as dampening the peak flows and increasing low flow, however, the effects are reduced further downstream due to the joining tributaries (Saraiva-Okello *et al*., 2015).

5.3 Chapter Summary

The model performed well in simulating the streamflow, especially the calibration period, the low performance indicators for the validation period can be attributed to the input data and the high discharge rates during calibration. However, due to the positive correlation between simulated and observed flow and the R^2 results, the model performance was accepted for this study. Based on the simulated streamflow and the observed streamflow trend, the catchment streamflow showed a decreasing trend for the period of study. The distribution of evapotranspiration and surface waterflow were highly influenced by forest plantation, grassland, and savannah/bushland. Evapotranspiration was higher in the middle reaches and surface runoff was low, but runoff was high in the areas covered by the bushland. The fact that cultivated areas and forest plantation are the biggest water users, the increase in LULC, such as forest plantation and cultivation might have accounted for the decrease in streamflow; this is also supported by Saraiva-Okelllo *et al*., (2015). Furthermore, an increase in evapotranspiration was observed from 1980 to 2020 as 36.3 mm to 533.1 mm, respectively, while surface runoff decreased from 32.79 in 1980 to 2.56 mm in 2020. Based on the decrease in surface runoff and streamflow, built-up areas, therefore, do not have much felt impacts on the hydrological response of the catchment, however, it was also shown that the streamflow dynamics in this catchment are highly affected by climate extremes - floods and droughts. Sheil (2018) indicated that climate and vegetation are interlinked, thus a decrease in streamflow could have led to the decrease in vegetation.

CHAPTER 6: CONCLUSION AND RECOMMENDATION

6.1 Conclusion

The aim of the study was to evaluate the impact of LULC on water resources of Crocodile River Catchment from 1981 to 2020 using remote sensing, QSWAT and QGIS. The catchment was reported to have been over-stressed and to have reached its limit. The CRC plays an important role in irrigation and as source of water supply to numerous communities in the areas of Kanyamazane, Mbombela, Matsulu. The QGIS platform was chosen as the GIS interface due to it being an open-source software and QSWAT was chosen due to its ability to integrate land-use management in simulating the hydrology of a catchment. The study used the SCP plug-in from QGIS to classify and the accuracy results from the classification were satisfactory.

There were changes in LULC observed between 1980 and 2020, with the aid of the classified maps; hotspot areas were mapped based on quaternary catchments and the NDVI value for each hotspot area was calculated. NSE, RSR, PBIAS and correlation were used to evaluate the SWAT model performance and it was concluded that the model gave an acceptable performance. The validation results, however, did not perform as well as the calibration simulation; this was attributed to the input data and the fact that there were more high flow discharges during calibration than validation.

The streamflow showed a negative trend over the study period, however, the streamflow of the catchment is not only affected by the changes in LULC, but it also varies with the climate, for example, the impacts of the 2000 flood and drought of 1982/83. The impacts on evapotranspiration and surface runoff were the focus components of the hydrological cycle. Surface runoff and evapotranspiration are also essential components of the water balance (Kumar *et al.,* 2012). These were used to indicate the changes in vegetation since 1980 because the modification of the nature and density of vegetation alter the hydrological cycle by affecting the evapotranspiration rates, therefore, modifying precipitation.

The study found that there was an increase in forest plantation, built-up areas, and cultivated lands between 1980 and 2020 and these have modified the catchment in LULC setting due to the decrease in natural vegetation cover, such as natural forests and grassland. Surface water flow was low in areas with high evapotranspiration rate

especially, middle catchment. Furthermore, the increase in forest plantation from 1980 to 2020 was consistent with the increase in evapotranspiration, and the decrease in runoff, consequently the decrease in streamflow. The decrease in streamflow could also be attributed to the increase in cultivation, thus, increasing irrigation requirements, however, the study concluded that the changes induced on the quantity of water resources - surface runoff and evapotranspiration - by built-up areas cannot be easily quantified at a catchment level. This is due to the fact that built-up areas only occupy a small area of the catchment (2.8%), hence, any changes are cancelled out by the changes induced by bigger LULC and bigger water users such as forest plantation and cultivation. The competition between cultivation and forest plantation was also indicated in a report by Bate *et al*. (1999) where it was reported that forest plantation reduce run-off and consequently, water flow in the upper and middle catchment, thus affecting water availability downstream for irrigation. Based on the results, forestry and cultivation lands seem to have more impact on the hydrological response of the catchment, thus on the streamflow and water resources, as indicated by several reports (Mpumalanga SoE, 2003); these effects, however are also coupled with the variation of weather patterns.

6.2 Recommendations

6.2.1. Development

The demand and competition for land is to be expected hence measures to regulate and balance economic growth, population and preservation should be put in place (MEGDP, 2011). It is imperative to understand the water resources risks associated with a specific land/water use activity prior to its implementation to ensure that proper measures are taken. As indicated in a number of the Mpumalanga SoE reports (2003, “Over-utilisation of water resources is not a function of the number of people within the catchment but is due to the over-use of water for agricultural and industrial purposes”. Nkosi *et a*l. (2021) emphasised the importance of measures focusing on water demand instead of water supply being at the centre of water management planning. The latter study reiterated the importance of planning all land development around existing water resources.

6.2.1.1. Climate Change

This study proved the vulnerability of CRC to climate extremes, drought and floods, therefore, given the projected increase in temperatures of 2% by 2035, measures that regulate the balance between LULC management, economic growth and water resources, should be strictly adhered to for sustainability (MPCOGTA, 2018). This includes measures such as adapting a holistic approach towards water management and planning and this can be achieved by integrating land reform policies and water management legislations (Nkosi *et al.*, 2021). Furthermore, technologies that reduce the loss of water during drought seasons can be implemented in large water bodies, and other strategies, such as regulating flow, should be strictly adhered to, as it has already been done on the catchment.

6.2.2. Model performance

For the accuracy of the model simulation, it is recommended that the input data be complete and be up to date; this can be ensured by improving monitoring of hydrometeorological variables throughout the CRC.

6.3 Limitations of the study

6.3.1 Model Input Data

The quality and accuracy of input data plays a crucial role in the successful simulation of a model (Thavhana, 2018). Due to the lack or incomplete meteorological data, a single weather station had to be used for all the simulated periods; this could have resulted in the over and/or underestimation of the rainfall distribution in the catchment. The current soil database is old, hence for the accuracy of the model, it is recommended that the soil databases used be updated, since the soil data used for this study was from 2001.

6.3.2 Land-use classification

Since some land-use occur in very small units and cannot be differentiated easily from others, they must be classified differently (Meyer and Turner, 1992). In this study, for example, there was some confusion between forest plantation and other irrigation crops like citruses, therefore, these were classified as “forest”, which could have led to an underestimation of the cultivation areas. The same goes for the natural forest and forest plantation classes.

Despite these mentioned challenges, this study showed the effectiveness of QSWAT, RS and QGIS in simulating and presenting the impacts of LULC changes in a catchment. The use of this model is, therefore, recommended for future monitoring of changes in the catchment, especially given that the catchment will continue to embrace development and built-up areas will continue to increase due to expanding settlements and urban areas. To quantify the changes induced on the hydrological response and water resources by the increase in built-up areas, a similar study, but at sub-catchment or quaternary catchment level is recommended.

REFERENCES

Abbaspour, K.C., Yang, J., Maximov, I., Siber, R., Bogner, K., Mieleitner, J., Zobrist, J. and Srinivasan, R., 2006. Modelling hydrology and water quality in the pre-alpine/alpine Thur watershed using SWAT. *Journal of Hydrology,* 333, 413-430.

Aduah, M.S., Jewitt, G.P.W. and Warburton Toucher, M.L., 2017. Assessing suitability of the ACRU hydrological model in a rainforest catchment in Ghana, West Africa. *Water Science*, 31, 198-214.

Aghsaei, H., Dinan, N. M., Asadolahi, Z., Delavar, M., Foherer, N. and Wagner, P.D., 2019. Effects of dynamic land use/land cover change on water resources and sediment yield in the Anzali wetland catchment, Gilan, Iran. *Science of the Total Environment*, 712. https://doi.org/10.1016/j.scitotenv.2019.136449

Albhaisi, M., Brendonck, L. and Batelaan, O., 2013. Predicted impacts of land use change on groundwater recharge of the upper Berg catchment, South Africa. *Water SA,* Vol. 39 No. 2.

Ali. M., 2013. Effects of Climate Change on Vegetation. In: Climate Change Impacts on Plant Biomass Growth. Springer, Dordrecht. https://doi.org/10.1007/978-94-007-5370-9_4 **DATE ACCESSED???**

Ang, R. and Oeurng, C., 2018. Simulating streamflow in an ungauged catchment of Tonlesap Lake Basin in Cambodia using Soil and Water Assessment Tool (SWAT) model. *Water Science*, 32 (2018) 89–101. https://doi.org/10.1016/j.wsj.2017.12.002

Arnold, J.G., Moriasi, D.N., Gassman, P.W., Abbaspour, K.C., White, M.J., Srinivasan, R., Santhi, C., Harmel, R.D., van Griensven, A., van Liew, M.W., Kannan, N. and Jha, M.K., 2012. SWAT: model use, calibration, and validation. *Model use, calibration and validation,* Vol. 55(4): 1491-1508.

Ashraf, A. and Ahmad, Z., 2012. Integration of Groundwater Flow Modelling and GIS. *Water Resources Management and Modeling*. Purna Nayak IntechOpen, doi: 10.5772/34257. [Online] Available from: https://www.intechopen.com/books/water-resources-management-and-

modeling/integration-of-groundwater-flow-modeling-and-gis [Accessed: 24/8/2018]

Asuero, A.G., Sayago, A. and Gonzales, A.G., 2006. The Correlation Coefficient: An Overview. *Critical Reviews in Analytical Chemistry*, 36, 41–59. doi: 10.1080/10408340500526766

Aynekulu, E., Kassawmar, T. and Tamene, L., 2008. Applicability of ASTER imagery in mapping land use/cover as a basis for biodiversity studies in drylands of northern Ethiopia. *Afr. J. Ecol.,* 46(Suppl. 1), 19–23

Azanga, E., Majaliw, M., Kansiime, F., Mushagalusa, N., Karume, K. and Tenywa, N.N., 2016. Land-use and land cover, sediment and nutrient hotspot areas changes in Lake Tanganyika Basin. *African Journal of Rural Development*, 1(1), pp. 75 – 90.

Baamonde, S., Cabana, M., Sillero, N., Penedo, M. G., Naveira, H. and Novo, J., 2019. Fully automatic multi-temporal land cover classification using Sentinel-2 image data. 23rd International Conference on Knowledge-Based and Intelligent Information & Engineering Systems. *Procedia Computer Science* 159 (2019) 650–657.

Baker, T.J. and Miller S.N., 2013. Using the Soil and Water Assessment Tool (SWAT) to assess land use impact on water resources in an East African watershed. *Journal of Hydrology*, 486 (2013), 100-111.

Basson, M.S. and Rossow, J.D., 2003. Inkomati Water Management Area overview of water resources availability and utilisation. Natural water resource strategy, final. P WMA 06/000/00/0203 **PUBLICATION DETAILS???**

Bate, R., Tran, R. and Mooney L., 1999. An econometric and institutional economic analysis of water use in the Crocodile River Catchment, Mpumalanga Province, South Africa. *WRC Report* No. 885/1/99, Pretoria.

Baus, D., 2017. Overpopulation and the Impact on the Environment. [Online] Available at: https://academicworks.cuny.edu/gc_etds/1906 [Accessed: 24/8/2018].

Berjak, L., 2003. *Water Resource Management in South Africa*. MSc Dissertation, University of Natal, Pietermaritzburg.

Boschet, C. and Rambonilaza, T., 2015. Integrating water resource management and land-use planning at the rural-urban interface: insights from a political economy approach. *Water resources and economics*, 9, 45–59. doi: 10.1016/j.wre.2014.11.005

Boucher, D., 2018. [Blog] The World's Population Hasn't Grown Exponentially for at Least Half a Century. Available at: https://blog.ucsusa.org/doug-boucher/world-population-growth-exponential **DATE ACCESSED???**

Brannstrom, E., 2019. A review on hydrological modelling tools for Nexus assessment-A comparative study. Stockholm, Sweden.

Broge, N.H., Thomsen, A.G. and Andersen, P.B., 2003. Comparison of selected vegetation indices as indicators of crop status. Geoinformation for European-wide integration, Benes (ed.), *Millpress,* Rotterdam, 591–596. ISBN 90-77017-71-2.

Broge, N.H. and Mortensen, J.V., 2002. Deriving green crop area index and canopy chlorophyll density of Winter wheat from spectral reflectance data. *Remote Sensing of Environment*, 81, 45–57.

Calder, I. R., Hall, R. L., Bastablea, H. G., Gunstona, H. M., Shela, O., Chirwab, A. and Kafundub, R., 1995. The impact of land use change on water resources in sub-Saharan Africa: a modelling study of Lake Malawi. *Journal of Hydrology*, 170(1995), 123–135.

Campbell, J. B. and Wynne, R. H., 2011. *Introduction to remote sensing*. (5th ed): The Guilford Press, New York.

Cavur, M., Duzgun, H.S., Kemec, S. and Demirkan, D.C., 2019. Land use and land cover classification of Sentinel 2-A: St Petersburg case study. https://doi.org/10.5194/isprs-archives-XLII-1-W2-13-2019 **DATE ACCESSED???**

Chai, T. and Draxler, R.R., 2014. Root mean square error (RMSE) or mean absolute error (MAE)? –Arguments against avoiding RMSE in the literature. *Geoscience Model Development* 7, 1247–1250. doi:10.5194/gmd-7-1247-2014

Chang, H., 2003. Basin hydrologic response to changes in climate and land use: The Conestoga River Basin, Pennsylvania. *Physical Geography*, 24, 222–247.

Chaves, J., Neill, C., Germer, S., Neto, S.G., Krusche, A. and Elsenbeer, H., 2008. Land management impact on runoff sources in small Amazon watersheds. *Hydrological Processes*, 22, 1766-1775. Doi: 10.1002/hyp.6803

Charlton, S., 2008. The state of land use management in South Africa. Second Economy Strategy: Inequality and Economic Marginalisation. Urban LandMark, South Africa.

Chemura, A., Rwasoka, D., Mutanga, O., Dube, T. and Mushore, T., 2020. The impact of land-use/land cover changes on water balance of the heterogeneous Buzi sub-catchment, Zimbabwe. *Remote Sensing Applications: Society and Environment*, 18. https://doi.org/10.1016/j.rsase.2020.100292

Choi, W. and Deal, B. M., 2008. Assessing hydrological impact of potential land use change through hydrological and land use change modelling for the Kishwaukee River Basin (USA). *Journal of Environmental Management,* 88, 1119–11130, 2008.

City of Mbombela, 2017. City of Mbombela Vision 2030-strategy, final draft.

Colwell, J.E., 1973. *Bidirectional spectral reflectance of grass canopies for determination of above ground standing biomass*. PhD Thesis, University of Michigan, University, Microfilm.

Congedo, L., 2014. Semi-Automatic Classification Plug-in User Manual. *QGIS, Technical Report*. 10.13140/RG.2.1.1219.3524.

Cosgrove, W. J. and Loucks, D. P., 2015. Water management: Current and future challenges and research directions, *Water Resource Research*, 51, 4823–4839. doi:10.1002/2014WR016869

Cuceloglu, G. and Ozturk, I., 2019. Assessing the impact of CFSR and local climate datasets on hydrological modelling performance in the Mountainous Black Sea Catchment. *Water*, 11, 2277.

Dabrwoski, J. M. and de Klerk, L. P., 2013. An assessment of the impact of different land use activities on water quality in the upper Olifants River catchment. *Water SA*, 39 (2), 231–244.

Dechmi, F., Burguete, J. and Skhiri, A., 2012. SWAT application in intensive irrigation systems: Model modification, calibration and validation. *Journal of Hydrology*; 227–238.

Deksissa, T., Ashton, P.J. and Vanrolleghem, P.A., 2003. Control options for river water quality improvement: A case study of TDS and inorganic nitrogen in the Crocodile River (South Africa). *Water SA*, 29(2), pp 209–218.

Department of Department of Cooperative Governance and Traditional Affairs, Mpumalanga Provincial Government (MPCOGTA), 2018. Spatial Challenges and Opportunities Report. Final draft, Mpumalanga Spatial Development Framework.

Department of Environmental Affairs (DEA), 2017. South Africa's 2nd annual Climate Change Report. Department of Environmental Affairs, Pretoria.

Department of Water Affairs, 2009. Inkomati Water Availability Assessment – Water Requirements. Department of Water Affairs, Pretoria. Report PWMA 05/X22/00/1708

DWA, 2014. Water Requirements and Availability Reconciliation Strategy for the Mbombela Municipal Area. Current and future water requirements and water resources. Department of Water Affairs, Pretoria.

DWA, 2013. Water Requirements and Availability Reconciliation Strategy for the Mbombela Municipal Area. Current and future water requirements and water resources, Final Strategy. Department of Water Affairs, Pretoria.

Dile, Y.T., Daggupati, P., George, C., Srinivasan, R. and Arnold, J., 2016. Introducing a new open-source GIS user interface for SWAT model. *Environmental*

Modelling & Software, 85, 129–138. https://doi.org/10.1016/j.envsoft.2016.08.004.

Din, M., Zheng, W., Rashid, M., Wang, S. and Shi, Z., 2017. Evaluating hyperspectral vegetation indices for leaf area index estimation of *Oryza sativa* L. At diverse phenological stages. *Frontier in Plant Science*, 40 (820). doi: 10.3389/fpls.2017.00820

Dlamini, L., 2013. *Modelling of Standardised Precipitation Index using remote sensing for improved drought monitoring*. MSc Thesis/Dissertation, Faculty of Engineering and Built Environment, University of Witwatersrand, Johannesburg, South Africa.

Donnenfeld, Z., Crookes, C. and Hedden, S., 2018. A delicate balance water scarcity in South Africa. *Southern Africa Report* 13, March 2018. Pretoria.

Duraisamy, V., Bendapudi, R. and Jadhav, A., 2018. Identifying hotspots in land use land cover change and the drivers in a semi-arid region of India. *Environmental Monitoring Assessment*, 190, 535. https://doi.org/10.1007/s10661-018-6919-5

Easton, Z.M. and Bock, E. (2015). *Hydrology basics and the hydrologic cycle. Virginia Cooperative Extension.* Virginia State University, Petersburg, USA. VT/1015/BSE-191P.

El-Sadek, A. and Irvem, A., 2014. Evaluating the impact of land use uncertainty on the simulated streamflow and sediment yield of the Seyhan River basin using the SWAT model. *Turkish Journal of Agriculture and Forestry*, 38, 515-330. doi:10.3906/tar-1309-89

Escobar, F., Hunter, G., Bishop, I. and Zerger, A., 2008. Introduction to GIS. Department of Geomatics, The University of Melbourne, Melbourne, Australia. http://www.sli.unimelb.edu.au/ **DATE ACCESSED???**

FAO and ISRIC, 2003. Soil and Terrain database for Southern Africa (1:2 million scale). FAO Land and Water Digital Media Series 25, ISRIC and FAO, Rome.

FAO, 2017. Sustainable Land Management (SLM) in practice in the Kagera Basin. Lessons learned for scaling up at landscape level - Results of the Kagera Transboundary Agro-ecosystem Management Project (Kagera TAMP). Food and Agriculture Organization of the United Nations, Rome, Italy. 440 pp

Ferrar, A. A. and Lotter, M. C., 2007. *Mpumalanga Biodiversity Conservation Plan Handbook.* Mpumalanga Tourism and Parks Agency, Nelspruit.

Feyen, L., Vázquez, R., Christiaens, K., Sels, O., Feyen, J., 2000. Application of adistributed physically-based hydrological model to a medium size catchment. *Hydrological Earth System Science,* 4, 47–63.

Fourie, L., Rouget, M. and Lotter, M., 2014. Landscape connectivity of the grassland biome in Mpumalanga, South Africa. *Austral Ecology*, doi:10.1111/aec.12169.

Franklin, S.E., He, Y., Pape, A., Guo, X. and McDermid, G.J., 2009. Landsat-comparable land cover maps using ASTER and SPOT images: A case study for large-area mapping programmes. *International Journal of Remote Sensing*, 32(8).

Gabiri, G., Leemhuis, C., Diekkruger, B., Naschen, S.S. and Thonfeld, F., 2019. Modelling the impact of land use management on water resources in a tropical inland valley catchment of central Uganda, East Africa. *Science of the Total Environment,* 653, 1052–1066.

Gandhi, M.G., Parthiban, S., Thummalu, N., and Christy, A., 2015. NDVI: Vegetation change detection using remote sensing and gis – A case study of Vellore District. 3rd International Conference on Recent Trends in Computing 2015 (ICRTC-2015) *Procedia Computer Science*, 57,1199–1210.

Gao, Q., Guo, Y., Xu, H., Ganjurjav, H., Li, Y., Wan, Y., Qin, X., Ma, X. and Liu, S., 2016. Climate Change and its impacts on vegetation distribution and net primary productivity of the alpine ecosystem in the Qinghai-Tibetan Plateau. *Science of the total environment*, 554-555, pp. 34–41. https://doi.org/10.1016/j.scitotenv.2016.02.131.

Garrity, G., 2009. Ground truth. *Standards in Genomic Sciences*, 1, 91–92. DOI:10.4056/sigs.50595

Gassman, P.W., Reyes, M.R., Green, C.H. and Arnold, J.G., 2007. The soil and water tool: historical development, applications and future research directions. *American Society of Agricultural and Biological Engineers*, 50(4), 1211–1250.

Gee, G.W., Fayer, M.J., Rockhold, M.L. and Campbell, M.D., 1992. Variation in recharge at the Hanford site. *Northwest Science*, 66, 237–250

Giardino, C., Bresciani, M., Villa, P. and Martinelli, A., 2010. Application of Remote Sensing in Water Resource Management: The Case Study of Lake Trasimeno, Italy. *Water Resources Management*, 24(14), pp. 3885–3899.

Golmohammadi, G., Prasher, S., Madani, A. and Rudra, R., 2014. Evaluating three hydrological distributed watershed models: MIKE-SHE, APEX, SWAT. *Hydrology*, 1, 20–39. doi:10.3390/hydrology1010020

Goodchild, M.F., 2011. Spatial Thinking and the GIS User Interface. International Conference: Spatial Thinking and Geographic Information Sciences 2011. *Procedia Social and Behavioral Sciences* 21, 3–9.

Graham, D.N. and Butts, M.B., 2015. *Flexible, integrated watershed modelling with MIKE SHE in Watershed Models*. Eds. VP Singh and Frevert, D.K. 245–272. CRC Press, Florida.

Guay, K. C., Beck, P. S. A., Berner, L. T., Goetz, S. J., Baccini, A. and Buermann, W., 2014. Vegetation productivity patterns at high northern latitudes: a multi-sensor satellite data assessment. *Global Change Biology*, 20(10), 3147–3158. https://doi.org/10.1111/gcb.12647.

Gumindoga, W., Rwasoka, D.T., Ncube, N., Kaseke, E. and Dube, T., 2018. Effect of landcover/land-use changes on water availability in and around Ruti Dam in Nyazvidzi catchment, Zimbabwe. *Water SA*, 44(1), 136–145. http://dx.doi.org/10.4314/wsa.v44i1.16

Gyamfi, C., Ndambuki, J.M. and Salim, R.W., 2016. Application of SWAT Model to the Olifants Basin: Calibration, Validation and Uncertainty Analysis. *Journal of*

Water Resource and Protection, 2016, 8, 397–410. http://dx.doi.org/10.4236/jwarp.2016.83033

Gyedu-Ababio, T.K. and Van Wyk, F., 2004. Effects of human activities on the Waterval River, Vaal River catchment, South Africa. *African Journal of Aquatic Science*, 29:1, 75–81, doi: 10.2989/1608591040950379

Ha, L.T., Bastiaanssen, W.G.M., van Griensven, A., van Dijk, A.I.J.M. and Senay, G.B., 2017. SWAT-CUP for Calibration of Spatially Distributed Hydrological Processes and Ecosystem Services in Vietnamese River Basin using Remote Sensing. *Hydrological Earth System Science discuss*, http://doi.org/10.5194/hess-2017-251 **DATE ACCESSED???**

Hadebe, X.M.J., 2001. *Determination of streamflow reduction associated with afforestation on a selected quaternary catchment of the Crocodile River, Mpumalanga.* MSc dissertation, Faculty of Science, University of Johannesburg, Johannesburg, South Africa.

Hamdan, A.N.A., Almuktar, S. and Scholz, M., 2021. Rainfall-runoff modeling using the HEC-HMS model for the Al-Adhaim River Catchment, Northern Iraq. *Hydrology*, 8, 58. https://doi.org/10.3390/hydrology8020058

He, C., 2003. Integration of geographic information systems and simulation model for watershed management. *Environmental Modelling and Software,* , 18, pp. 809–813.

Herpertz, D., 1994. *Modellierung der hydrologischen prozessdynamik in einzugsgebietsmodell ACRU*. MSc dissertation, Bonn University, Germany.

Hosseini, M., Geissen, V. and González-Pelayo, O., 2017. Effects of fire occurrence and recurrence on nitrogen and phosphorus losses by overland flow in maritime pine plantations in north-central Portugal. *Geoderma,* 289, 97–106.

Inkomati Water Management Area, 2008. *The development of comprehensive water conservation and water demand management strategy and business plans - domestic sector*. Mbombela Local Municipality, Mpumalanga.

Isbaex, C. and Coelho, A. M., 2021. The Potential of Sentinel-2 satellite images for land-cover/land-use and forest biomass estimation: A review, forest biomass - from trees to energy, Ana Cristina Gonçalves, Adélia Sousa and Isabel Malico. *IntechOpen*, DOI: 10.5772/intechopen.93363

Jackson, B., 2014. *An Adaptive operational water resources management framework for the crocodile river catchment*. MSC dissertation, Centre of Water Resources Research, University of KwaZulu-Natal, Pietermaritzburg, South Africa.

Jamil, R.M., 2020. A Development of a 'ArcSWAT' Surface Runoff Model for Estimating Urban Precipitation Recharge. 2nd International Conference on Tropical Resources and Sustainable Sciences. *IOP Conf. Series: Earth and Environmental Science*, 549. doi:10.1088/1755-1315/549/1/012010

Jin, X., Jin, Y. and Mao, X., 2019. Land Use/Cover Change Effects on River Basin Hydrological Processes Based on a Modified Soil and Water Assessment Tool: A Case Study of the Heihe River Basin in Northwest China's Arid Region. *Sustainability,* 11, 1072. doi:10.3390/su11041072

Joerin, F., Theriault, M. and Musy, A., 2001. Using GIS and Outranking Multicriteria Analysis for Land-Use Suitability Assessment. *International Journal of Geographical Information Science*. 15(2), 153–174.

Jordan, C.F., 1969. Derivation of leaf-area index from quality of light on the forest floor. *Ecology,* 50(4), pp. 663 – 666.

Jung, C.-G, Lee, D.-R. and Moon, J.-W., 2016. Comparison of the Penman-Monteith method and regional calibration of the Hargreaves equation for actual evapotranspiration using SWAT-simulated results in the Seolma-cheon basin, South Korea. *Hydrological Sciences Journal,* 61,4,793–800. doi: 10.1080/02626667.2014.943231

Kanianska, R., 2016. Agriculture and its impact on land use, environment, and ecosystem services. A. Almusaed (Ed.), *Landscape Ecology - The Influences of Land Use and Anthropogenic Impacts of Landscape Creation,* InTech Pub, pp. 3–26, 10.5772/63719 Chapter 1

Kaushal, S.S., Gold A.J. and Mayer, P.M., 2017. Land use, climate, and water resources – Global stages on interaction. *Water, 9, 815.* doi:10.3390/w9100815

Khan, S. and Mohiuddin, K., 2018. Evaluating the parameters of ArcGIS and QGIS for GIS applications. *International Journal of Advance Research in Science and Engineering*, 7(3).

Khatam, S. and Khazaei, B., 2014. Benefits of GIS Application in Hydrological Modeling: A Brief Summary. *Journal of Water Management and Research*, 70, 41–49.

Kleynhans, C.J., Thirion, C., Roux, F., Hoffmann, A., Marais, H. and Diedericks, G., 2013. Eco-status of the Crocodile River Catchment, Inkomati River System. Inkomati-Usuthu Catchment Area, Mpumalanga. **PUBLICATION DETAILS???**

Konapala, G., Mishra, A.K., Wada, Y. and Mann, M.E., 2020. Climate change will affect global water availability through compounding changes in seasonal precipitation and evaporation. *National Communication*, 11, 3044

Krause, P., Boyle, D.P. and Base, F., 2005. Comparison of different efficiency criteria for hydrological model assessment. *Advances in Geosciences,* 5, 89–97.

Kuemmerle, T., Levers, C., Erb, K., Estel, S., MartinR Jepsen, M.R., Müller, D., Plutzar, C., Stürck, J., VerkerK, P.J., Verburg, P.H. and Reenberg, A., 2016. Hotspots of land use change in Europe. *Environmental Research Letters,* 11 (2016) 064020. doi:10.1088/1748-9326/11/6/064020

Kumar, N., Tischbein, B., Kusche, J., Beg, M.K. and Bogardi, J. J., 2017. Impact of land-use change on the water resources of the Upper Kharun Catchment, Chhattisgarh, India. *Regional Environmental Change*, 17, 2373–2385.

Kusangaya, S., Warburton, M. and van Garderen, E.A., 2017. Use of ACRU, a distributed hydrological model, to evaluate how errors from downscaled rainfall are propagated in simulated runoff in uMngeni catchment, South Africa. *Hydrological Sciences Journal,* 62:12, 1995–2011, doi: 10.1080/02626667.2017.1349317

Lekha, S. L and Kumar, S. S., 2018. Classification and Mapping of Land Use Land Cover change in Kanyakumari district with Remote Sensing and GIS techniques. *International Journal of Applied Engineering Research*, 13(1), pp. 158–166.

Liu, J., Zhang, C., Kou, L. and Zhou, Q., 2017. Effects of climate and land use change on water resources in the Taoer River. *Advances in Meteorology*, 2017, doi.org/10.1155/2017/1031854

Lo, C.P., Quattrochi, D.A. and Luvall, J.C., 1997. Application of high-resolution thermal infrared remote sensing and GIS to assess the urban heat island effect. International. *Journal of Remote Sensing*, 18, pp. 287–303.

Luo, J., Zhou, X., Rubinato, M., Li, G., Tian, Y. and Zhou, J., 2020. Impact of Multiple Vegetation Covers on Surface Runoff and Sediment Yield in the Small Basin of Nverzhai, Hunan Province, China. *Forests*, 11, 329. doi:10.3390/f11030329

Ma, L., He, C., Bian, H. and Sheng, L., 2016. MIKE SHE modeling of ecohydrological processes:Merits, applications, and challenges. *Ecological Engineering*, 96, 137-149. http://dx.doi.org/10.1016/j.ecoleng.2016.01.008

Madani, E.M., Jansson, P.E. AND Babelon, I., 2018. Differences in water balance between grassland and forest watersheds using long-term data, derived using the CoupModel. *Hydrology Research*, 49.1, 72–89.

Mancino, G., Ferrara, A., Padula, A. and Nole, A., 2020. Cross-Comparison between Landsat 8 (OLI) and Landsat 7 (ETM+) Derived Vegetation Indices in a Mediterranean Environment. *Remote Sensing,* 12, 291. doi:10.3390/rs12020291

Marwa, A., Okke, B. and Willy, B., 2011. *Application of SWAT Model in land-use change in the Nile River Basin: A Review*. SWAT.

Masereka, E.M., Ochieng, G.M. and Snyman, J., 2018. Statistical analysis of annual maximum daily rainfall for Nelspruit and its environs. J*àmbá: Journal of Disaster Risk Studies* 10(1), a499. https://doi.org/10.4102/jamba.v10i1.499

Masindi, V. and Dunker, L.C., 2016. *State of Water and Sanitation in South Africa*. CSIR Built Environment. CSIR, Pretoria.

Masud, M.J. and Bastiaanssen, W.G.M. 2017. *Remote sensing and GIS applications in Water Resources Management.* Chapter 16, in: Alla Bakhsh and Muhammad Rafiq (Eds), Choudhry University of Agriculture, Faisalabad, Pakistan, pp. 351 -373.

Mathieu, R. and Yves, R., 2005. Intensity and spatial extent of drought in Southern Africa. *Geophysical Research Letters,* 32, L15702. doi:10.1029/2005GL022436

Mbombela State of Environment, 2003. Identification of key environmental indicators. [Online] Available at: http://soer.deat.gov.za/dm_documents/MbombelaSoERKeyIndicators_e3z70.pdf [Accessed 15/05/2018]

Mbombela Local Municipality, 2011. Spatial Development FINAL Draft 2011 – 2030 Spatial Development Framework (SDF) http://www.mbombela.gov.za/part%201%20sdf%202012.10.pdf [Accessed: 21/05/2018]

McMichael, C.E. and A.S. Hope, 2007. Predicting Streamflow Response to Fire-Induced Landcover Change: Implications of Parameter Uncertainty in the MIKE SHE Model. *Journal of Environmental Management*, 84:245-256.

Mengistu, A.G., van Rensburg, L.D. and Woyessa, Y.E., 2019. Techniques for calibration and validation of SWAT model in data scarce arid and semi-arid catchments in South Africa. *Journal of Hydrology: Regional Studies*, 25(2019) 100621.

Meyer, B. M. and Turner II, B. L., 1992. Human population growth and global land-use/cover change. *Annual Review of Ecological Syst*em 23:39–61. https://www.jstor.org/stable/2097281

Molobela, I.P. and Sinha, P., 2011. Management of water resources in South Africa: A review. *African Journal Environmental Science and Technology*, 5(12), pp. 993–1002. doi: 10.5897/AJEST11.136

Moore, D. S., Notz, W. I, and Flinger, M. A., 2013. *The basic practice of statistics* (6th ed.). New York, NY: W. H. Freeman and Company.

Morán-Tejeda, E., Zabalza, J., Rahman, K., Gago-Silva, A., 2015. Hydrological impacts of climate and land-use changes in a mountain watershed: uncertainty estimation based on model comparison. *Ecohydrology,* 8, 1396–1416.

Moriasi, D.N., Arnold, J.G., Van Liew, M.W., Bingner, R.D., Harmel, R.D. and Veith, T.L., 2007. Model Evaluation guidelines for systematic quantification of accuracy in watershed simulations. *American Society of Agricultural and Biological Engineers,* 50(3), 885–990.

Mosimanegape, K., 2016. Integration of physicochemical assessment of water quality with remote sensing techniques for the Dikgathong Damin Botswana. [Online] Available at: http://researchdatabase.ac.zw/5828 [Accessed 31 8 2018]

Mpumalanga Economic Growth & Development Path (MEGD), 2011. Mpumalanga.

MMDC (Mpumalanga Maputo Development Corridor and Spatial Development Initiative). 1998. *Resource Opportunities and Constraints Report.* Undertaken by Mpumulelo Consortium for Mpumalanga Provincial Government in May 1998. Mpumalanga.

Mucina, L. and Rutherford, M.C., 2006. *The Vegetation of South Africa, Lesotho and Swaziland*. Strelitzia 19. South African National Biodiversity Institute, Pretoria.

Mukheibir, P. and Sparks, D., 2003. Water resource management and climate change in South Africa: Visions, driving factors and sustainable development indicators. *Report for Phase I of the Sustainable Development and Climate Change project.* Energy and Development Research Centre, University of Cape Town, Cape Town, South Africa.

Muller, M., Schreiner, B., Smith, L., van Koppen, B., Sally, H., Aliber, M., Cousins, B., Tapela, B., van der Merwe-Botha, M., Karar, E. and Pietersen, K., 2009*. Water security in South Africa. Development Planning Division*. Working Paper Series No.12, DBSA: Midrand

Municipal Area, 2014. Current and Future Water Requirements and Water Resources. Final February 118|Page. DWA Report Number PWMA 05/X22/00/2012/3. [Online] Available at: http://www.dwa.gov.za/Projects/WRAR/Documents/Mbombela%20Reconciliation%20Strategy%20%20FINAL%20signed.pdf [Accessed 14/05/2018]

Mussa, F.E.F., Zhou, Y., Maskey, S., Masih, I. and Uhlenbrook, S., 2015. Groundwater as an emergency source for drought mitigation in the Crocodile River Catchment, South Africa. *Hydrological Earth System Science*, 19, 1093–1106. doi:10.5194/hess-19-1093-2015.

Mutamba, J. and Busari, O., 2011. Water Resources Assessment for Mbombela Local Municipality in South Africa. *British Library Conference Proceedings*. [Online] Available at: http://www.wseas.us/e-library/conferences/2011/Cambridge/GEWACO/GEWACO-10.pdf [Accessed: 19/05/2018]

Namugize, J.N., Jewitt, G. and Graham, M., 2018. Effects of land use and land cover changes on water quality in the uMngeni River catchment, South Africa. *Physical Chemistry Earth*, 105:247–264.

National Department of Agriculture, 2005. Strategic Plan for the National Department of Agriculture. Directorate Agricultural Information Services, Pretoria. 8http://www.nda.agric.za/docs/strat_plan_05.htm

National Water Act, 1998. Department of Water Affairs, Pretoria.

Nel, V., 2009. Can the South African land use management system be an effective tool in creating low(er) carbon cities? 45th ISOCARP Congress. Porto, Portugal 18-22 October 2009.

Nel, J.L. and Driver, A., 2015. National River Ecosystem Accounts for South Africa. *Discussion document for Advancing SEEA Experimental Ecosystem Accounting Project, October 2015*. South African National Biodiversity Institute, Pretoria.

New Jersey Stormwater, 2016. Chapter 1: Impacts of development on runoff. New Jersey stormwater best management Practices Manual. New Jersey.

Nhamo, L., Mabhaudi, T. and Modi, A.T., 2019. Preparedness or repeated short-term relief aid? Building drought resilience through early warning in southern Africa. W*ater SA.* 45(1), 75–85.

Nkosi, M., Mathivha, F.I. and Odiyo, J.O., 2021. Impact of land management on water resources, a South African Context. *Sustainability*, 13, 701. https://doi.org/10.3390/su13020701

Nugroho, P., Marsonob, D., Sudirac P. and Suryatmoj, H., 2013. Impact of land-use changes on water balance. The 3rd International Conference on Sustainable Future for Human Security SUSTAIN 2012. *Procedia Environmental Science,* 17(2013), 256–262.

Oleyiblo, J.O. and Li, Z.-j., 2010. Application of HEC-HMS for flood forecasting in Misai and Wan'an catchments in China. *Water Science Engineering*, 3, 14–22.

Owuor, S.O., Butterbach-Bahl, K., Guzha, A.C., Rufino, M.C., Pelster, D.E., Diaz-Pines, E. and Breuer, L., 2016. Groundwater recharge rates and surface runoff response to land use and land cover changes in semi-arid environments. *Ecological Processes,* 5, 16. doi 10.1186/s13717-016-0060-6

Oxford Dictionaries, https://www.lexico.com/defination/hotspot [Accessed 9 April 2020]

Para, V., Arumi, J.L. and Munoz, E., 2019. Isentifying a suitable model for low-flow simulation in watersheds of South-Central Chile: A study based on a sensitivity analysis. *Water,* 11(7). doi:10.3390/w1107506

Peters, N. E., Meybeck, M. and Chapman, D. V., 2006. Effects of Human Activities on Water Quality. Available online: http://onlinelibrary.wiley.com/doi/10.1002/0470848944.hsa096/abstract **DATE ACCESSED???**

Petersen, C.R., Jovanovic, N.Z., Le Maitre, D.C. and Grenfell, M.C., 2017. Effects of land use change on streamflow and stream water quality of a coastal catchment. *Water SA,* 43(1), 139–152. https://dx.doi.org/10.4314/wsa.v43i1.16

Phukoetphim, P., 2014. *Multi-model approach for combined outputs of rainfall-runoff models.* PhD thesis, The University of Auckland, Auckland, New Zealand.

Pretorius, D.J., 2009. *Mapping Land Use Systems at National Scale for Land Degradation Assessment Analysis in South Africa*. In support of the soil protection programme. Department of Agriculture, Pretoria, South Africa.

Pugnaire, F.I., Morillo, J.A., Penuelas, J., Reich, P.B., Bardgett, R.D., Gaxiola, A., Wardle, D.A. and van der Putten, 2019. Climate change effects on plant-soil feedbacks and consequences for biodiversity and functioning of terrestrial ecosystems. *Science Advances*, 5(11), pp. 1 – 11.

Quan, Z., Xianfeng, Z. and Miao, J., 2011. Eco-environment variable estimation from remote sensed data and eco-environment assessment: models and system. *Acta Botanica Sinica*, vol. 47, pp. 1073–1080.

Ques10, 2020. Diagram of hydrological cycle and aquifers. Availabe at: https://www.ques10.com/p/28761/diagram-of-hydrological-cycle-and-aquifers-1/ [Accessed on 23/07/2021]

Rahbeh, M., Chanasyk, D. and Miller, J., 2011. Two-Way Calibration-Validation of SWAT Model for a Small Prairie Watershed with Short Observed Record. *Canadianm Water Resources Journal / Revue canadienne des ressources hydriques,* 36:3, 247-270, doi: 10.4296/cwrj3603884

Refsgaard, J.C. and Abbott, M.B., 1996. The role of distributed hydrological modelling in water resource management. In: MB Abbott, JC Refsgaard, (eds.). *Distributed hydrological modelling*. Netherlands: Kluwer Academic Publishers, pp. 55–69.

Reif, M., Piercy, C., Jarvis, J., Sabol, B., Macon, C., Loyd, R., Colarusso, P., Dierssen, H. and Aitken, J., 2012. *Ground Truth Sampling to Support Remote Sensing Research and Development: Submersed Aquatic Vegetation Species Discrimination Using an Airborne Hyperspectral/Lidar System*. U.S Army Engineer Research and development center. ERDC TN-DOER-E30.

Richardson, A.J. and Weigand, C., 1977. Distinguishing vegetation from soil background information. *Photogrammetric Engineering and Remote Sensing*, 43(12), pp. 1541 – 1552.

Riddell, E., Pollard, S., Mallory, S. and Sawunyama, T., 2014. A methodology for historical assessment of compliance with environmental water allocations: lessons from the Crocodile (East) River. *South Africa, Hydrological Sciences Journal,* 59:3-4, 831-843, doi: 10.1080/02626667.2013.853123

Ridwansyah, I., 2010. *Applying SWAT and GIS To Predict Impact of Land use Change on Water Yield and Land use Optimazing In Upper Cimanuk Catchment Area.* 5th International Remote Sensing & GIS workshop Series on Demography, Land use - Land Cover and Disaster conference Proceedings, Bandung, Indonesia, January 2012.

Rimba, A. B., Chapagain, S. K., Masago Y, *et al*., 2019. Investigating water sustainability and land use/land cover change (LULC) as the impact of tourism activity in Bali, Indonesia. In: IGARSS 2019–2019 IEEE International Geoscience and Remote Sensing Symposium. https://ieeexplore.ieee.org/document/8900060 , Yokohama, Japan, Japan, pp 6531–6534. Accessed 28 July-2 Aug 2019

Ritter, A. and Muñoz-Carpena, R., 2013. Performance evaluation of hydrological models: Statistical significance for reducing subjectivity in goodness-of-fit assessments. *Journal of Hydrology*, Vol. 480, pp. 33–45. https://doi.org/10.1016/j.jhydrol.2012.12.004.

Rodgers, J. L. and Nicewander, W. A., 1998. Thirteen ways to look at the elation coefficient. *The American Statistician*, 42, 59–66

Rostamian, R., Jaleh, A., Afyuni, M., Mousavi, S. F., Heidarpour, M., Jalalian, A. And Abbaspour, K.C., 2008. Application of a SWAT model for estimating runoff and sediment in two mountainous basins in central Iran. *Hydrological Sciences Journa*l, 53:5, 977–988, doi: 10.1623/hysj.53.5.977

Rouault, M., Monyela, B., Kounge, R.A.I., Njouodo, A.S.N., Dieppois, B., Illig, S. and N., Keenlyside, 2019. *Ocean Impact on Southern African Climate Variability and Water Resources*. Pretoria, South Africa, WRC Report No. 2425/1/18.

Rouse Jr, J.W., Haas, R., Schell, J. and Deering, D., 1974. Monitoring vegetation systems in the great plains with erts. *NASA Special Publication*, pp. 351-30.

Rowe, T.J., 2015. *Development and assessment of rules to parameterize the ACRU model for design flood estimation*. MSc dissertation, University of KwaZulu-Natal, Pietermaritzburg.

Rwanga, S.S. and Ndambuki, J.M., 2017. Accuracy Assessment of Land Use/Land Cover Classification Using Remote Sensing and GIS. *International Journal of Geosciences*, 8, 611–622. https://doi.org/10.4236/ijg.2017.84033

Saeedrashed, Y.S., 2020. Hydrologic and Hydraulic Modelling of the Greater Zab River-Basin for an Effective Management of Water Resources in the Kurdistan Region of Iraq Using DEM and Raster Images. In *Environmental Remote Sensing and GIS in Iraq*. Springer: Cham, Switzerland, pp. 415–446.

Saraiva-Okello, A.M.L, Masih, I., Uhlenbrook, S., Jewitt, G.P.W., van der Zaag, P. and Riddell, E., 2015. Drivers of spatial and temporal variability of streamflow in the Incomati River basin. *Hydrological Earth System Science,* 19, 657–673. doi:10.5194/hess-19-657-2015

Satellite Imaging Corporation, 2021. Sentinel-2A (10m) Satellite Sensor. Available at: https://www.satimagingcorp.com/satellite-sensors/other-satellite-sensors/sentinel-2a/ [Accessed on: 4 June 2021]

Sauka, S., 2016. *Flood Risk Assessment of the Crocodile River, Mpumalanga.* Masters, School of Geography and Archaeology and Environmental Studies. University of the Witwatersrand, Johannesburg.

Scanlon, B.R., Reedy, R.C. and Tachovsky, J.A., 2007. Semiarid unsaturated zone chloride profiles: archives of past land use change impacts on water resources in the southern High Plains, United States. *Water Resource Research*, 43(6), W06423. doi:10.1029/2006WR005769

Scharffenberg, W., Ely, P., Daly, S., Fleming, M. and Pak, J., 2010. *Hydrologic Modeling System (HEC-HMS): Physically-Based Simulation Components*. 2nd Joint Federal Interagency Conference, Las Vegas, NV, June 27 – 1 July 2010.

Schulze, R.E and Smithers, J.C., 2004. *The ACRU agrohydrological modelling system as of 2002: Background, concepts, structure, output, typical applications and operations.* ***PUBLICATION DETAILS???***

Sead, A., 2009. *Analysis of the impact of land use change and climate change on the flows in the Blue Nile River using SWAT*. MS thesis, Department of Hydrology and Hydraulic Engineering, Vrije Universiteit Brussel, Belgium.

Senthil Lekha, S. L. and Kumar, S. S., 2018. Classification and Mapping of Land Use Land Cover change in Kanyakumari district with Remote Sensing and GIS techniques. *International Journal of Applied Engineering Research,* 13(1), pp. 158–166.

Shafiei, M.K., Porhemmat, J., Sedghi, H. and Hosseni, M., 2018. Application of SWAT model in assessing the impact of land use change in runoff of Maroon River in Iran. *Applied Ecology and Environmental Research*, 16(5):5481–5502. http://dx.doi.org/10.15666/aeer/1605_54815502

Shakak, N., 2015. Integrationof Remote Sensing and Geographic information system in Ground Water Quality Assessment and Management. *ISPRS - International Archives of the Photogrammetry, Remote Sensing and Spatial Information Sciences.* Volume XL-7/W3, pp. 1483–1490.

Sheffield, J., Wood, E. F., Pan, M., Beck, H., Coccia, G., Serrat-Capdevila, A., & Verbist, K. (2018). Satellite remote sensing for water resources management: Potential for supporting sustainable development in data-poor regions. *Water Resources Research*, 54, 9724–9758. https://doi.org/10.1029/ 2017WR022437

Sheil, D., 2018. Forests, atmospheric water and an uncertain future: the new biology of the global water cycle. *Forest Ecosystem*, 5,19. https://doi.org/10.1186/s40663-018-0138-y

Singh, P., Gupta, A. and Singh, M., 2014. Hydrological inferences from watershed analysis for water resource management using remote sensing and GIS

techniques. *The Egyptian Journal of Remote Sensing and Space Science*, 17(2), pp. 111–121

Singo, L.R. 2014. *Integration of GIS and Remote sensing techniques to evaluate the impacts of land cover change on the hydrology and water resources of Luvuvhu River Catchment in Limpopo Province, South Africa*. PhD thesis, School of Environmental Science, University of Venda, Thohoyandou, South Africa.

Sipe, N. G. and Dale, P., 2003. Challenges in using geographic information systems to understand and control malaria in Indonesia. *Malaria Journal,* 2(26) https://doi.org/10.1186/1475-2875-2-36

Skidmore, A. K., Bijker, W., Schmidt, K. and Kumar, L., 1997. Use of remote sensing and GIS for sustainable land management. *Itc Journal,* 3(4), pp. 302–315.

Smithers, J.C., Chetty, K.T., Frezghi, M.S., Knoesen, D.M. and Tewolde, M.H., 2013. Development and assessment of a daily time-step continuous simulation modelling approach for design flood estimation at ungauged locations: ACRU model and Thukela Catchment case study. *Water SA*, 39(4), 467–476. https://dx.doi.org/10.4314/wsa.v39i4.4

Smithers, J.C., Schulze, R.E. and Jewitt, G.P.W., 2001. A hydrological perspective of the February 2000 floods: A case study in the Sabie River Catchment. *Water SA,* 27(3).

Smithers, J.C., Schulze, R.E. and Kienzle, S., 1997. Design flood estimation using a modelling approach: a case study using the ACRU model. *Sustainability of Water Resources Under Increasing Uncertainty*, 240: 365–375.

Soko, M.I. and Gyedu-Ababio, 2015. The Spatial and Temporal Variations of Ichythyofauna and Water Quality in the Crocodile River (East), Mpumalanga, South Africa. *Journal of Water Resource and Protection*, 7, pp. 152-170.

State of rivers reports (2001). Crocodile, Sabie-sand & Olifants River systems. WRC Report no. TT 147/01

Stehr, A., Debels, P., Romero, F. and Alcayaga, H., 2008. Hydrological modelling with SWAT under conditions of limited data availability: evaluation of results from a

Chilean case study. *Hydrological Sciences Journal*, 53:3, 588–601, doi: 10.1623/hysj.53.3.588

Sterling, S.M., Ducharne, A. and Polcher, J., 2013. The impact of global land-cover changes on the terrestrial water cycle. *National Climate Change,* 3:385–390

Susantoro, T.M., Wikantika, K., Saepuloh, A. and Harsolumakso, A.H., 2018. Selection of vegetation indices for mapping the sugarcane condition around the oil and gas field of North-West Java Basin, Indonesia. *IOP Conference Series Earth and Environmental Science,* 149, 012001. doi:10.1088/1755-1315/149/1/012001

Sy, S. and Quesada, B., 2020. Anthropogenic land cover change impact on climate extremes during the 21st century. *Environmental Research Letters*, 15, 034002

Sykes, M. T., 2009. Climate Change Impacts: Vegetation. In: *Encyclopedia of Life Sciences* (ELS). John Wiley & Sons, Ltd: Chichester. doi: 10.1002/9780470015902.a0021227

Tadesse, W., Tsegaye, T. D., and Coleman, T. L., 2001. Land use/cover change detection of the city of Addis Ababa, Ethiopia using remote sensing and geographic information system technology. *International Geoscience and remote sensing symposium*, 1:462–464

Tahiru, A. A., Doke, D. A. and Baatuuuwie, B. N., 2020. Effect of land use and land cover changes on water quality in the Nawuni Catchment of the White Volta Basin, Northern Region, Ghana. Applied Water Science, 10:198 https://doi.org/10.1007/s13201-020-01272-6 **DATE ACCESSED???**

Tassew, B.G., Mulugeta, A.B. and Miegel, K., 2019. Application of HEC-HMS Model for Flow Simulation in the Lake Tana Basin: The Case of Gilgel Abay Catchment, Upper Blue Nile Basin, Ethiopia. *Hydrology, 6,21. doi:10.3390/hydrology6010021*

Teillet, P.M. and Ren, X., 2008. Spectral band difference effects on vegetation indices derived from multiple satellite sensor data. *Canadian Journal of Remote Sensing,* 34, 159–173.

Thakur, J.K., Singh, S.K. and Ekanthalu, V.S., 2017. Integrating remote sensing, geographic information systems and global positioning system techniques with hydrological modelling. *Applied Water Sciences*, 7, 1595–1608. doi 10.1007/s13201-016-0384-5

Thavhana, M.P., 2018. *Runoff simulation using the SWAT model for flood frequency analysis and design flood estimations in the Luvuvhu River catchment, South Africa.* MSc, School of Agriculture, Earth and Environmental Sciences, University of KwaZulu-Nata, Pietermaritzburg, South Africa.

Thomson, M., Abayomi, K., Barnston, A.G., Levy, M. and Dilley, M., 2003. El Nino and Drought in Southern Africa. *Lancet*, 361, 437–438. 10.1016/S0140-6736(03)12421-X

Tian, K.D., Shen, B. and Jia, X., 2016. Application of MIKE-SHE model in runoff simulation of Bahe River Basin. *Journal of Water Resources and Water Engineering*, 27: 91–95.

Trung, N. H., Tri, L. Q., van Mensvoort, M. E. F. and Bregt, A. K., 2006. Application of GIS and Multi-criteria evaluation for land use planning in the coastal zone of the Mekong Delta, Vietnam. *International Symposium on Geoinformatics for Spatial Infrastructure Development in Earth and Allied Sciences*. [Online] Available at: http://library.wur.nl/webquery/wurpubs/346567 [Accessed 24 August 2018].

Tsihrintzis, V. A., Hamid, R. and Fuentes, H. R., 1996. Use of Geographic Information Systems (GIS) in water resources: A review. *Water Resources Management,* , 10(4), pp. 251–277.

Tucker, C.J., 1979. Red and Photographic Infrared linear combination for monitoring vegetation. *Remote sensing of environment*, 8, 127–150.

USGS, 2021. Ndvi Foundation Remote Sensing Phenology. Available at: https://www.usgs.gov/core-science-systems/eros/phenology/science/ndvi-foundation-remote-sensing-phenology?qt-science_centre_objects=0#qt-science_centre_objects [Accessed 10 June 2021]

USGS, 2021. USGS Eros archive-Sentinel-2. Available at: https://www.usgs.gov/centers/eros/science/usgs-eros-archive-sentinel-2?qt-science_center_objects=0#qt-science_center_objects [Accessed 4 June 2021]

USGS, 2016. Landsat-earth observation satellite (ver. 1.2, April 2020): U.S. Geological Survey Fact Sheet 2015-3081, 4 p., https://doi.org/10.3133/fs20153081

Utamahadi, M.A., Pandjaitan, N.H. and Rau, M.I., 2018. Land use change impacts on discharge analysis using SWAT model at Ciherang Pondok Dam catchment area. *IOP Conf. Series: Earth and Environmental Sciences,* 149. doi: 10.1088/1755-1315/149/1/012015

Van Bladeren, D. and Van Der Spuy, D., 2000. *The February 2000 Flood - The Worst in Living Memory? Southern Africa Floods of February 2000*. Department of Civil Engineering, University of Pretoria. Pretoria, South Africa.

van der Laan, M., van Antwerpen, R. and Bristow, K. L., 2012. River water quality in the northern sugarcane-producing regions of South Africa and implications for irrigation: A scoping study. *Water SA*, 38(1) PP. 87–96.

Verstraete, M., 2015. Re: Can I obtain comparable NDVI and GVI values from Landsat 7 (ETM+) and Landsat 8 (OLI), images as well as MSS vs TM images?. Retrieved from: https://www.researchgate.net/post/Can_I_obtain_comparable_NDVI_and_GVI_values_from_Landsat_7_ETM_and_Landsat_8_OLI_images_as_well_as_MSS_vs_TM_images/54d3c4a1d11b8bf46b8b461f/citation/download [Accessed 05 August 2021]

Versveld, D. B., Le Maitre, D. C., and Chapman, R. A.,1998. *Alien invading plants and water resources in South Africa: A preliminary Assessment.* Water Research Commission, Pretoria, South Africa, WRC Report No. TT 99/98.

Wagner, P.D., Kumar, S. and Schneider, K., 2013. An assessment of land use change impacts on the water resources of the Mula and Mutha Rivers catchment upstream of Pune, India. *Hydrological Earth System Science*, 17, 2233–2246. doi:10.5194/hess-17-2233-2013

Wang, X.X., Sun, Y.M., Hu, Y. and Zhu, Q.J., 2019. Impact of weeds on surface runoff and soil loss in a navel orange orchard. *Journal of Weed Science*, 37, 23–28.

Warburton, M.L., Schulze, R.E. and Jewitt, G.P.W., 2010. Confirmation of ACRU model results for applications in land use and climate change studies. *Hydrological Earth System Science,* 14, 2399–2414.

Willis, K.J. and Bhagwat, S.A., 2009. Biodiversity and climate change. *Science,* 326(5924), pp. 806 –807.

Wilson, G.M., 2005. Landcover classification of the City of rocks National Reserve Using ASTER Satellite imagery. Upper Columbia Basin Network, Inventory and Monitoring Program. Project Number UCBN-000001 National Park Service.

Wu, J., Zheng, H. and Xi, Y., 2019. SWAT-Based runoff simulation and Runoff responses to climate change in the headwaters of the Yellow River, China. *Atmosphere,* 10(9), pp.509. doi: 10.3390/atmos10090509

WWF-SA 2016, Water: Facts & Futures. WWF-SA, Cape Town, South Africa.

Xue, J. and Su, B., 2017. Significant remote sensing vegetation indices: A review of developments and applications. *Journal of Sensors*, 17. https://doi.org/10.1155/2017/1353691

Yamagata, K., Butts, M.B., Grooss, J. and Clausen, T.H., 2012. OpenMI coupling of FEFLOW and Mike SHE. 34th Hydrology and Water Resources Symposium, 19-22 November, Sydney, Australia.

Yeom, J., Jung, J., Chang, A., Ashapure, A., Maeda, M., Maeda, A. and Landivar, J., 2019. Comparison of Vegetation Indices Derived from UAV Data for Differentiation of Tillage Effects in Agriculture. *Remote Sensing*, 11, 1548. doi:10.3390/rs11131548

Yuan, Y., Nie, W. and Sanders, E., 2015, *Problems and Prospects of SWAT Model Application On An Arid/Semiarid Watershed In Arizona*. SEDHYD 2014 Joint Conference, Reno, NV, 23-24 March 2014.

Yue, W., Xu, J., Tan, W. and Xu, L., 2007. The relationship between land surface temperature and NDVI with remote sensing: application to Shanghai Landsat 7

ETM+ data. *International Journal of Remote Sensing*, 28:15, 3205–3226, doi: 10.1080/01431160500306906

Yuksel, A., Akay, A.E. and Gundogan, R., 2008. Using ASTER imagery in Land use/cover Classification of Eastern Mediterranean Landscapes according to CORINE Land Cover Project. *Sensors (Basel)*, 8(2), 1237–1251. doi: 10.3390/s8021287

Zacharias, I., Dimitriou, E. and Koussouris, T.H. 2009. Estimating land cover changes and associated environmental impacts on wetlands by coupling remote sensing and hydrogical modelling. *Water Resources system – water availability and global change (Proceedings of symposium HS02a held during IUGG2003 al Sapporo, July 2003*). IAHS Publ. no. 280, 247–254

Zang, C. and Mao, G. 2019. A Spatial and Temporal Study of the Green and Blue Water Flow Distribution in Typical Ecosystems and its Ecosystem Services Function in an Arid Basin. *Water*, 11, 97. doi:10.3390/w11010097

Zewdie, M., Worku, H. and Bantider, A., 2017. Temporal Dynamics of the Driving Factors of Urban Landscape Change of Addis Ababa During the Past Three Decades. *Environmental Management*. 61. 1–15. 10.1007/s00267-017-0953-x.

Zhang, B., Wu, D., Zhang, L., Jiao, Q. and Li, Q., 2012. Application of hyperspectral remote sensing for environment monitoring in mining areas. *Environmental Earth Sciences*, vol. 65, no. 3, 649–658.

Zhang, Z., Wang, S., Sun, G., McNulty, S.G., Zhang, H., Li, J., Zhang, M., Klaghofer, E. and Strauss, P., 2008. Evaluation of Mike-SHE model for application in the Loess Plateau, China. *Journal of American Water Resources Association*, 44(5), 1108–1120. doi: 10.1111/j.1752-1688.2008.00244.x

Zhang, M., Zhang, J. and Song, Y., 2019. Preliminary Research and Application of MIKE SHE Model in Jialingjiang River Basin. International Conference on Civil and Hydraulic Engineering. *IOP Conf. Series: Earth and Environmental Science*, 304. doi:10.1088/1755-1315/304/2/022088

Zhou, F., Xu, Y., Chen, Y., Xu, C-Y., Gao, Y. and Du, J. 2013. Hydrological response to urbanization at different spatio-temporal scales simulated by coupling of

CLUE-S and the SWAT model in the Yangtze River Delta region. *Journal of Hydrology*, 485, 113–125

Zhu, C. and Li, Y., 2014. Long-term hydrological impacts of land use/land cover change from 1984 to 2010 in the Little River Watershed, Tennessee. *International Soil and Water Conservation Research*, 2 (2), 11–22.

Zubair. O.A., Ji, W. and Festus, O., 2019. Urban Expansion and the Loss of Prairie and Agricultural Lands: A Satellite Remote-Sensing-Based Analysis at a Sub-Watershed Scale. *Sustainability*, 11, 4673. doi:10.3390/su11174673.

Appendix A: Correlation results

	1980	2000	2020
CAIBRATION	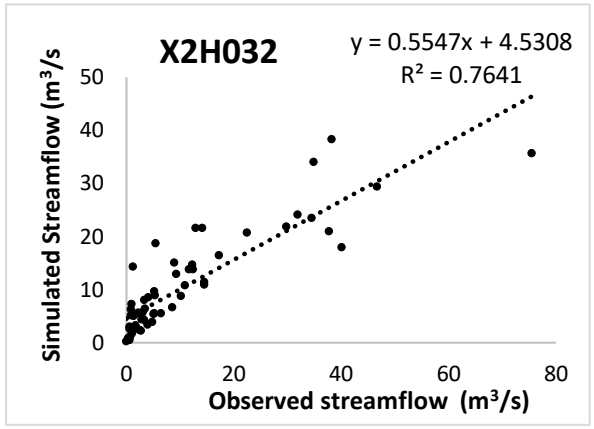	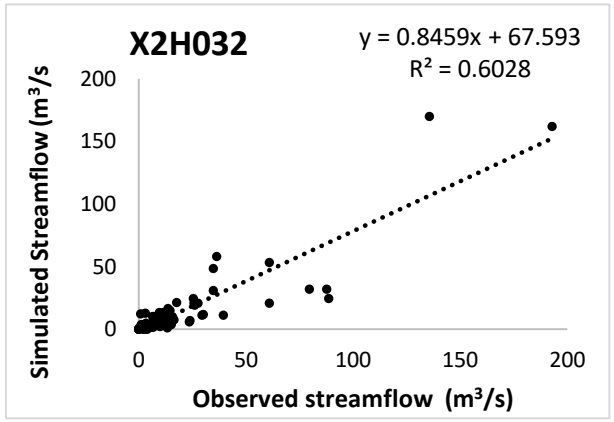	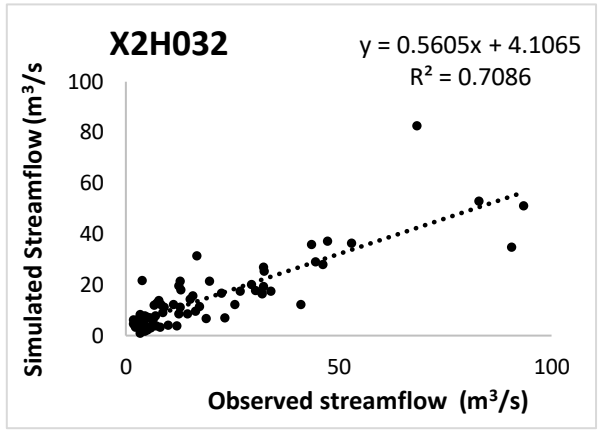
VALIDATION	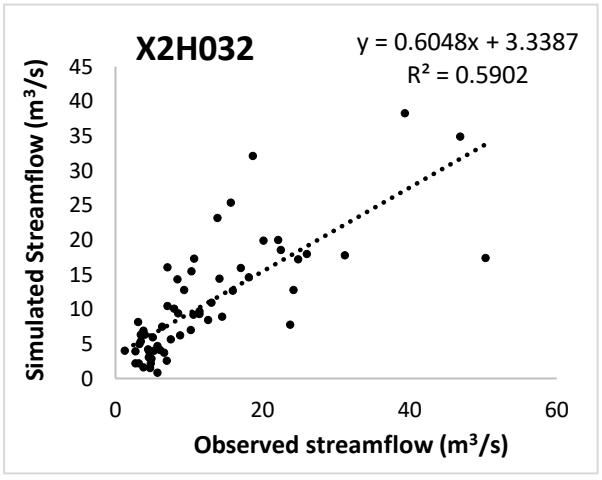	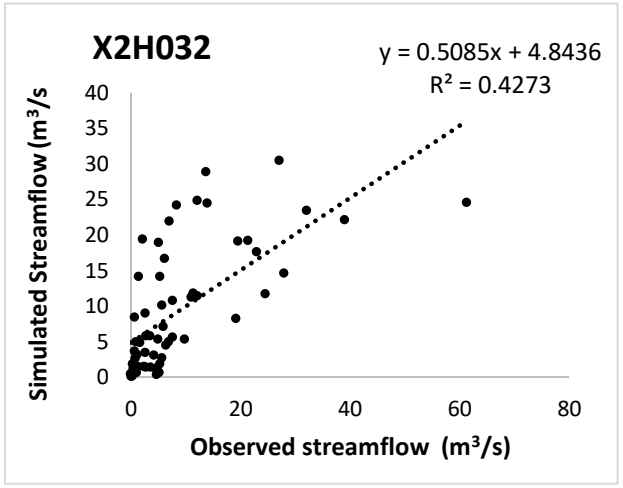	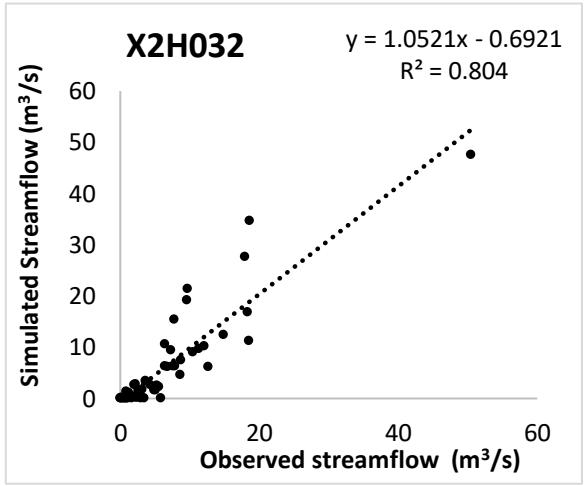

A1)

	1980	2000	2020
CAIBRATION	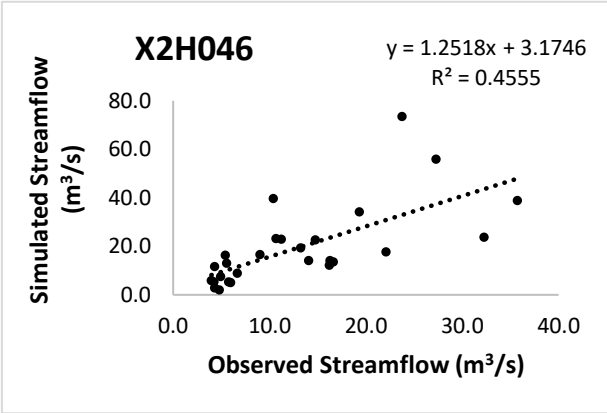	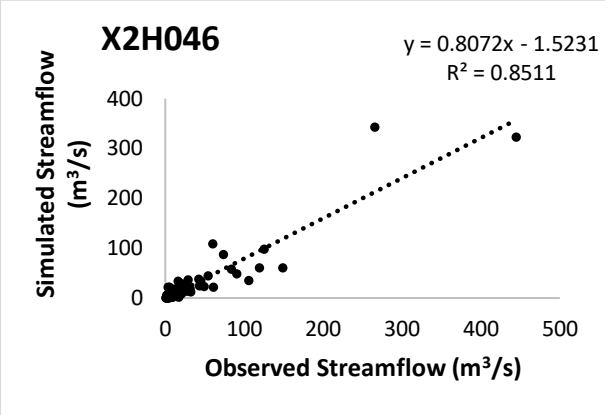	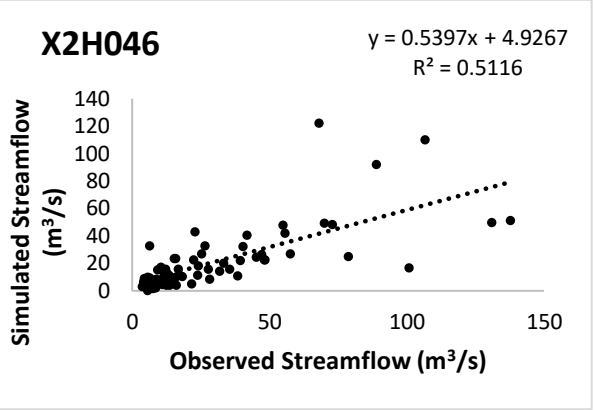
VALIDATION	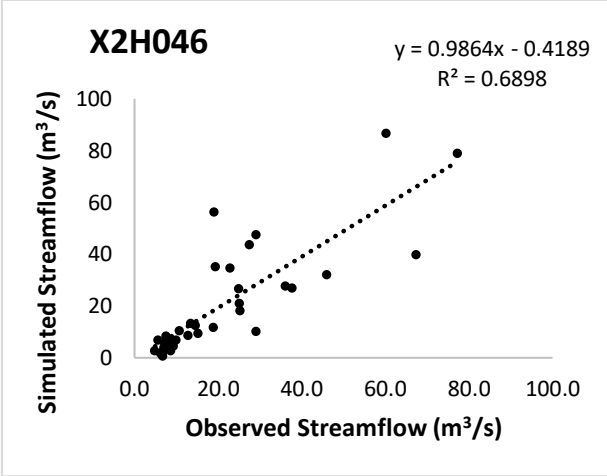	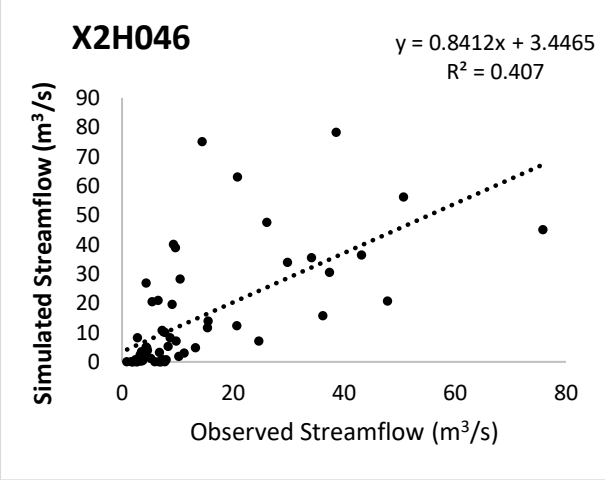	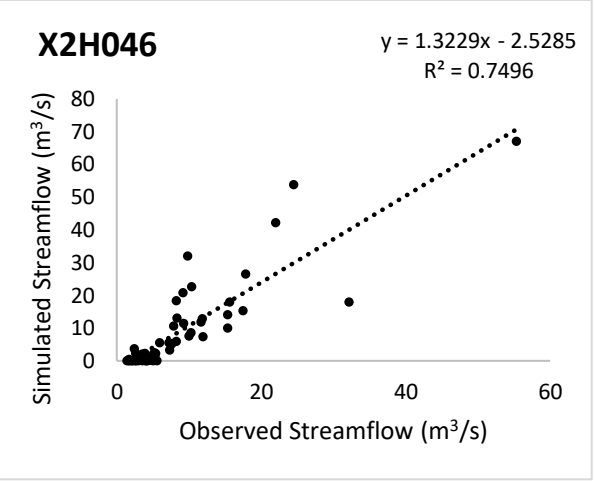

A2)

	1980	2000	2020
CAIBRATION	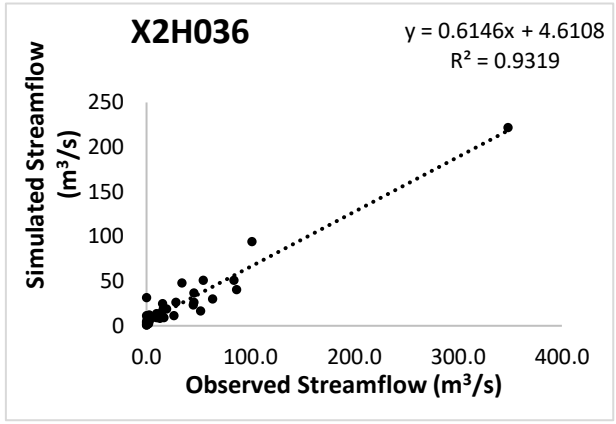	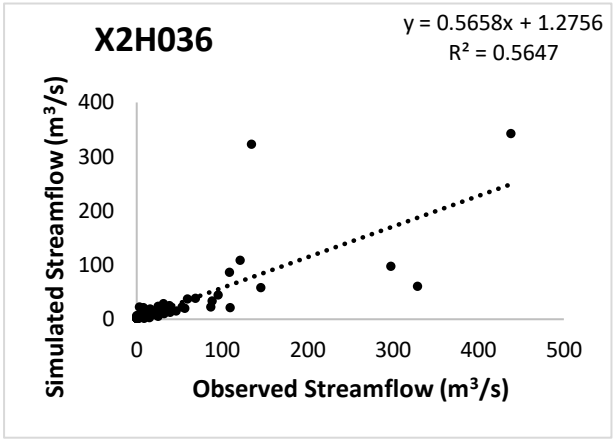	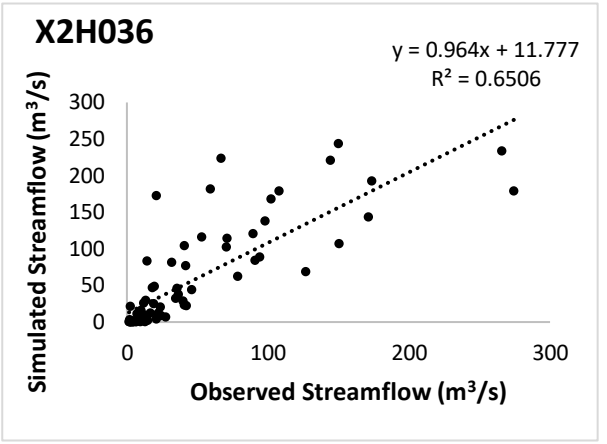
VALIDATION	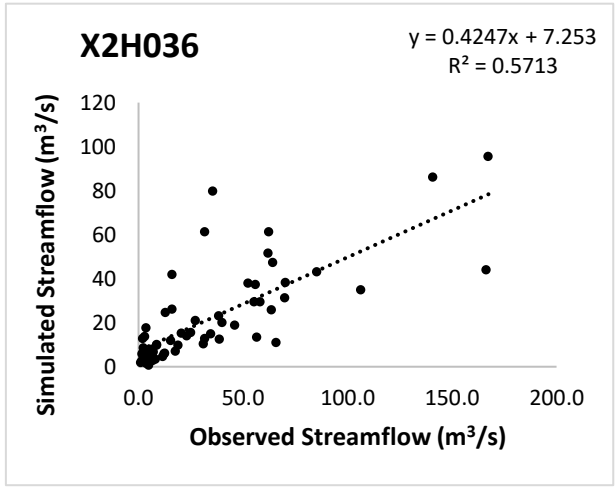	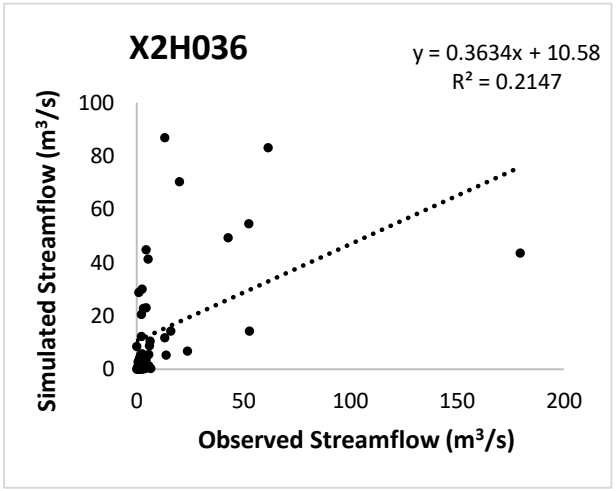	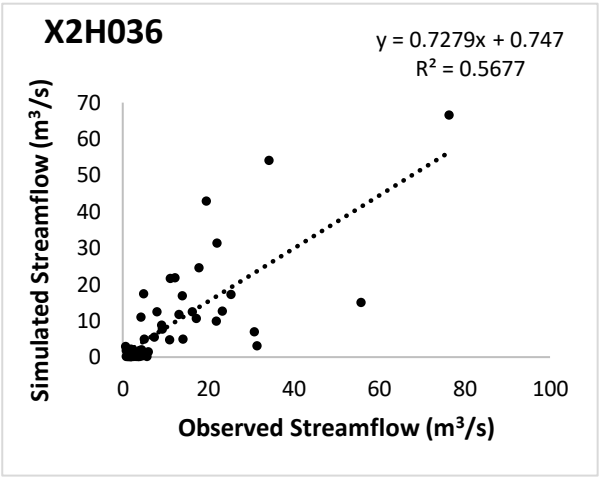

A3)

Appendix B: Simulated hydrological cycle/Water balance

B1) 2000

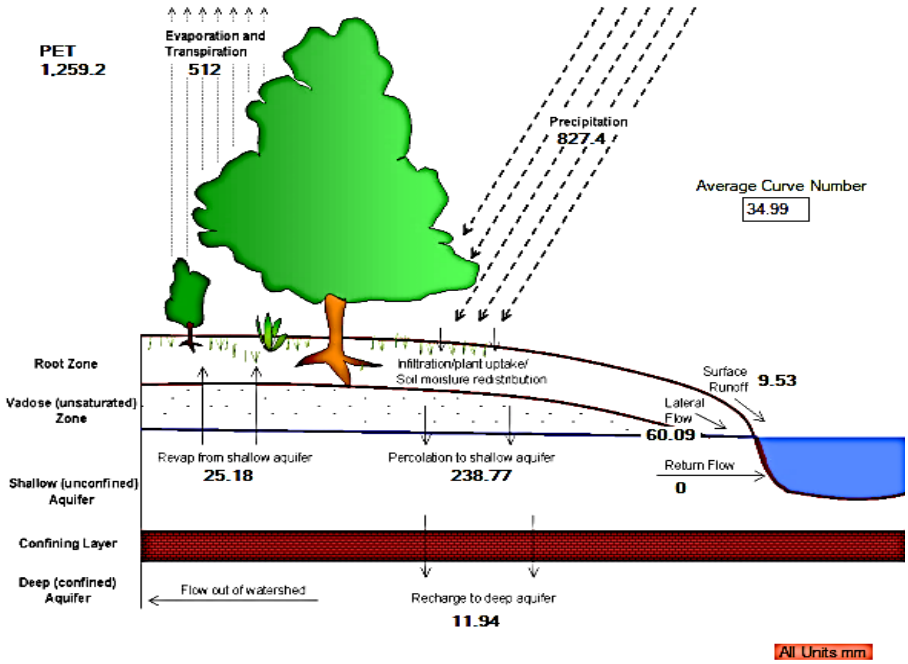

B2) 2020